

ADDIS ABABA UNIVERSITY
SCHOOL OF GRADUATE STUDIES

Normal Pulse Polarographic Determination of
Kinetic Parameters

by

Bizuneh Workie

Chemistry Department
Science Faculty

Approved by:

Dr. Theodros Solomon
Advisor

Prof. Bengt Nygård
Examiner

Dr. Carol Anderson
Examiner

Dr. H. Bartelt
Examiner

Theodros Solomon

Bengt Nygård

Carol G. Anderson

H. Bartelt

DEDICATION

To My Parents

1
2
3
4
5
6
7
8
9
10
11
12
13
14
15
16
17
18
19
20
21
22
23
24
25
26
27
28
29
30
31
32

Table of Contents

	<u>Page</u>
ACKNOWLEDGEMENTS	i
List of Figures	iii
List of Tables	v
Symbols and Abbreviations	vii
ABSTRACT	x
1. INTRODUCTION	1
2. THEORY	5
2.1 Kinetics of Simple Electrode reactions	5
2.2 Normal Pulse Polarography	11
2.3 Determination of Kinetic Parameters of Simple Electrode Reactions by Normal Pulse Polarography	17
2.3.1 Method of J.H. Christie	18
2.3.2 The Logarithmic Matsuda Equation	19
2.3.3 Method of Oldham and Parry	24
2.3.4 Method of P. Merican	24
3. EXPERIMENTAL	29
4. RESULTS AND DISCUSSION	31
4.1 Zn(II)-NaNO ₃ System	31
4.1.1 Determination of Kinetic Para- meters	31
4.1.1.1 Method of J.H Christie	31

	<u>Page</u>
4.1.1.2 Method of P. Mericam	45
4.1.1.3 The Logarithmic Matsuda Equation	50
4.1.2 Discussion	51
4.2 Cr(III)-NaClO ₄ System	54
4.2.1 Determination of Kinetic Para- meters	56
4.2.1.1 Method of Oldham and Parry	56
4.2.1.2 Method of P. Mericam	62
4.2.1.3 The Logarithmic Matsuda Equation	65
4.2.2 Discussion	67
4.3 Ni(II)-KNO ₃ System	69
4.3.1 Determination of Kinetic Para- meters	70
4.3.2 Discussion	81
5. CONCLUSION	85
6. APPENDIX	87
I. Computer Programme for The Theoretical Calculation of $(E^{\circ} - E_{V2})$ and $(E_{3/4} - E_{V4})$ for Simple Electrode Reactions as Functions of $\log k^{\circ}$ and α	87
II. Theoretical Values of $(E^{\circ} - E_{V2})$ and $(E_{3/4} - E_{V4})$ for the analysis of Irreversible Electrode reactions	89
IIa. Cr(III)-NaClO ₄ System	89

	<u>Page</u>
Iib. Ni(II)-KNO ₃ System	92
III. Derivation of Eq. (19a)	95
7. REFERENCES	96

ACKNOWLEDGEMENTS

I would like to express my gratitude and record my indebtedness to my advisor Dr. Theodros Solomon, whose effort as a research advisor and valuable guidance of this project was indispensable.

I am greatly indebted to Professor P. Mericam of Universite de Pau (France) who had kindly sent me his original computer programme for the theoretical calculations. I would also like to thank Ato Alebachew Demoz, who is on a study leave in FRG, for the very useful reprints he sent me, Ato Yilma Tamiru for typing manuscript, and Ato Amare Meriga, Ato Tekele Habte, Ato Abdu De Tango, and Ato Adenew Geletu for their invaluable assistance in the materialization of this work.

It would take me pages to list the names of all who have contributed to have a successful outcome of the computer work, but mention should be made of Dr. C. Anderson, Ato Micheal Shebelle, W/t Woubalem Taye and Ato Genene Zewge whose precious assistance is highly acknowledged. I should also like to thank all staff members of the Department of Chemistry, colleagues and friends, Dr. Chandravanshe, Aberra Fura, Alemayehu Abebaw, Hailemicheal Alemu, Shimeles Admassie, Omer Kekyu, Endalkachew Sahele, Berhanu Mekonen, Bekele Dinku, Getachew Atnafu and all others not mentioned for their valuable assistance and continuous encouragements given during the course of this work.

Finally, it is a pleasure for me to express my gratitude to the Department of Chemistry of AAU for providing me with every facilities needed for the accomplishment of the work.

List of Figures

<u>Figure</u>	<u>Page</u>
1. Sampling scheme for normal pulse polarography	12
2a,2b. $(E^{\circ} - E_{\sqrt{2}})$ and $(E_{3/4} - E_{\sqrt{4}})$ dependence on $\log k^{\circ}$ at various α values	26
3. $\log k^{\circ}$ vs α diagram at constant $(E^{\circ} - E_{\sqrt{2}})$ and constant $(E_{3/4} - E_{\sqrt{4}})$	28
4. $\log \left(\frac{i}{i_d - i} \right)$ vs E plot of Zn(II)-0.49M NaNO ₃ system	33
5. Plot of $\sqrt{\pi x} \exp(x^2) \operatorname{erfc}(x)$ vs x	35
6a,6b,	
6c. NPP polarograms of 0.19mM Zn(II) in 0.49, 1.05, and 2.45M of NaNO ₃	36,37,38
7a,7b,	
7c. $\log k$ vs E plot of Zn(II) in 0.45, 1.05, and 2.45M of NaNO ₃	42,43,44
8a,8b. $(E^{\circ} - E_{\sqrt{2}})$ and $(E_{3/4} - E_{\sqrt{4}})$ vs $\log k^{\circ}$ diagram at various α values for the analysis of the Zn(II)-NaNO ₃ systems	46,47
9a,9b. $\log k^{\circ}$ vs α diagram at the experimental $(E^{\circ} - E_{\sqrt{2}})$ and $(E_{3/4} - E_{\sqrt{4}})$ values of the Zn(II)-NaNO ₃ systems	49
10a,10b,	
10c. NPP polarograms of 0.2mM Cr(III) in 0.2,	

<u>Figure</u>	<u>Page</u>
11. Log y vs -E plot of Cr(III) in 0.2, 0.5, and 1.0M of NaClO ₄	61
12. (E ⁰ - E _{1/2}) vs log k ⁰ diagram at various α values for the analysis of the Cr(III)-NaClO ₄ systems	64
13a, 13b,	
13c, 13d. NPP polarograms of 0.2mM Ni(II) in 0.1 0.15, 0.2, and 0.26M of KNO ₃	71, 72, 73
	74
14. Log y vs -E plot of Ni(II) in 0.10, 0.15, 0.20 and 0.26M of KNO ₃	75
15. (E ⁰ - E _{1/2}) vs log k ⁰ diagram at various α values for the analysis of the Ni(II)-KNO ₃ systems	79
16. Experimental (k ⁰ - E _{1/2}) and (E _{1/2} - E _{1/2}) values for the reduction of Ni(II) in the various concentrations of KNO ₃	79
17. Experimental (k ⁰ - E _{1/2}) and (E _{1/2} - E _{1/2}) values for the reduction of Ni(II) in the various concentrations of KNO ₃	79

List of Tables

<u>Table</u>	<u>Page</u>
1. Equations for the analysis of the Zn(II)-NaNO ₃ systems	32
2. The values of $E_{1/2}^R$ of Zn(II) reduction in various concentrations of NaNO ₃	34
3,4,	
5. The values of $\Lambda_2^0 v \theta_s$, $k v \theta_s$, and $\log k$ at different potentials of Zn(II) reduction in 0.49, 1.05 and 2.45M NaNO ₃	39,41
6. Apparent values of the kinetic parameters for the Zn(II) reduction for the various concentrations of NaNO ₃	53
7. Equations for the analysis of the Cr(III)-NaClO ₄ and Ni(II)-KNO ₃ systems	55
8. Apparent values of the kinetic parameters for Cr(III) reduction for the various concentrations of NaClO ₄	68
9. Values of k^0 and α obtained using the method of Oldham and Parry for Ni(II) reduction in the various concentrations of KNO ₃	76
10. Experimental $(E^0 - E_{1/2})$ and $(E_{3/4} - E_{1/4})$ values for the reduction of Ni(II) in the various concentrations of KNO ₃	77

<u>Table</u>		<u>Page</u>
11.	Experimental values ($E_{1/2} - E^0$) and ($E_{3/4} - E^0$) for the reduction of Ni(II) in the various concentrations of KNO_3	78
12.	Apparent values of the kinetic parameters for the reduction of Ni(II) in the various concentrations of KNO_3	83

Symbols and Abbreviations

α	= Cathodic transfer coefficient
θ_s	= Sampling time in normal pulse polarography
ϕ_2	= Electrical potential of the outer Helmholtz plane referred to the bulk of the solution (unit V)
A	= Surface area of electrode
C_O^0	= Bulk concentration of oxidized species
$C_O(x=0)$	= Concentration of oxidized species at the electrode surface
$C_R(x=0)$	= Concentration of reduced species at the electrode surface
D_O	= Diffusion coefficient of oxidized species
D_R	= Diffusion coefficient of reduced species
E	= Electrode potential referred to some reference electrode (unit V)
E^0	= Formal electrode potential
E_2	= Step potential applied in normal pulse polarography
$E_{V/2}$	= Half wave potential
$E_{V/2}^r$	= Polarographic reversible half wave potential
$E_{V/4}$	= Potential where $i/i_d = 1/4$
$E_{3/4}$	= Potential where $i/i_d = 3/4$
F	= Faraday constant
$\exp(x)$	= Exponential of x
$\operatorname{erf}(x)$	= Error function of x

- $\operatorname{erfc}(x)$ = Error function complement of x
- i = Electric current
- i_a = Anodic current
- i_c = Cathodic current
- i_{NPP}^c = Normal pulse polarographic cathodic current
- i_d = Diffusion current
- $(i_d^c)_{\text{Cott}}$ = Cottrel diffusion current
- \overrightarrow{k} = Heterogenous rate constant for reduction
(unit cm s^{-1})
- \overleftarrow{k} = Heterogenous rate constant for oxidation
(unit cm s^{-1})
- \overrightarrow{k}^0 = Heterogenous rate constant for reduction
at $E = 0V$ (unit cm s^{-1})
- \overleftarrow{k}^0 = Heterogenous rate constant for oxidation
at $E = 0V$ (unit cm s^{-1})
- k^0 = Standard heterogenous rate constant (unit
 cm s^{-1})
- n = Number of electrons per mole of a substance
reduced
- O = Oxidized species
- R = Gas constant /Reduced species
- T = Absolute temperature (unit K)
- t = Time
- V_b = The rate of the backward reaction (unit
 $(\text{mol s}^{-1} \text{cm}^{-2})$)
- V_f = The rate of the forward reaction (unit $\text{mol s}^{-1} \text{cm}^{-2}$)

V_n	=	The net rate of reaction (unit mol s ⁻¹ cm ⁻²)
DME	=	Dropping mercury electrode
NHE	=	Normal hydrogen electrode
SCE	=	Saturated calomel electrode
dcp	=	Direct current polarography
NPP	=	Normal pulse polarography

ABSTRACT

The procedure that has been developed by P. Mericam, M. Astruc, and X. Andrieu [1] for the determination of kinetic parameters of simple electrode reactions using normal pulse polarography has been tested by applying the technique to quasi-reversible polarographic electrode reduction of Zn(II) and, to irreversible polarographic electrode reductions of Cr(III) and Ni(II). The obtained kinetic parameters have been compared with values computed with previously established methods.

An alternative simpler procedure for the evaluation of kinetic parameters of simple electrode reactions by normal pulse polarography has been proposed. The method has been devised by formulating simultaneous equations from the logarithmic form of Matsuda's equation [2] for the rate constant and using experimental parameters of the NPP wave, namely, the half wave potential $E_{1/2}$ and three quarter wave potential $E_{3/4}$. This technique has been tested on the above mentioned electrode reduction of Zn(II), Ni(II), and Cr(III). Results obtained are in good agreement with values computed by other methods.

Attempts have also been made to study the effect of the supporting electrolyte concentration on the kinetic parameters.

1. INTRODUCTION

Normal pulse polarography (NPP) was developed originally by G.C. Barker [3] as an outgrowth of his work on square wave polarography. Nowadays, NPP has become one of the most powerful and applicable electroanalytical techniques because of its higher sensitivity [4-7]. A great potentiality of NPP has been recognized also for the determination of kinetic parameters of simple electrode reactions thereby lending itself to wider utility in electrochemical studies.

A general theory of NPP current-potential curve has been developed by Matsuda [2] for a simple electrode reaction proceeding at the expanding plane electrode. Other extensive theoretical studies have also been made by various workers [8-12].

Following the studies of Parry and Osteryoung [4] on reversible waves, several papers have dealt with NPP for studying the kinetics of simple electrode reactions. From the current-potential relation of Barker and Gardner [12], J.H. Christie et. al [13] have developed a method for evaluating kinetic parameters and they applied the method to the reduction of Zn(II) in varying concentrations of NaNO_3 . Koryta [14] has studied this system by rapid polarography. Using the same current-potential equation of Barker and Gardner, Oldham and Parry [15] have also proposed a logarithmic expression for a totally

irreversible electrode reduction from which kinetic parameters are determinable. The relation of Oldham and Parry can also be developed from the equation of Matsuda [2.]. L. Canacho et. al [16] have also suggested different mathematical relationships for an irreversible electrode reduction from the solution given by Galvez and Serna [8].

Recently, P. Mericam et. al [1] have developed a new graphical procedure for the determination of kinetic parameters of simple electrode reaction by NPP. The graphical methods of these workers have been devised from systematic variation of the kinetic parameters introduced either in closed form solutions or in digital simulations. The method has been applied to the reduction of zinc in potassium nitrate solution which had already been used as a test [17]. The possible application of the method for an irreversible electrode reduction has also been suggested [1].

In this work the method of P. Mericam et. al [1] has been applied and tested on the quasi-reversible polarographic electrode reduction of Zn(II) in varying concentration of NaNO_3 that had already been studied by NPP [13] and rapid polarography [14]. The test has also been extended to the polarographic electrode reduction of Ni(II) in varying concentration of KNO_3 as a supporting electrolyte. Ni(II) had been studied [18] by dc polarography in 0.1 M KNO_3 . Different works on the electrode

kinetics of Zn(II) and Ni(II) can be found in reference 19. The applicability of the P. Mericam method is also checked for the totally irreversible polarographic electrode reduction of Cr(III) in different concentration of NaClO_4 as a supporting electrolyte. The reduction of Cr(III) at the dropping mercury electrode had been studied as a function of both electrode potential and NaClO_4 concentration by R. Andreu et al. [20] using rapid polarography. The rate of reduction of Cr(III) at DME using normal dc polarographic method has also been studied by F.C anson et al. [21], and by R. Parsons and E. Passeron [22] in an attempt to search for the potential dependence of the transfer coefficient. Various studies on the electrode kinetics of Cr(III) have been compiled in reference 19. The validity of the P. Mericam et al. method is established by comparing the results obtained with values computed using the techniques of J.H. Christie et al. [13] and Oldham and Parry [15].

In this study simpler means of extracting the kinetic parameters of simple electrode reactions has been proposed. The technique has been developed by formulating simultaneous equations from the logarithmic form of Matsuda's equation [2] for the rate constant and the experimental values of the three quarter wave potential $E_{3/4}$ and the half wave potential $E_{1/2}$ of the NPP wave. The method devised has been tested on the previously mentioned quasi-reversible electrode reduction of Zn(II)

and the totally irreversible electrode reductions of Cr(III) and Ni(II). The results obtained are in good agreement with values determined by the above mentioned techniques of J.H. Christie et al., Oldham and Parry, and P. Mericam et al.

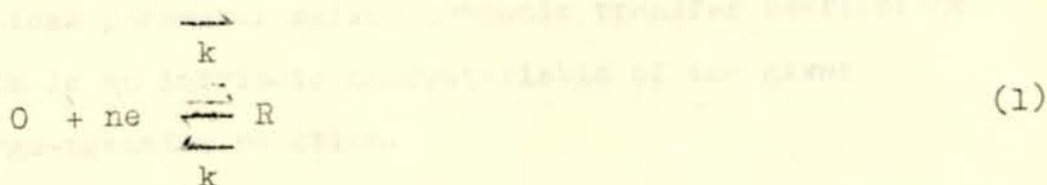
The work has also been extended to the study of the influence of supporting electrolyte concentration on the electrode kinetics from the effect on the experimentally determined apparent values of the kinetic parameters.

2. THEORY

Electrode reactions are heterogenous processes whose kinetics depend on the rate of charge transfer, mass transfer, possibly the rate of chemical reactions coupled with charge transfer, and other surface reaction, such as adsorption, desorption, or crystallization. Because of the heterogenous nature of electrode processes, their kinetics is profoundly affected by the double-layer structure and by adsorption of reactants, products, supporting electrolyte, and any additive. The simplest reaction involves only mass transfer of reactants to the electrode, heterogenous electron-transfer involving nonadsorbed species and mass transfer of the product to the solution. In this chapter kinetics of such simple electrode reactions and methods of determining their kinetic parameters by normal pulse polarography will be discussed.

2.1 Kinetics of Simple Electrode Reactions

Consider a simple electrode reaction, designated by



where both reactants O and R are assumed to be soluble in solution or in the dropping mercury

electrode (DME). The rate of the forward reaction V_f ($\text{mol s}^{-1} \text{ cm}^{-2}$) and the backward reaction V_b ($\text{mol s}^{-1} \text{ cm}^{-2}$) are given by

$$V_f = \vec{k} C_O(x=0) = i_c/nFA \quad (2a)$$

$$V_b = \overset{\leftarrow}{k} C_R(x=0) = i_a/nFA \quad (2b)$$

where \vec{k} and $\overset{\leftarrow}{k}$ are the forward and backward heterogeneous rate constants respectively and have a dimension of cm s^{-1} if the concentrations are expressed in mol cm^{-3} .

The rate constants are dependent on potential, E and can be expressed as

$$\vec{k} = \vec{k}^0 \exp \left[\frac{-\alpha nFE}{RT} \right] \quad (3a)$$

$$\overset{\leftarrow}{k} = \overset{\leftarrow}{k}^0 \exp \left[\frac{(1-\alpha)nFE}{RT} \right] \quad (3b)$$

where \vec{k}^0 and $\overset{\leftarrow}{k}^0$ are the value of \vec{k} and $\overset{\leftarrow}{k}$ when $E=0$, on an arbitrary potential scale and α is a dimensionless parameter called cathodic transfer coefficient which is an intrinsic characteristic of the given charge-transfer reaction.

A far more useful potential at which to define the rate constants is the formal standard redox couple E^0 where E^0 has the usual thermodynamic significance.

When $E=E^0$, $C_O(x=0) = C_R(x=0)$ and $V_f = V_b$. Thus $\overrightarrow{k} = \overleftarrow{k}$ and

$$\overrightarrow{k}^0 \exp \left[\frac{-\alpha n F E^0}{RT} \right] = \overleftarrow{k}^0 \exp \left[\frac{(1-\alpha) n F E^0}{RT} \right] = k^0 \quad (4)$$

k^0 denotes the heterogenous rate constant at E^0 and is termed the standard rate constant.

Equation (4) may be substituted in Eqs. (3a) and (3b) to yield:

$$\overrightarrow{k} = k^0 \exp \left[\frac{-\alpha n F (E - E^0)}{RT} \right] \quad (5a)$$

$$\overleftarrow{k} = k^0 \exp \left[\frac{(1-\alpha) n F (E - E^0)}{RT} \right] \quad (5b)$$

The value of k^0 is characteristic of a given electrode process. Its physical interpretation is straight forward. It is simply a measure of the kinetic facility of a redox couple. A system with large k^0 will achieve equilibrium on a short time scale, but a system with small k^0 will be sluggish.

The cathodic transfer coefficient, α , which characterizes the electrode kinetics together with k^0 , determines what fraction of the electrical energy resulting from the displacement of the potential from the equilibrium value affects the rate of electrochemical tran-

sformation. In terms of free energy-vs-reaction coordinate diagrams [23,24] it can be proposed that the height of the activation energy of the forward reaction is altered by some fraction α of the total free energy change resulting from the potential difference at the electrode-solution interface when the reduction occurs. The same assumption requires that the activation energy for the reverse reaction is altered by $1-\alpha$ of the total free energy. The value of α lies between 0 and 1.

The net rate, V_n , which determines the magnitude of the current i , is given by the difference between the forward and reverse rates, so that

$$V_n = V_f - V_b = \vec{k} C_O(x=0) - \overset{\leftarrow}{k} C_R(x=0) = \frac{i}{nFA} \quad (6)$$

Thus:

$$i = nFA [\vec{k} C_O(x=0) - \overset{\leftarrow}{k} C_R(x=0)] = i_c - i_a \quad (7)$$

Using Eqs. (6) and (7) the complete current-potential equation is written as

$$i = nFA k^0 \left\{ C_O(x=0) \exp \left[\frac{-\alpha nF(E-E^0)}{RT} \right] - C_R(x=0) \exp \left[\frac{(1-\alpha)nF(E-E^0)}{RT} \right] \right\} \quad (8)$$

For very rapid electrode kinetics, or for reversible

processes it can be shown that the general current-potential relation (Eq. (8)) reduces to the Nernst relation:

$$E = E^{\circ} + \frac{RT}{nF} \ln \frac{C_o(x=0)}{C_R(x=0)} \quad (9)$$

This class of electrode processes are characterized by large value of k° , and the current magnitude at all potentials is considered to be independent of k° , k , or \overleftarrow{k} within the limit of experimental error of method of measurement.

When the electrode kinetics are very sluggish (k° is very small), the anodic and cathodic terms of Eq. (8) are never simultaneously significant. That is when an appreciable net cathodic current is flowing, the second term has a negligibly small effect, and vice versa. For such kinds of electrode reactions, the reduction process is solely governed by \overleftarrow{k} and the oxidation process by \overrightarrow{k} . This type of electrode processes are called totally irreversible electrode processes.

Electrode reactions are not always very facile or very sluggish, and the whole i - E characteristic must sometimes be considered. For these types of electrode processes called quasi-reversible electrode processes, the complete mathematical description requires inclusion of terms involving both \overleftarrow{k} and \overrightarrow{k} . In this class of electrode processes the magnitude of \overleftarrow{k} and \overrightarrow{k} are comparable.

In experimental determination of the kinetic parameters, the reacting species in the initial and final states of the reaction are usually to be located on the solution side of the double layer. As a consequence of this assumption the parameters are affected by the structural change of the double layer. For example the standard rate constant k^0 for a given electrode reaction might be a function of the nature of supporting electrolyte or the supporting electrolyte concentration, even when no apparent bulk reaction involving electrolyte ions occurs. These effects can be understood and interpreted in terms of the variations of the potential in the double layer region. The basic concepts were described by Frumkin [44] and the effect is sometimes called Frumkin effect.

Under the assumption that the electrode reaction proceeds at the outer Helmholtz plane, the Frumkin double layer effect on the kinetic parameters is given by the following equations:

$$\alpha = \alpha_t + [(Z_0 - n\alpha_t)/n] (\partial\phi_2/\partial E) \quad (10a)$$

$$k^0 = k_t^0 \exp [(\alpha_t - Z_0) F\phi_2/RT] \quad (10b)$$

where the parameters with the subscript "t" denotes the parameters corrected for Frumkin effect, Z_0 the charge number (with sign) of the species O, and ϕ_2 is

the electrical potential of the outer Helmholtz layer referred to the bulk of solution.

The overall effect of the double layer on kinetics is that the apparent quantities, k^0 and α , are functions of potential, through the variation of ϕ_2 with E . They are function of the supporting electrolyte concentration, as well, since ϕ_2 depends on the supporting electrolyte concentration.

2.2 Normal Pulse Polarography

In pulse polarography a single rectangular pulse of short duration per mercury drop is applied late in the drop life [3-6]. Since the capacitance current decays much more rapidly than the faradic current, the current measured at 20 - 40 ms after the pulse application is essentially faradic. The polarogram is a plot of the faradic current produced by the pulses versus the applied potential. Analytically the chief advantage of pulse polarographic methods over conventional dc polarography is their ability to discriminate charging current. Depending on the applied voltage function and the method of current determination, various kinds of pulse polarography may be distinguished, of which the two most important are differential and normal pulse polarography (NPP). What follows is a theoretical discussion about the latter.

In NPP the electrode is held at a constant, adjustable base voltage (E_1), at which negligible electrolysis occurs (Fig. 1). After a fixed waiting period \bar{c} , measured from the birth of the drop, the value is changed abruptly to another constant value E_2 for a short period.

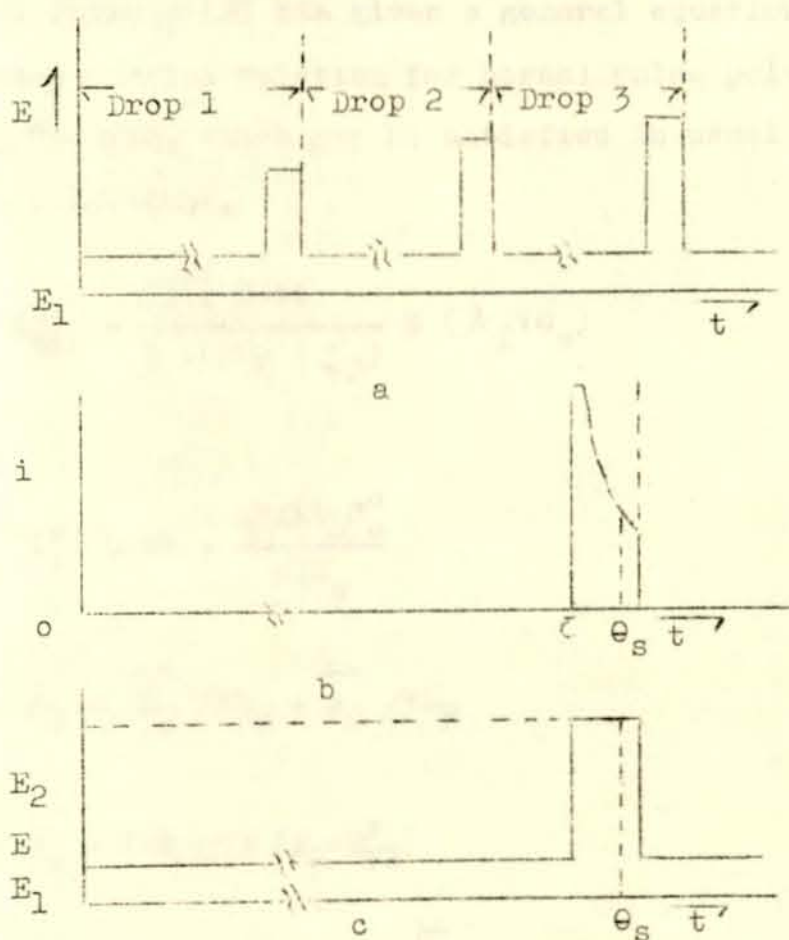


Fig. 1. Sampling scheme for normal pulse polarography (a) Potential programme (b) Current and (c) Potential during a single drop's life time

The potential pulse is ended by a return to a base value E_1 . The current is sampled at a time θ_s near the end of the pulse, and a signal proportional to this sampled value is recorded. The drop is dislodged just after the pulse ends, and the whole cycle is repeated with a series of pulses of increasing height. The plot is the output current versus step potential E_2 . The i/E curve obtained resembles an ordinary polarogram.

H. Matsuda [2] has given a general equation for the current-potential relation for normal pulse polarography. For $\theta_s/\bar{C} \leq 1/30$, which may be satisfied in usual experimental conditions,

$$i_{NFP}^c = \frac{(i_d^c) \text{ Cott}}{1 + \exp(\zeta_2)} \vartheta(\lambda_2 \sqrt{\theta_s}) \quad (11)$$

where

$$(i_d^c) \text{ Cott} = \frac{nFAVD_0 C_0^0}{\sqrt{\pi\theta_s}} \quad (12a)$$

$$\lambda_2 = \frac{k_2}{\sqrt{D_0}} + \frac{k_2}{\sqrt{D_R}} \quad (12b)$$

$$\lambda_2 = (nF/RT) (E_2 - E_{V/2}^r) \quad (12c)$$

$$E_{V/2}^r = E^0 - (RT/nF) \ln \sqrt{\frac{D_0}{D_R}} \quad (12d)$$

$$\vartheta(\lambda_2 \sqrt{\theta_s}) = \sqrt{\pi} \lambda_2 \sqrt{\theta_s} \exp(\lambda_2^2 \theta_s) \text{erfc}(\lambda_2 \sqrt{\theta_s}) \quad (12e)$$

In order to examine the behavior of a pulse polarogram, it is convenient to derive an expression similar to the log-plot in dc polarography.

Considering the limiting case of reversible waves, $\phi(\lambda_2 \nu \theta_s)$ is equal to unity within an error of 2%, when $(\lambda_2 \nu \theta_s) \geq 5$. Matsuda [2] has shown that this inequality can be expressed as:

$$(k_o \nu \theta_s) / \nu D \geq 5[\alpha^\alpha (1-\alpha)^{(1-\alpha)}] \quad (13a)$$

where

$$D = D_o^{1-\alpha} D_R^\alpha \quad (13b)$$

Under such condition, Eq. (11) can be simplified into

$$i_{NPP}^c = (i_d^c)_{Cott} / [1 + \exp(\frac{E_2}{E_2^R})] \quad (14)$$

or, solving Eq. (14) with respect to E_2 ,

$$E_2 = E_{v/2}^R - (RT/nF) \ln [x/(1-x)] \quad (15a)$$

where

$$x = i_{NPP}^c / (i_d^c)_{Cott} \quad (15b)$$

For normal pulse polarograms of quasi-reversible and irreversible systems, a new log plot was derived

by Matsuda [2] using an approximate equation of ϕ derived by Oldham and Parry [15].

It has been shown [15] that for any $\lambda_2 v \theta_s$ value, $\phi(\lambda_2 v \theta_s)$ can be expressed as:

$$\phi(\lambda_2 v \theta_s) = \frac{2}{1 + \sqrt{1 + E(\lambda_2 v \theta_s) / \lambda_2^2 \theta_s}} \quad (16a)$$

where the function $E(\lambda_2 v \theta_s)$ can be approximated by:

$$E(\lambda_2 v \theta_s) \approx 3[1.75 + \phi^2(\lambda_2 v \theta_s)]/4 \quad (16b)$$

Substituting Eq. (16b) into Eq. (16a) and solving for $\lambda_2 v \theta_s$,

$$\lambda_2 v \theta_s = \frac{\sqrt{3}}{4} \left[\frac{1.75 + \phi^2}{1 - \phi} \right]^{-1/2} \phi \quad (17)$$

Introducing Eqs. (5a) and (5b) into Eq. (12b) and using the definition of D given in Eq. (13b), λ_2 can be expressed as:

$$\lambda_2 = (k^0 / VD) [\exp(-\alpha \xi_2) + \exp\{(1-\alpha) \xi_2\}] \quad (18)$$

It can be shown (see Appendix III) that the use of Eqs. (11), (17) and (18) yields, upon some rearrangements,

$$E_2 = E^* - \frac{RT}{\alpha nF} \ln \left\{ x \left[\frac{1.75 + x^2(1 + \exp(\xi_2))^2}{1 - x(1 + \exp(\xi_2))} \right]^{1/2} \right\} \quad (19a)$$

where

$$E^* = E_{1/2}^r + \frac{RT}{\alpha n F} \ln \left\{ \frac{4 k^0 v e_s}{\sqrt{3} \sqrt{D}} \right\} \quad (19b)$$

Equation (19a) is a convenient log-plot for NPP waves.

Equation (19a) can further be simplified for a totally irreversible waves. The term $\exp(\frac{1}{2})$ in Eq. (19a) can be neglected compared with unity in the whole potential region concerned. Thus Eq. (19a) will be reduced to

$$E = E^* - \frac{RT}{\alpha n F} \ln \left\{ x \left[\frac{1.75 + x^2}{1 - x} \right]^{\sqrt{2}} \right\} \quad (20)$$

This is the same equation that was previously proposed by Oldham and Farry [15] for totally irreversible waves.

The half wave potential of totally irreversible waves can be obtained from Eq. (20) as

$$E_{1/2} = E^0 + \frac{RT}{\alpha n F} \ln \left[2.31 k^0 \sqrt{\frac{\theta_s}{D_0}} \right] \quad (21)$$

Equation (21) shows that the half wave potential for an irreversible reduction will be a function of sampling time, θ_s , i.e., drop time governs the time scale in dc polarography, whereas θ_s is the equivalent parameter in NPP.

The preceding relations show that the basis for the classification of NPP waves into reversible, quasi-reversible or irreversible applies equally to dc and NPP. However, a reversible reaction in dc polarography may be classified as quasi-reversible when examined by NPP and one which is quasi-reversible may be observed as totally irreversible with shorter time scale of NPP.

2.3 Determination of Kinetic Parameters of Simple Electrode Reactions by Normal Pulse Polarography

Various techniques of extracting kinetic parameters of simple electrode reactions by NPP have been designed by different workers [1,13,15]. J.H. Christie et al. [13] have used the current-potential equation of Barker and Gardner [12] to devise a method for evaluating kinetic parameters of quasi-reversible electrode reaction. Using the same current-potential relation of Barker and Gardner, Oldham and Parry [15] have also developed a method for evaluating kinetic parameters of totally irreversible electrode reduction. These two procedures can also be obtained from the general current potential equation of Matsuda [2] (Equation (11)). Recently P. Merican et al. [1] have designed a graphical procedure using computer plots obtained by systematic variation of kinetic parameters introduced in the equation of Matsuda (Equation (11)). A relatively

simple technique of extracting kinetic parameters by NPP can also be deduced from the logarithmic form of Matsuda equation (Equation (19a)). In this section a theoretical discussion of these various techniques will be presented.

2.3.1 Method of J.H. Christie

Introducing Eqs. (12a) and (12e) into Eq. (11) and using the expression of λ_2 given in Eq. (18), it can be shown that

$$i_{NPP}^c = \frac{nFA C_o^o D_o^{\alpha/2} k^o}{D_R^{\alpha/2}} \left\{ \exp \left[\frac{-nF(E_2 - E_2^r)}{RT} \right] \exp \left(\lambda_2^2 \theta_s \right) \operatorname{erfc}(\lambda_2 \sqrt{t} \theta_s) \right\} \quad (22)$$

Equation (22) obtained from the general equation of Matsuda (Equation (11)) is the current potential relation for NPP originally developed by Barker and Gardner [12]. Equation (22) had been used by J.H. Christie et al. [13] to formulate the technique for determining kinetic parameters of quasi-reversible electrode reaction.

Since Eq. (11) can also be written as:

$$\frac{i_{NPP}^c}{(i_d^c)_{Cott}} \left[1 + \exp \frac{nF}{RT} (E_2 - E_2^r) \right] = \sqrt{\pi} \lambda_2 \sqrt{t} \theta_s \left[\exp(\lambda_2^2 \theta_s) \operatorname{erfc}(\lambda_2 \sqrt{t} \theta_s) \right] \quad (23)$$

equation (23) indicates that the value of $\lambda_2 v\theta_s$ corresponding to any value of i/i_d of the experimental NPP polarogram may be determined from the theoretical plot of $\sqrt{\pi} \lambda_2 v\theta_s \exp(\lambda_2^2 \theta_s) \operatorname{erfc}(\lambda_2 v\theta_s)$ vs $\lambda_2 v\theta_s$.

From the value of $\lambda_2 v\theta_s$, a new parameter $k v\theta_s$ defined by

$$k v\theta_s = \lambda_2 v\theta_s \left[1 + \exp\left(\frac{nF(E_2 - E_{1/2}^r)}{RT}\right) \right]^{-1} \quad (24)$$

will be determined.

Using Eqs. (18) and (13b), Eq. (24) can be rewritten as:

$$k v\theta_s = \frac{k^0 v\theta_s}{D_R^{\alpha/2} \cdot D_0^{(1-\alpha)/2}} \exp\left[\frac{-\alpha nF(E_2 - E_{1/2}^r)}{RT}\right] \quad (25)$$

Equation (25) shows that a plot of $\log k$ vs E_2 should be linear with a slope $-(\alpha nF/2.303RT)$. The plot of $\log k$ vs E_2 thus gives α from its slope. At $E_{1/2}^r$ Eq. (25) will be reduced to

$$\log k = \log k^0 - (\alpha/2) \log D_R - \frac{(1-\alpha)}{2} \log D_0 \quad (26)$$

Using the value of $\log k$ at $E_{1/2}^r$, Eq. (26) gives k^0 if D_0 , D_R , and α values are available.

2.3.2 The Logarithmic Matsuda Equation

A convenient technique of determining the sets of

kinetic parameters (k^0 and α) can also be derived from the logarithmic form of Matsuda's equation [2] (Equation (19a)). Equation (19a) can be rewritten as

$$\overline{\ln k_2} = \ln a + \ln b \quad (27a)$$

$$\text{where } a = \frac{\sqrt{3}VD_0}{4V\theta_s} \quad \text{and } b = x \left[\frac{1.75+x^2(1+\exp(\xi_2))^2}{1-x(1+\exp(\xi_2))} \right]^{1/2} \quad (27b)$$

This relation can be derived from Eq. (19a) by taking into account the relations given by Eqs. (5a), (12d), and (13b).

Considering the expression of $\overline{k_2}$ at $E_{1/2}$ and $E_{3/4}$

$$\overline{k_{E_{1/2}}} = k^0 \exp \left[\frac{-\alpha nF(E_{1/2} - E^0)}{RT} \right] \quad (28a)$$

$$\overline{k_{E_{3/4}}} = k^0 \exp \left[\frac{-\alpha nF(E_{3/4} - E^0)}{RT} \right] \quad (28b)$$

Eq. (27a) can be written either as

$$\log k^0 = \log a + \log b + \frac{\alpha nF}{2.303RT} (E_{1/2} - E^0) \quad (29a)$$

$$\text{with } x = 0.5 \text{ and } \xi_2 = nF/RT (E_{1/2} - E_{1/2}^R) \quad (29b)$$

or

$$\log k^0 = \log a + \log b + \frac{\alpha nF}{2.303RT} (E_{3/4} - E^0) \quad (30a)$$

$$\text{with } x = 0.75 \text{ and } \xi_2 = nF/RT (E_{3/4} - E_{1/2}^r) \quad (30b)$$

It is possible to obtain simultaneous equations from Eqs. (29a) and (30a) if the experimental $E_{1/2}$ and $E_{3/4}$ values of NPP polarogram are available. The solution of the simultaneous equation yields the set of kinetic parameters (k^0 and α).

For a totally irreversible electrode-reduction an expression which enable one to compute α from the wave width ($E_{3/4} - E_{1/4}$) of NPP polarogram can be deduced. Taking $\ln \bar{k}_2$ at $E_{1/4}$ and using Eq. (27a), it is possible to have the following relation:

$$\begin{aligned} (E_{3/4} - E_{1/4}) = & - \frac{RT}{\alpha nF} \ln \left[\frac{4V\theta_s}{\sqrt{3D_0}} \right] - \frac{RT}{\alpha nF} \ln k^0 + \\ & \frac{RT}{\alpha nF} \ln x \left[\frac{1.75 + x^2(1 + \exp(\xi_2))^2}{1 - x(1 + \exp(\xi_2))} \right]^{1/2} + \\ & (E_{3/4} - E^0) \end{aligned} \quad (31a)$$

with

$$x = 0.25 \text{ and } \xi_2 = \frac{nF}{RT} (E_{1/4} - E_{1/2}^r) \quad (31b)$$

For totally irreversible electrode reduction k^0 can be written as

$$k^0 = \frac{\sqrt{D_0} \lambda_2}{\exp \left[\frac{-\alpha nF}{RT} (E_2 - E^0) \right]} \quad (32)$$

Equation (32) can be obtained from Eq. (12b) by discarding the second term, assuming the effect the backward (oxidation) process to be negligible and taking into account Eq. (5a). Since for an irreversible system $\exp(\xi_2)$ can be neglected compared with unity Eq. (17) will also be reduced to

$$\lambda_2 v \theta_s = \sqrt{3/4} \left[x \left(\frac{1.75 + x^2}{1 - x} \right)^{\sqrt{2}} \right] \quad (33)$$

Using Eqs. (32) and (33) and performing some rearrangements, Eq. (31a) will be reduced to the form

$$E_{3/4} - E_{1/4} = \frac{RT}{\alpha n F} \ln \left[\frac{x' \left(\frac{1.75 + x'^2}{1 - x'} \right)^{\sqrt{2}}}{x'' \left(\frac{1.75 + x''^2}{1 - x''} \right)^{\sqrt{2}}} \right] \quad (34)$$

with $x' = 0.25$ and $x'' = 0.75$. Eq. (34) is the same as

$$E_{3/4} - E_{1/4} = \frac{RT}{2\alpha n F} \ln 0.029 \quad (35)$$

Eq. (35) indicates that the wave width of NPP polarogram to be independent of the rate constant for a totally irreversible electrode reduction as proposed by P. Mericam et al. [1]. The experimental wave width of NPP polarogram of totally irreversible electrode reduction furnishes the α value using Eq. (35).

For totally irreversible electrode reactions the

term $\exp(\xi_2)$ in b of equation (27a) can be neglected compared with unity. Equations (29a) and (30a) derived from Eq. (27a) can thus further be reduced to:

$$\log k^0 = \log a + \log \left\{ x \left[\frac{1.75 + x^2}{1 - x} \right]^{1/2} \right\} + \frac{\alpha n F}{2.303 RT} (E_{1/2} - E^0) \quad (36a)$$

$$\log k^0 = \log a + \log \left\{ x \left[\frac{1.75 + x^2}{1 - x} \right]^{1/2} \right\} + \frac{\alpha n F}{2.303 RT} (E_{3/4} - E^0) \quad (36b)$$

Since x in Eqs. (36a) and (36b) is 0.5 and 0.75 respectively (see equations (29b) and (30b), Eqs. (36a) and (36b) will be simplified to:

$$\log k^0 = \log a + \frac{\alpha n F}{2.303 RT} (E_{1/2} - E^0) \quad (37a)$$

$$\log k^0 = \log a + 0.358 + \frac{\alpha n F}{2.303 RT} (E_{3/4} - E^0) \quad (37b)$$

The solution of the simultaneous equations from equations (37a) and (37b) furnishes the values of k^0 and α . Equation (37a) and (37b) also indicate the kinetic parameters of irreversible system can be determined using E^0 values without any knowledge of $E_{1/2}^r$.

2.3.3 Method of Oldham and Parry

Oldham and Parry [15] had developed Eq. (20) of irreversible waves independently of Matsuda's equation using the current potential relation of Barker and Gardner [12] (Eq. (22)).

Equation (20) can be rewritten in the form

$$\frac{2.303RT}{2\alpha nF} \log \left[\frac{x^2(1.75+x^2)}{(1-x)} \right] = E_{V/2} - E_2 \quad (38)$$

Equation (38) indicates that a plot of $\log \left[\frac{x^2(1.75+x^2)}{1-x} \right]$ vs $(-E)$ of the experimental NPP polarogram gives a straight line with a slope of $(2\alpha nF)/2.303RT$ enabling one to evaluate α . The intercept of the plot is $E_{V/2}$ and yields k^0 on application of Eq. (21).

2.3.4 Method of P. Mericam

P. Mericam et al. [1] have developed systematic method of evaluating kinetic parameters of simple electrode reaction using parameters of easy experimental access, namely, the half wave potential $E_{V/2}$ and wave width $(E_{3/4} - E_{V/4})$ of NPP polarogram. Their method has been developed by systematic calculation of $(E_{V/2} - E^0)$ and $(E_{3/4} - E_{V/4})$ from the set of kinetic parameters introduced into the general current-potential equation of Matsuda (Equation (11)). The calculations were performed with a computer using a programme shown in Appendix I.

The obtained dependence of $(E^0 - E_{1/2})$ and $(E_{3/4} - E_{1/4})$ on $\log k^0$ for different values of α is shown in Figs. 2a and 2b.

In the reversible situation ($\log k^0 > -0.5$) no information can be obtained on the actual values of k^0 and α . In totally irreversible region ($\log k^0 < -2.5$) the situation is rather simple. The experimental wave width $(E_{3/4} - E_{1/4})$, furnishes the α -value, since the width $(E_{3/4} - E_{1/4})$ is determined by α only as shown in Fig. 2b. It has been reported [1] that expression of Eq. (35) for the wave width holds true. The experimental shift of $E_{1/2}$ vs the standard potential gives $\log k^0$ corresponding to the evaluated α value using Fig. 2a where half wave potential is linearly dependent on $\log k^0$.

In the quasi-reversible domain of the electrode-reactions there is no such simple relationship in evaluating kinetic parameters as that of totally irreversible electrode reactions. The experimental characteristics of the NPP polarogram depend both on the standard rate constant and the transfer coefficient. Thus the quantitative evaluation of the kinetic parameters using the simple procedure of totally irreversible electrode reactions is not possible. A graphical procedure has thus been elaborated. The pairs of values (k^0, α) corresponding to fixed $(E^0 - E_{1/2})$ or/and $(E_{3/4} - E_{1/4})$ values can be evaluated from Figs. 2a and 2b, and plotted in a $\log k^0$ vs α

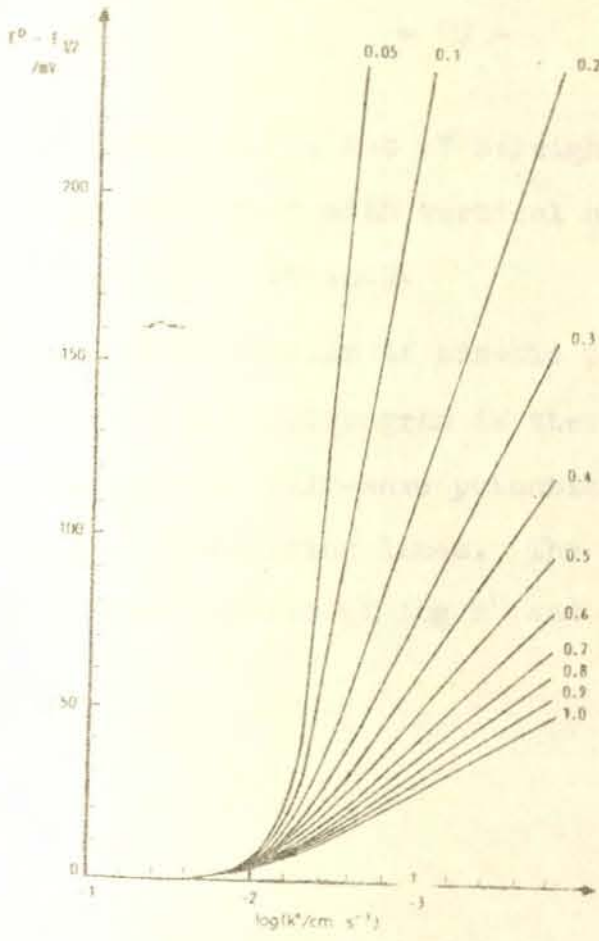


Fig. 2a. $E^0 - E_{1/2}$ dependence on $\log k^0$ at various α values [1]

$E_{3/4} - E_{1/4}$
/mV

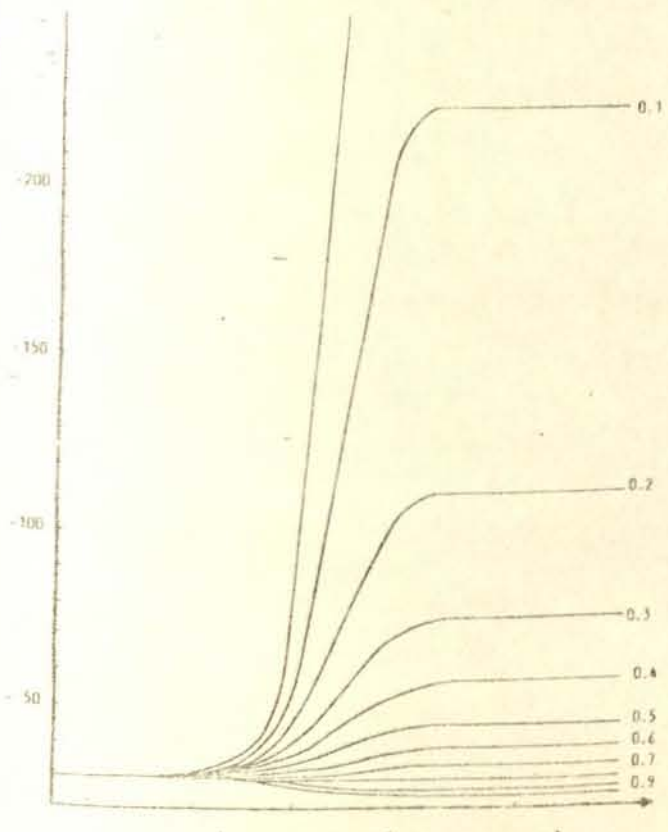


Fig. 2b $E_{3/4} - E_{1/4}$ dependence on $\log k^0$ at various α values [1]

diagram (Fig. 3). A set of straight lines for the first, and a set of curves with vertical asymptotes for the second had been obtained.

The determination of kinetic parameters from the experimental NPP polarogram is then straight forward: the shift of the half-wave potential and the wave-width belong to two-crossing lines. The intersection coordinates define the set of $\log k^0$ and α values (Fig. 3)

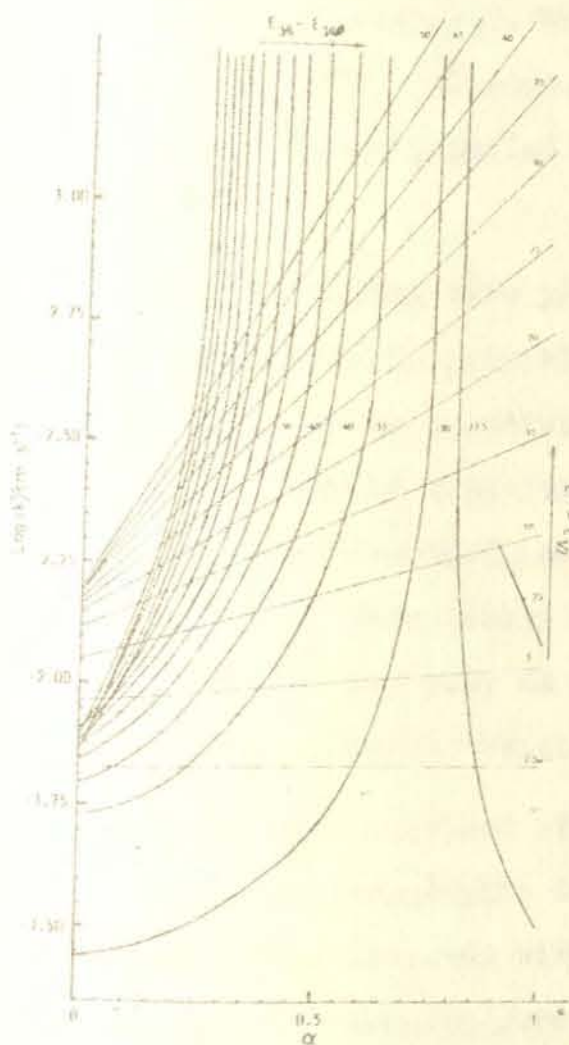


Fig. 3. $\log k^0$ vs α diagram at constant $(E^0 - E_{1/2})$ and constant $(E_{3/4} - E_{1/4})$ [1]

3. EXPERIMENTAL

The chemicals used were $Zn(NO_3)_2$ (Riedel de Haen), $NaNO_3$ (Analar, BDH), $Ni(NO_3)_2$ (Riedel de Haen), KNO_3 (Analar, Hopkin and Williams), $Cr(NO_3)_3$ (BDH), $HClO_4$ (BDH) and $NaClO_4$ (BDH). Polarographic experiments were performed using mercury purified according to procedure in reference 26.

The $Zn(II)$ solutions were prepared from a stock solution standardized by EDTA titration with Erichrome Black T indicator [27]. Stock solution of $Cr(III)$ ($10^{-2}M$ $Cr(III)$) was prepared by dissolving $Cr(NO_3)_3$ in a ten times more concentrated $HClO_4$ solution [20]. All solutions were prepared using doubly distilled water. All polarograms were run for 0.19 mM $Zn(II)$, 0.20 mM $Ni(II)$, and 0.2 mM $Cr(III)$ concentrations.

Polarograms were obtained with a Metrohm polarecord E506, and the NPP polarographic technique with a drop-time of 1 second was achieved with a Metrohm polarographic stand E505. All measurements were taken at a scan rate of 0.5 nV per second. The experiments were carried out under thermostatic condition at $25 \pm 5^\circ C$ using a water-jacketed polarographic cell. All solutions were flushed with pure grade helium for 10 minutes and then blanketed with an atmosphere of helium while recording the polarograms. For $Zn(II)$ and $Ni(II)$, potential measurements were taken against the $Ag/AgCl$, KCl (satd.) reference electrode. The reference

electrode compartment of the Cr(III) system contained supporting electrolyte and the reference electrode was Ag/AgCl immersed in saturated NaCl instead of KCl to prevent the precipitation of $KClO_4$. NPP polarograms were obtained at a base potential of -0.8V for Zn(II) and -0.6V for both Ni(II) and Cr(III) systems. The potential values used were extrapolated from the recorded polarograms and have an error of $\pm .002$ V.

In the NPP technique the pulses were generated in the last 200 ms of each droplife using the Metrohm polarograph E506 and the current was measured for 20 ms at the end of each pulse duration. For the determination of θ_s Matsuda [2] has developed the following relation:

$$\theta_s = \theta_1 + \Delta\theta/2 \quad (39)$$

where θ_1 : the time at which the current measurement is started.

$\Delta\theta$: the time duration in which the current is measured.

Equation (39) is applicable when θ_1 is larger than $3/2 (\Delta\theta)$. For our experimental condition where θ_1 , 180 ms, is greater than $3/2 (\Delta\theta)$, 30 ms, evaluation of θ_s using equation (39) is a justified approach. The experimental θ_s was thus computed to be 190 ms.

4. RESULTS AND DISCUSSION

4.1 Zn(II)-NaNO₃ System

Zn(II) was studied in 0.49M, 1.05M, and 2.45M NaNO₃ as supporting electrolyte. The set of kinetic parameters were determined using the techniques of J.H. Christie, P. Merican and the logarithmic Matsuda equations. The diffusion coefficient values used in all the three methods were infinitely dilute values and were $D_0 = D_R = 7.2 \times 10^{-6} \text{ cm}^2 \text{ s}^{-1}$ [25]. The equations of the various techniques employed in the analysis of the different systems are compiled in Table 1.

4.1.1 Determination of Kinetic Parameters

4.1.1.1 Method of J.H. Christie

The value of $E_{\sqrt{2}}^R$ used in this technique was determined by means of the extrapolation method [13,14,28-30]. Normal dc polarograms taken with a droptime of about 6 s were used to plot $\log\left(\frac{i}{i_d - i}\right)$ vs E. Values of $E_{\sqrt{2}}^R$ were obtained as the potentials at which the straight line tangent to the $\log\left(\frac{i}{i_d - i}\right)$ vs E plot at the most anodic potential intersect the $\log\left(\frac{i}{i_d - i}\right) = 0$ axis.

See Fig. 4 for the determination of $E_{\sqrt{2}}^R$ for Zn(II)- 0.49M NaNO₃ system. The values of $E_{\sqrt{2}}^R$ for the three systems are indicated in

Table 1. Equations used for the analysis of the
Zn(II)-NaNO₃ Systems

Method of analysis	Equations used	Equation number	Comment
J.H.Christie	$\frac{i_{NPP}^c}{i_a} \left[1 + \exp \frac{nF}{RT} (E_2 - E_{\sqrt{2}}^r) \right] = \sqrt{\pi} \lambda_2 \nu \theta_s \left[\exp(\lambda_2^2 \theta_s) \operatorname{erfc}(\lambda_2 \nu \theta_s) \right]$	23	Used for the determination of $\lambda_2 \nu \theta_s$
	$k \nu \theta_s = \lambda_2 \nu \theta_s \left[1 + \exp \left(\frac{nF(E_2 - E_{\sqrt{2}}^r)}{RT} \right) \right]^{-1}$	24	Used for the determination of k
	$k \nu \theta_s = \frac{k^0 \nu \theta_s}{D_R^{\alpha/2} \cdot D_o^{(1-\alpha)/2}} \exp \left[\frac{-\alpha nF(E_2 - E_{\sqrt{2}}^r)}{RT} \right]$	25	Used for determination of α (log k vs E_2)
	$\log k = \log k^0 - (\alpha/2) \log D_R - \frac{(1-\alpha)}{2} \log D_o$	26	Used for the determination of $\log k^0$
Logarithmic natsuda Equation	$\log k^0 = \log a + \log b + \frac{\alpha nF}{2.303RT} (E_{\sqrt{2}} - E^0)$	29a	
	$\log k^0 = \log a + \log b + \frac{\alpha nF}{2.303RT} (E_{3/4} - E^0)$	30a	

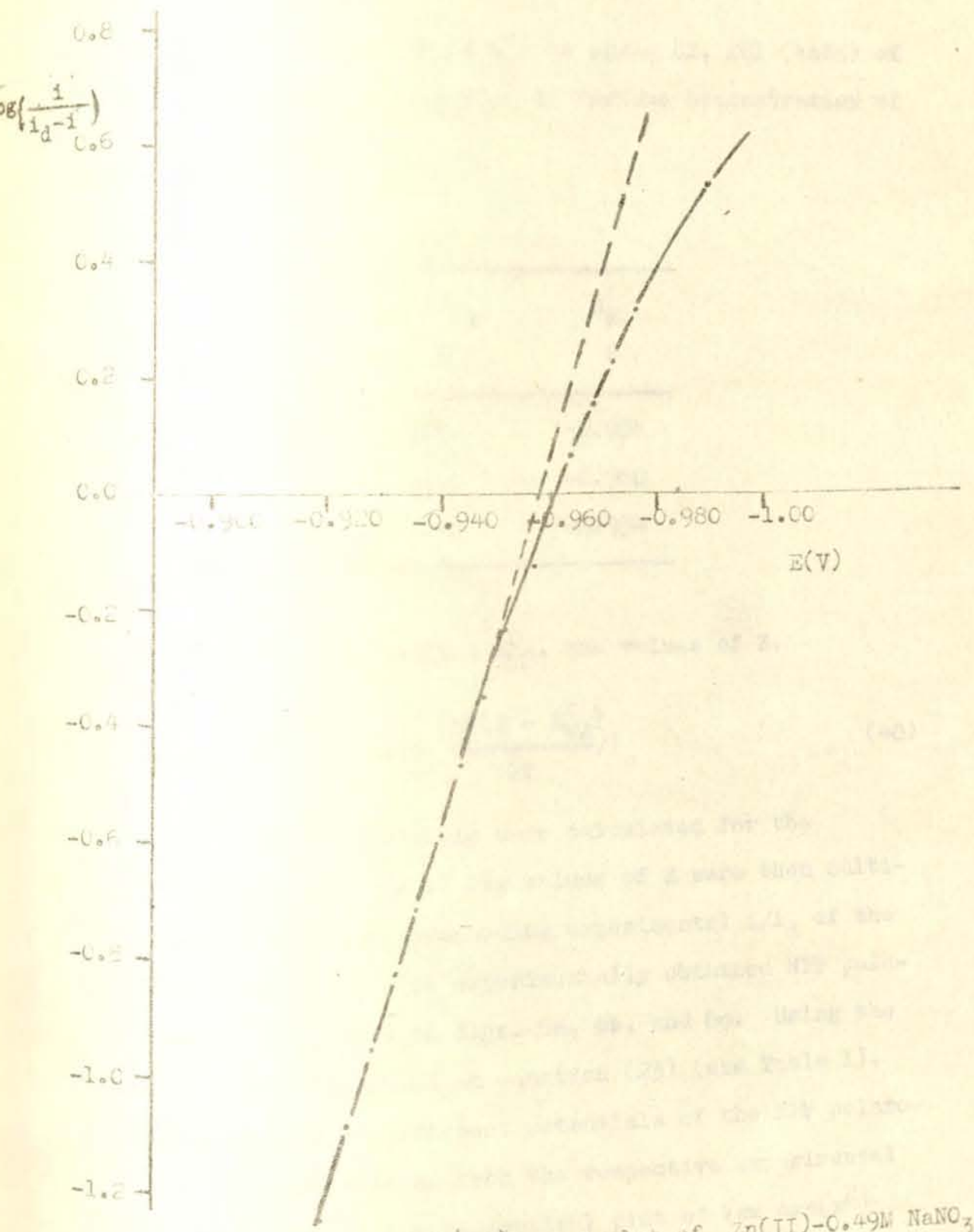


Fig. 2. $\log\left(\frac{i}{i_d - i}\right)$ vs E plot of Zn(II)-0.49M NaNO₃ system

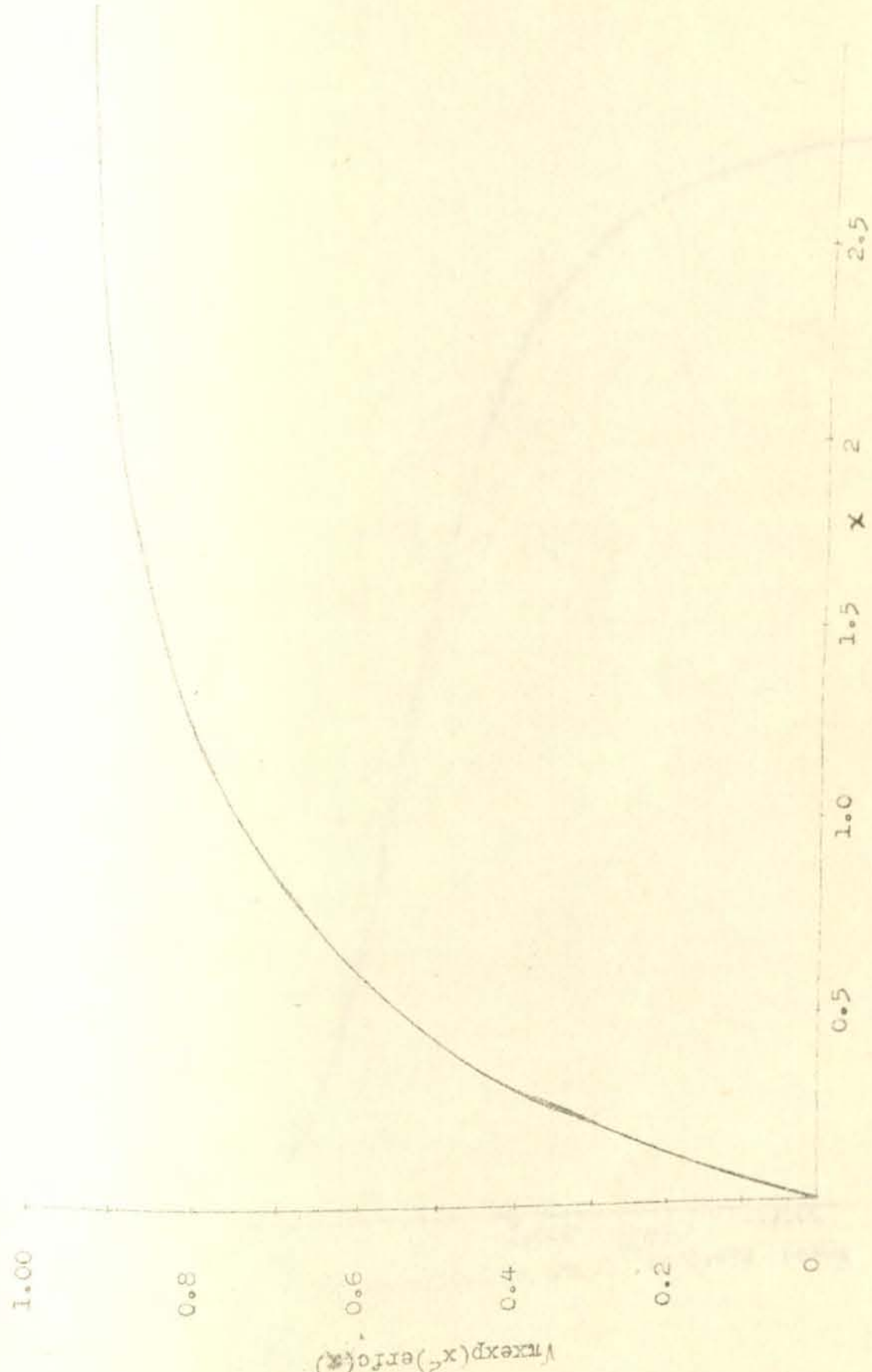
Table 2. The values of $E_{V/2}^R$ vs Ag/Ag Cl, KCl (satd) of Zn(II) Reduction in Various Concentration of NaNO_3

NaNO_3 M	$E_{V/2}^R$ V
0.49	-0.958
1.05	-0.960
2.45	-0.954

Using this experimental $E_{V/2}^R$, the values of Z,

$$Z = \left[1 + \exp\left(\frac{nF(E - E_{V/2}^R)}{RT}\right) \right] \quad (40)$$

at different potentials were calculated for the evaluation of $\lambda_2 \nu \theta_s$. The values of Z were then multiplied with the corresponding experimental i/i_d of the NPP polarogram. The experimentally obtained NPP polarograms are shown in Figs. 6a, 6b, and 6c. Using the relation established in equation (23) (see Table 1), $\lambda_2 \nu \theta_s$ values at different potentials of the NPP polarogram were determined from the respective experimental $Z \left(\frac{i}{i_d}\right)$ terms and the theoretical plot of $\sqrt{\max \exp(x^2) \operatorname{erfc}(x)}$ versus x shown in Fig. 5. The values of $\exp(x^2)$ and $\operatorname{erfc}(x)$ versus x were obtained from the



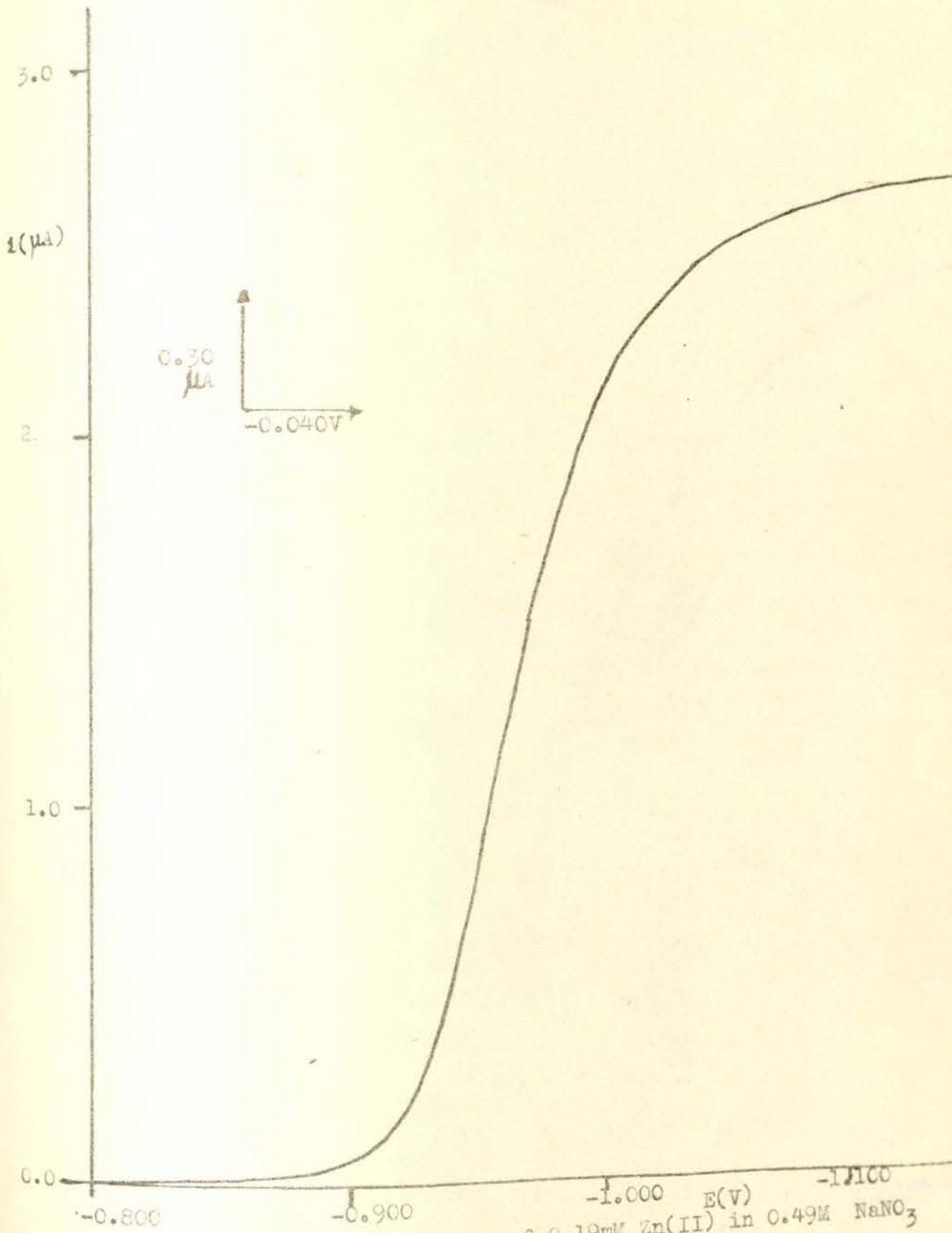


Fig. 6a NPP polarogram of 0.19mM Zn(II) in 0.49M NaNO_3

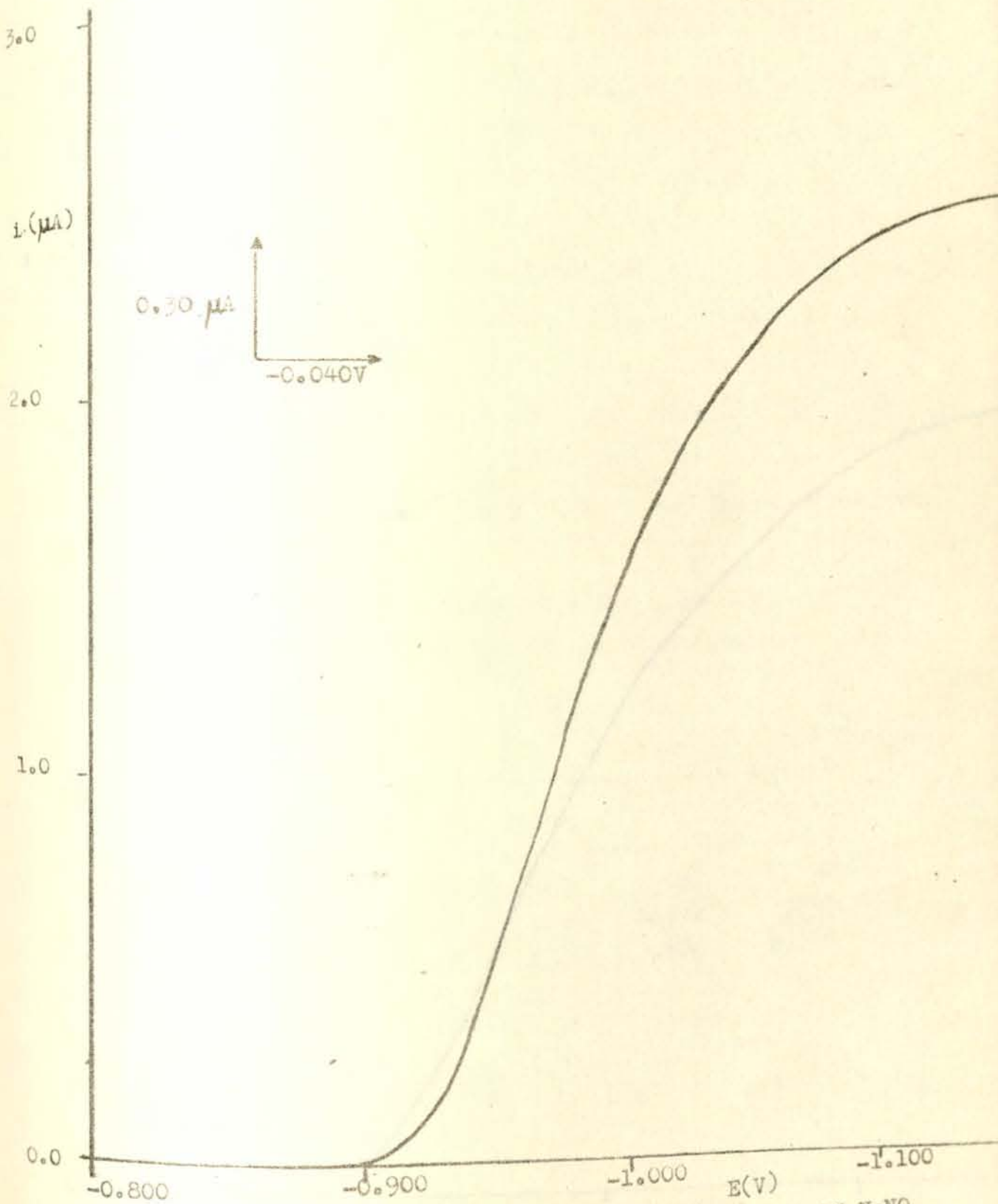


Fig. 6b NPP polarogram of 0.19 mM Zn(II) in 1.05 M NaNO_3

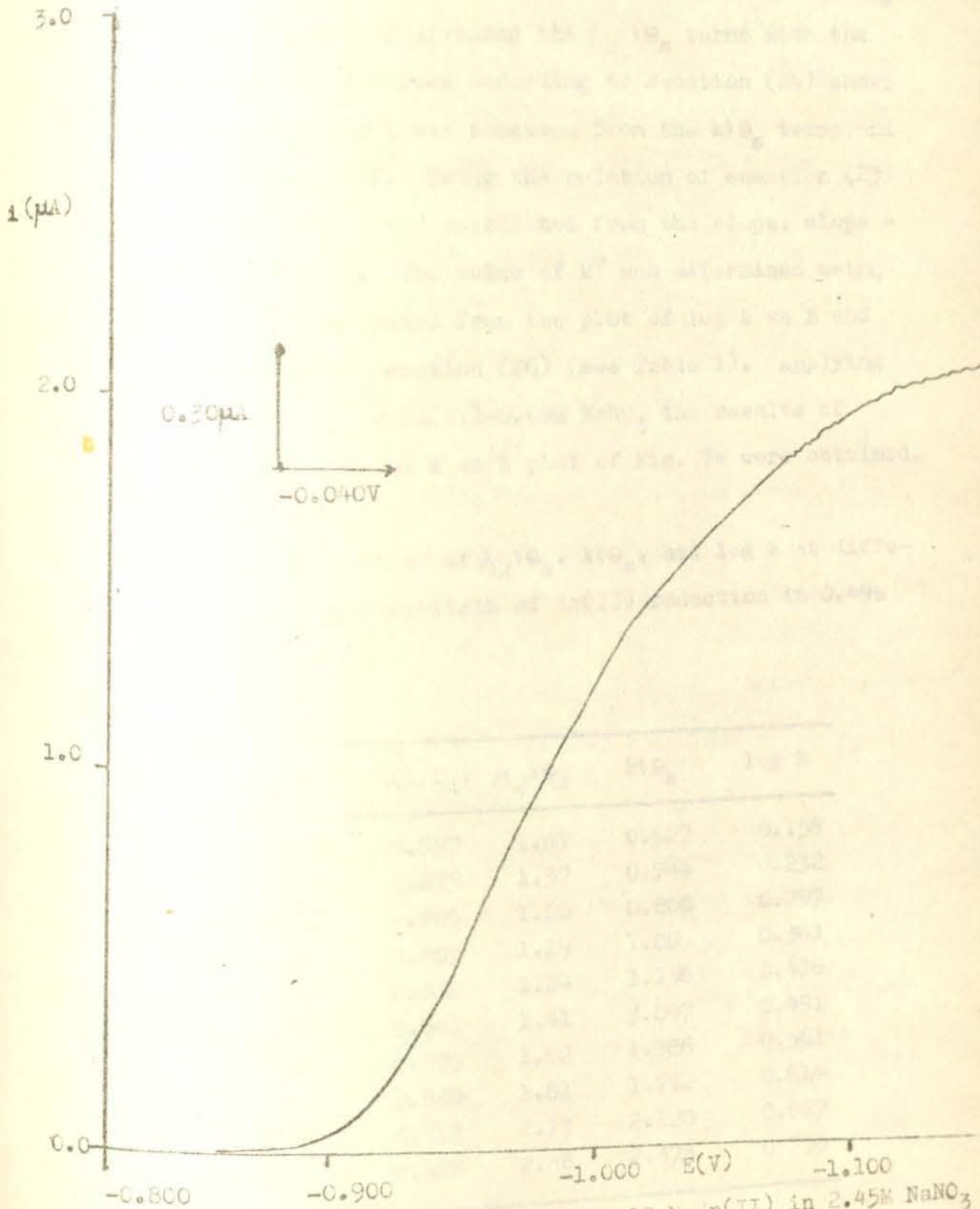


Fig. 6c. NPP polarogram of 0.19mM Zn(II) in 2.45M NaNO₃

literature [31].

To evaluate the kinetic parameters, values of $kV\theta_s$ were calculated by dividing the $\lambda_2 V\theta_s$ terms with the corresponding Z values according to equation (24) shown in Table 1. Log k was computed from the $kV\theta_s$ terms and plotted against E. Using the relation of equation (25) (see Table 1), α was calculated from the slope, slope = $(-\alpha nF)/2.303RT$. The value of k^0 was determined using log k at $E_{1/2}^R$ obtained from the plot of log k vs E and the relation of equation (26) (see Table 1). Applying this procedure to Zn(II)-0.49M NaNO₃ the results of Table 3 and the log k vs E plot of Fig. 7a were obtained.

Table 3. The values of $\lambda_2 V\theta_s$, $kV\theta_s$, and log k at different Potentials of Zn(II) reduction in 0.49M NaNO₃

E(V)	Z	Z(i/i _d)	$\lambda_2 V\theta_s$	$kV\theta_s$	log k
-0.950	2.67	0.877	1.67	0.627	0.158
-0.960	1.84	0.835	1.37	0.744	0.232
-0.970	1.39	0.805	1.20	0.800	0.297
-0.980	1.19	0.805	1.19	1.00	0.361
-0.990	1.09	0.812	1.24	1.136	0.416
-1.000	1.04	0.842	1.41	3.097	0.491
-1.010	1.02	0.870	1.62	1.586	0.561
-1.020	1.01	0.889	1.81	1.792	0.614
-1.030	1.00	0.914	2.13	2.120	0.687
-1.040	1.00	0.928	2.38	2.373	0.736

The values of $\lambda_2 v \theta_s$ versus E of Table 3 for Zn(II)-0.49M NaNO₃ system indicate an initial decrease of $\lambda_2 v \theta_s$ in the lower negative potentials region at increasing negative values of E. But after reaching a minima, $\lambda_2 v \theta_s$ values increase with an increase of -E in the higher negative potentials region. This trend of $\lambda_2 v \theta_s$ is the same as that of J.H. Christie et al. [13] at sampling times of 20 ms and 40 ns. The value of log k on the other hand shows a linear dependence on E as shown in Fig. 7a. This dependence of log k on E is in agreement with the theoretical prediction of equation (25). From the plot of log k vs E, k^0 (cm s⁻¹) and α were calculated to be 4.34×10^{-3} and 0.21 respectively.

The data for systems of Zn(II)-1.05 M NaNO₃ and Zn(II)-2.45 M NaNO₃ are given in Table 4 and 5 from which the log k vs α plots of 7b and 7c were obtained. The pairs: (k^0 , α) for Zn(II)-1.05 M NaNO₃ and Zn(II)-2.45 M NaNO₃ were determined to be (2.19×10^{-3} cm s⁻¹, 0.21) and (1.89×10^{-3} cm s⁻¹, 0.22) respectively.

Results of Table 4 of the Zn(II)-1.05 M NaNO₃ system shows that the trend of $\lambda_2 v \theta_s$ with respect to E is the same as that of Zn(II)-0.49 M NaNO₃ system. The linear dependence of log k on E is also shown in Fig. 7b. Unlike the Zn(II)-0.49 M NaNO₃ system, log k has now negative values in the lower negative potential regions which indeed is the source of variation in the evaluated values of the rate constant. The values in Table 5 also

show that $\lambda_2 v \theta_s$ and $\log k$ vs E (Fig. 7c) have the same trend.

Table 4. The Values of $\lambda_2 v \theta_s$, and $\log k$ at different potentials of Zn(II) Reduction in 1.05 M NaNO_3

$E(V)$	Z	$Z(\frac{i}{i_d})$	$\lambda_2 v \theta_s$	$k v \theta_s$	Log k
-0.960	2.08	0.680	0.72	0.345	-0.101
-0.964	1.78	0.642	0.67	0.376	-0.064
-0.968	1.56	0.618	0.63	0.403	-0.033
-0.972	1.41	0.604	0.60	0.427	-0.009
-0.976	1.29	0.601	0.59	0.456	0.020
-0.980	1.21	0.604	0.60	0.496	0.050
-0.984	1.15	0.609	0.61	0.529	0.085
-0.992	1.08	0.627	0.64	0.593	0.134
-1.000	1.04	0.666	0.73	0.702	0.206
-1.020	1.01	0.755	0.99	0.982	0.352
-1.060	1.00	0.823	1.30	1.298	0.470

Table 5. The Values of $\lambda_2 v \theta_s$, $k v \theta_s$, and $\log k$ at different Potentials of Zn(II) Reduction in 2.45 M NaNO_3

$E(V)$	Z	$Z(i/i_d)$	$\lambda_2 v \theta_s$	$k v \theta_s$	Log k
-0.940	4.120	0.817	1.27	0.308	-0.15
-0.950	2.380	0.662	0.72	0.302	-0.16
-0.960	1.614	0.576	0.55	0.345	-0.101
-0.970	1.272	0.555	0.51	0.397	-0.04
-0.980	1.121	0.578	0.56	0.500	0.06
-0.990	1.054	0.619	0.63	0.602	0.14
-1.000	1.024	0.663	0.73	0.712	0.21
-1.010	1.010	0.714	0.86	0.850	0.29
-1.020	1.004	0.757	1.00	0.998	0.36
-1.030	1.000	0.803	1.20	1.195	0.44
-1.040	1.000	0.842	1.41	1.615	0.57

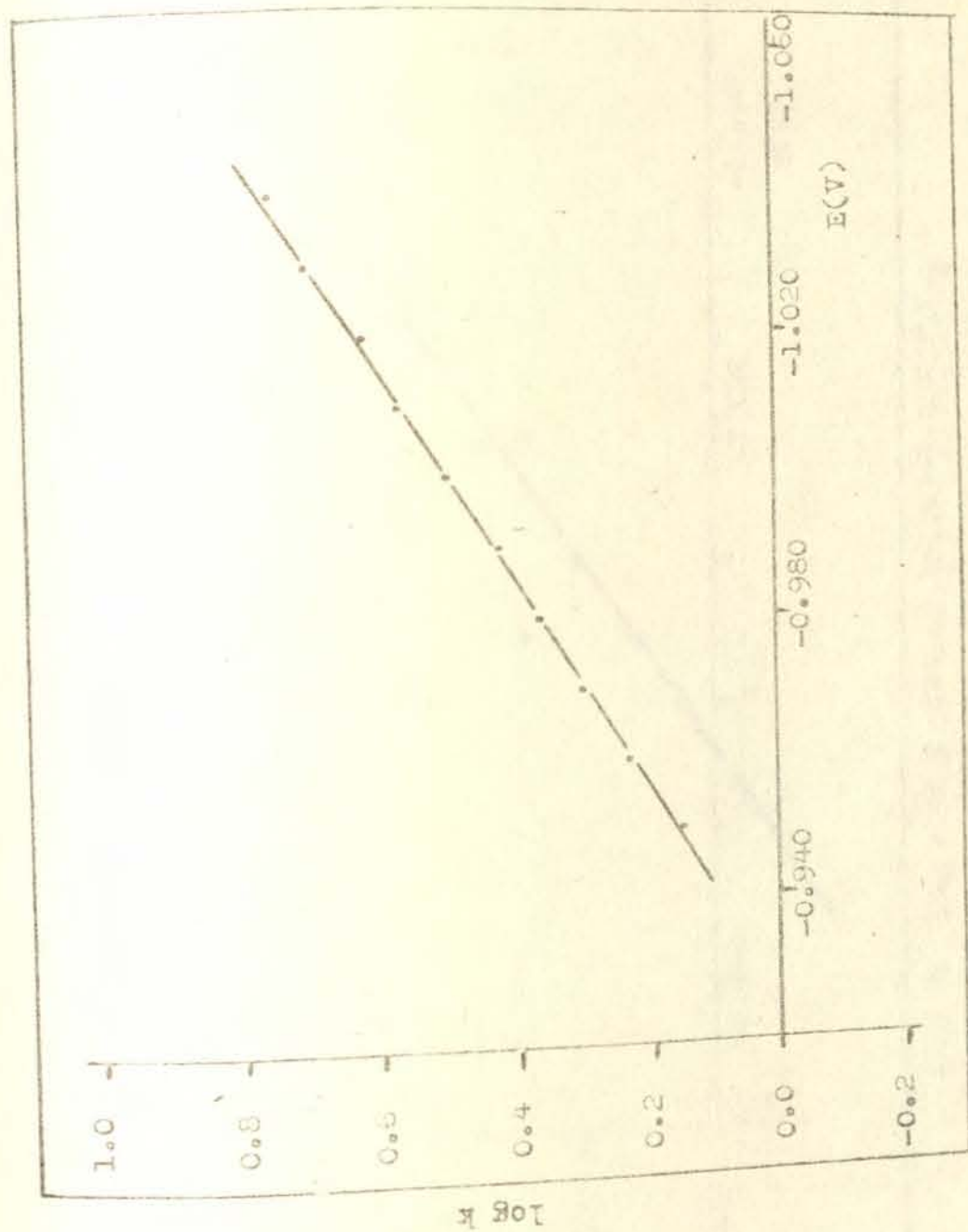


Fig. 7a $\log k$ Vs E plot of $Zn(II)$ - $0.49M$ NH_4NO_3

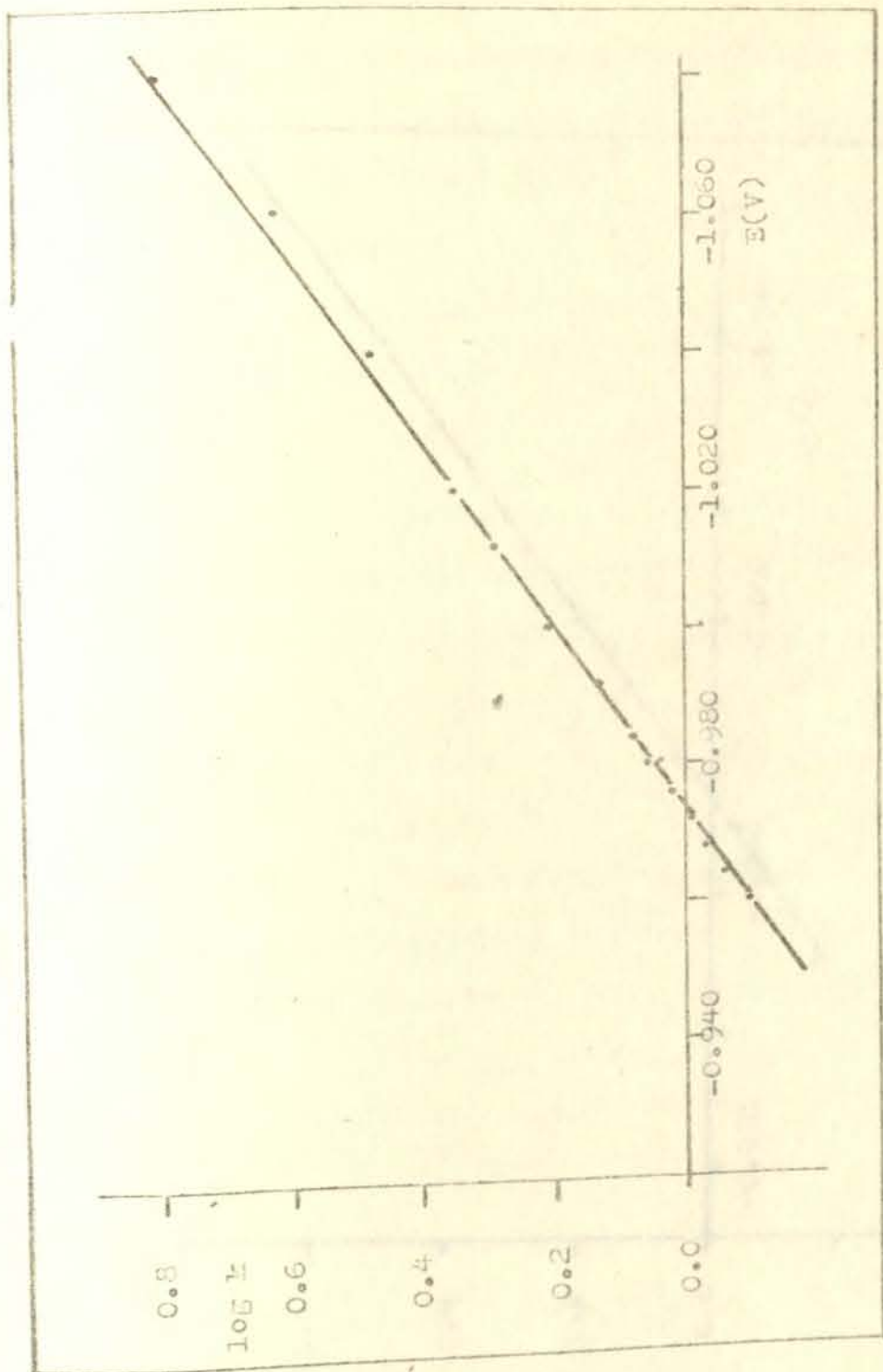


Fig. 7b $\log k$ Vs E plot of $Mn(II) \rightarrow 1.0M NaClO_3$

Repeat the procedure of P. Series of the

for values the following manner in the

values of k were used:

$$k = 0.01 - 0.02$$

$$k = 0.02 - 0.03$$

$$k = 0.03 - 0.04$$

$$k = 0.04 - 0.05$$

$$k = 0.05 - 0.06$$

$$k = 0.06 - 0.07$$

$$k = 0.07 - 0.08$$

$$k = 0.08 - 0.09$$

$$k = 0.09 - 0.10$$

$$k = 0.10 - 0.11$$

$$k = 0.11 - 0.12$$

$$k = 0.12 - 0.13$$

$$k = 0.13 - 0.14$$

$$k = 0.14 - 0.15$$

$$k = 0.15 - 0.16$$

$$k = 0.16 - 0.17$$

$$k = 0.17 - 0.18$$

$$k = 0.18 - 0.19$$

$$k = 0.19 - 0.20$$

$$k = 0.20 - 0.21$$

$$k = 0.21 - 0.22$$

$$k = 0.22 - 0.23$$

$$k = 0.23 - 0.24$$

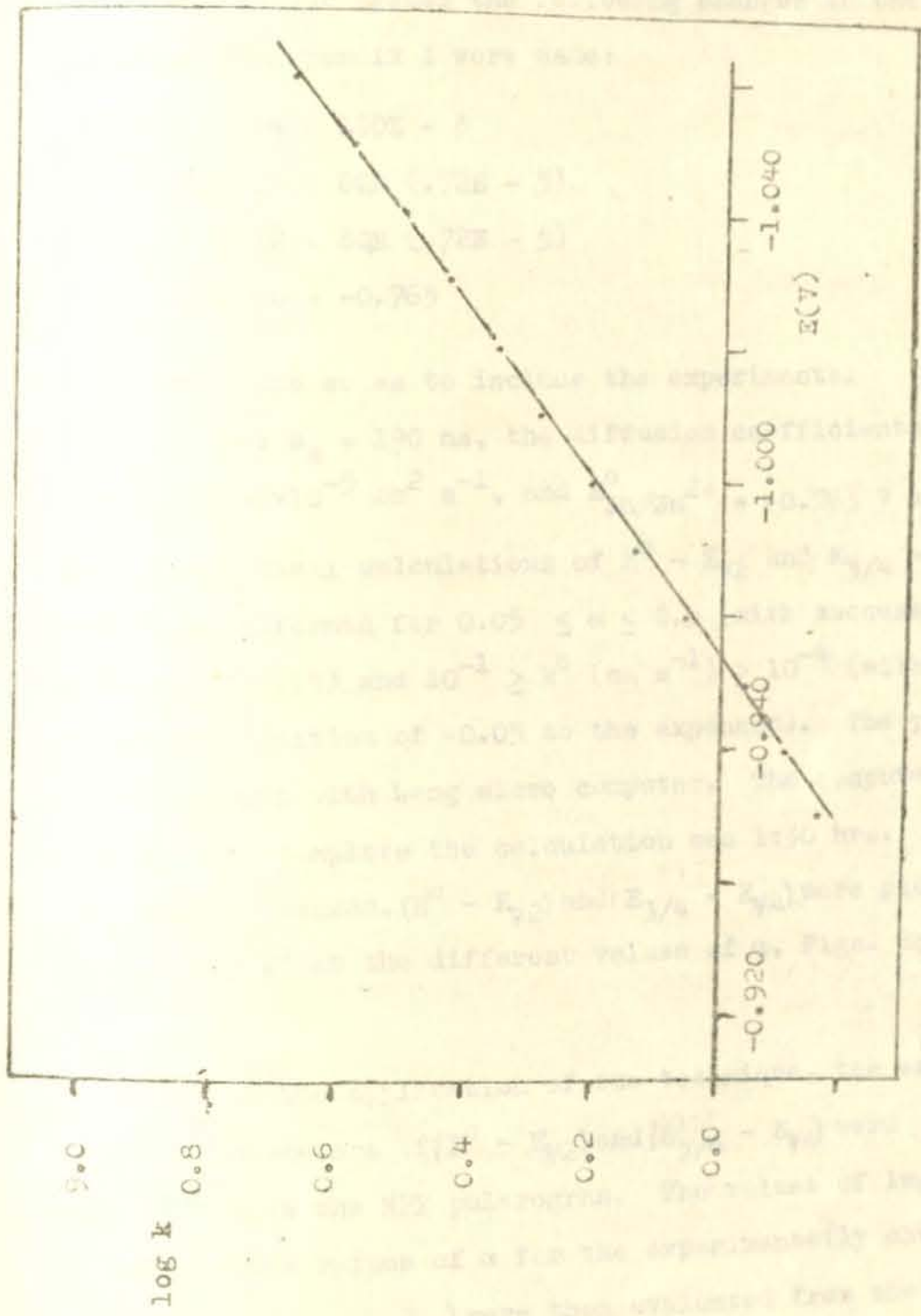


FIG. 7c $\log k$ Vs E Plot of $\Delta n(II)$ -2.45M N:NC₅

4.1.1.2 Method of P. Mericam

To adjust the procedure of P. Mericam to the conditions of our system the following changes in the programme of Appendix I were made:

80 C4 = 190E - 3
100 D1 = SQR (.72E - 5)
105 D2 = SQR (.72E - 5)
110 E0 = -0.763

These were done so as to include the experimental sampling time $\theta_s = 190$ ms, the diffusion coefficients $D_o = D_R = 0.72 \times 10^{-5}$ cm² s⁻¹, and $E_{Zn/Zn^{2+}}^o = -0.763$ V vs NHE. Theoretical calculations of $E^o - E_{1/2}$ and $E_{3/4} - E_{1/4}$ were then performed for $0.05 \leq \alpha \leq 0.5$ (with successive addition of 0.05) and $10^{-1} \geq k^o$ (cm s⁻¹) $\geq 10^{-4}$ (with successive addition of -0.05 to the exponent). The programme was run with Wang micro computer. The computer time used to complete the calculation was 1:30 hrs. From the computed values, $(E^o - E_{1/2})$ and $(E_{3/4} - E_{1/4})$ were plotted against $\log k^o$ at the different values of α , Figs. 8a and 8b.

For the application of the technique, the experimental parameters of $(E^o - E_{1/2})$ and $(E_{3/4} - E_{1/4})$ were extracted from the NPP polarogram. The values of $\log k^o$ at the various values of α for the experimentally obtained $(E^o - E_{1/2})$ and $(E_{3/4} - E_{1/4})$ were then evaluated from the respective theoretical plots of Figs. 8a and 8b. $\log k^o$

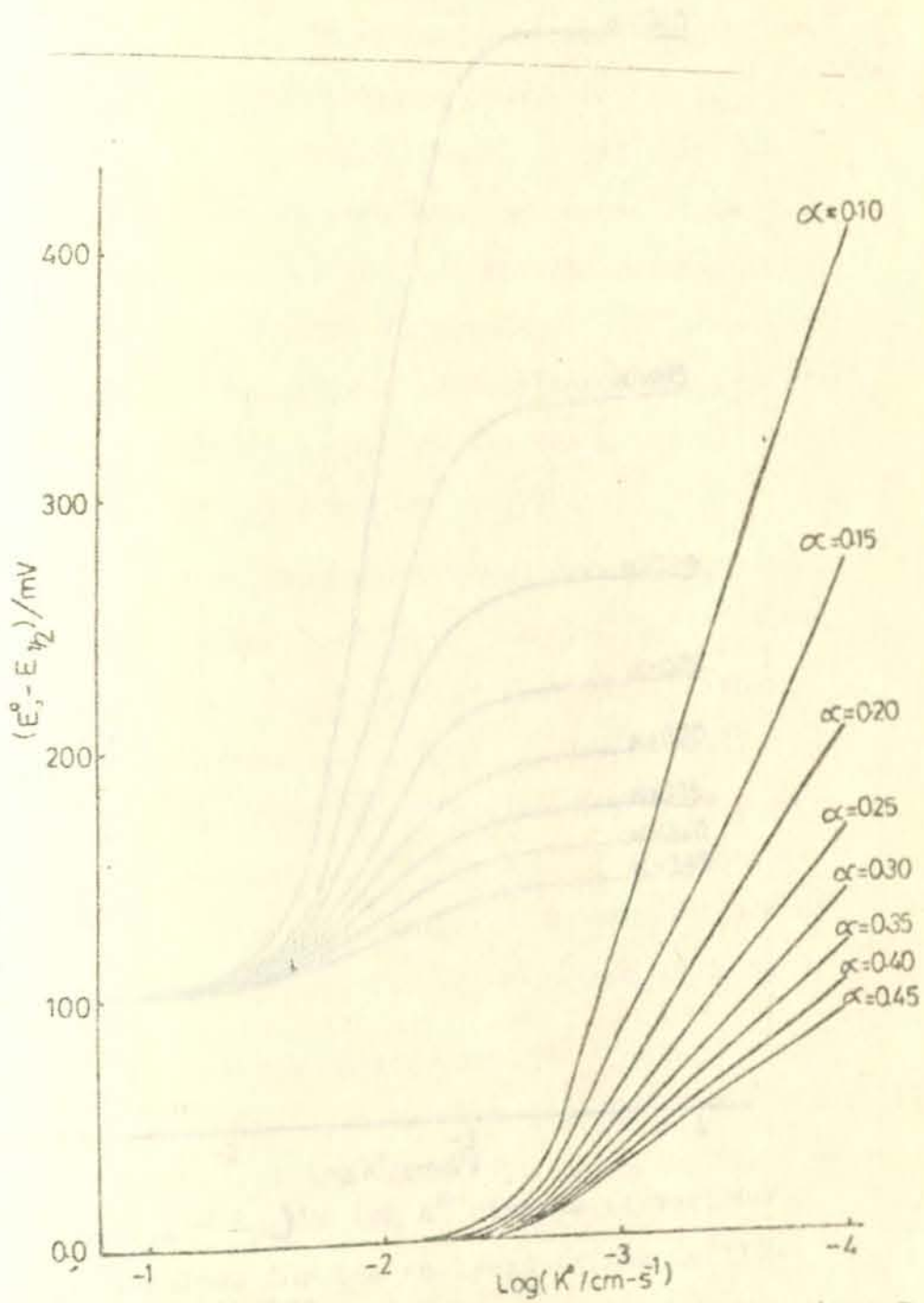


Fig. 8a $(E^0 - E_{1/2})$ Vs $\log k^0$ diagram at various α values for the analysis of the $Zn(II)-NaNO_3$ systems

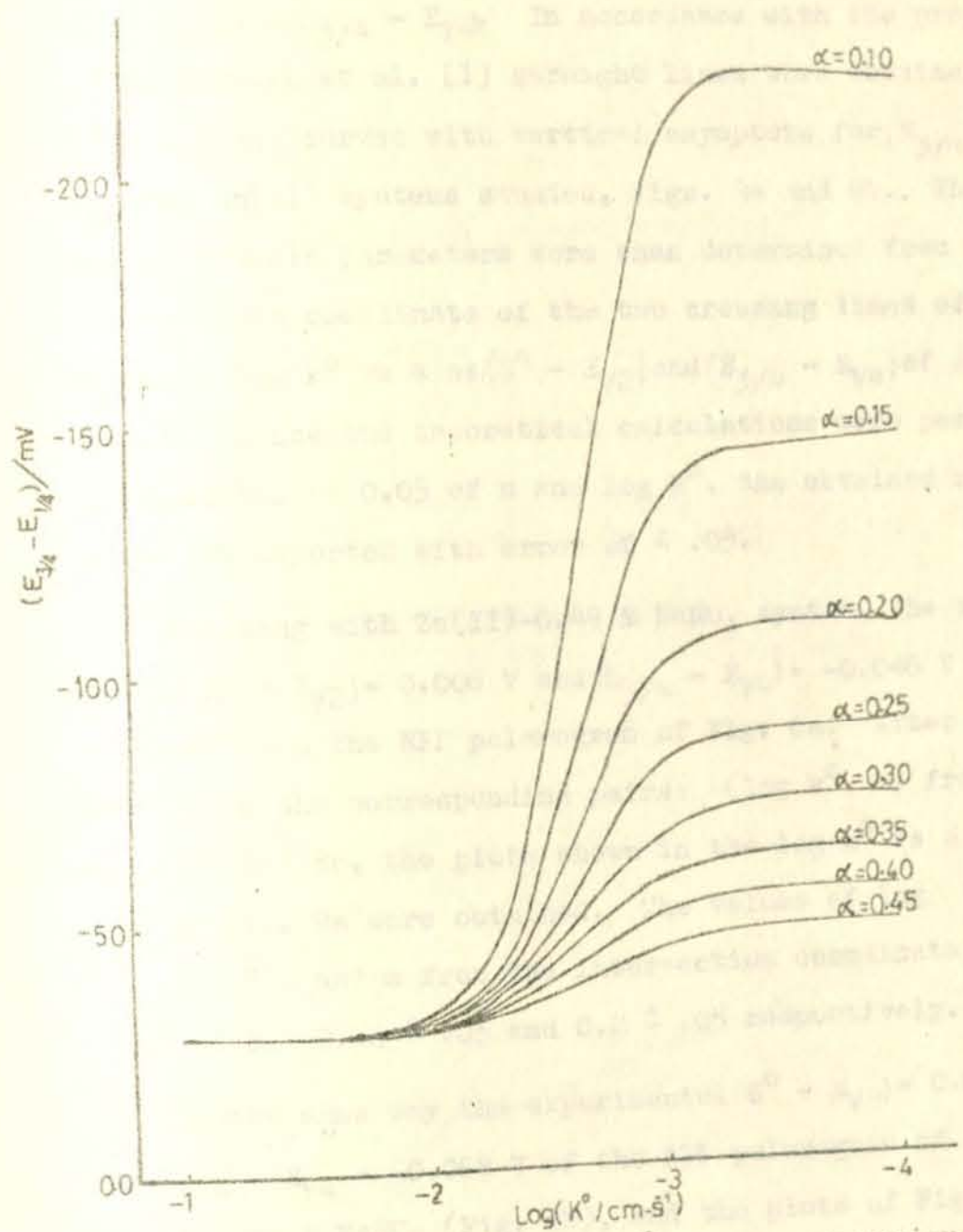


Fig. 8b $(E_{3/4} - E_{1/4})$ vs $\log k^0$ diagram at various α values for the analysis of the Zn(II)- $NaNC_3$ system

was then plotted against α for these fixed values of $(E^{\circ} - E_{1/2})$ and $(E_{3/4} - E_{1/4})$. In accordance with the proposal of P. Mericam et al. [1] straight lines were obtained for $(E^{\circ} - E_{1/2})$ and curves with vertical asymptote for $(E_{3/4} - E_{1/4})$ for Zn(II) systems studied, Figs. 9a and 9b. The set of kinetic parameters were then determined from the intersection coordinate of the two crossing lines of the plots of $\log k^{\circ}$ vs α at $(E^{\circ} - E_{1/2})$ and $(E_{3/4} - E_{1/4})$ of each system. Since the theoretical calculations were performed at intervals of 0.05 of α and $\log k^{\circ}$, the obtained results are reported with error of $\pm .05$.

Starting with Zn(II)-0.49 M NaNO_3 system, the experimental $(E^{\circ} - E_{1/2}) = 0.006$ V and $(E_{3/4} - E_{1/4}) = -0.046$ V were obtained from the NPP polarogram of Fig. 6a. After extracting the corresponding pairs: $(\log k^{\circ}, \alpha)$ from Figs. 8a and 8b, the plots shown in the $\log k^{\circ}$ vs α diagram of Fig. 9a were obtained. The values of $\log(k^{\circ}/\text{cm s}^{-1})$ and α from the intersection coordinate were found to be $-2.40 \pm .05$ and $0.2 \pm .05$ respectively.

In the same way the experimental $(E^{\circ} - E_{1/2}) = 0.018$ V and $E_{3/4} - E_{1/4} = -0.068$ V of the NPP polarogram of Zn(II)-1.05 M NaNO_3 (Fig. 6b), and the plots of Figs. 8a and 8b yield the respective plots in Fig. 9b. The values of $\log(k^{\circ}/\text{cm s}^{-1})$ and α from the plot in Fig. 9b were then evaluated to be $-2.61 \pm .05$ and $0.19 \pm .05$ respectively.

Using $(E^{\circ} - E_{1/2}) = 0.018$ V and $(E_{3/4} - E_{1/4}) = -0.076$ V

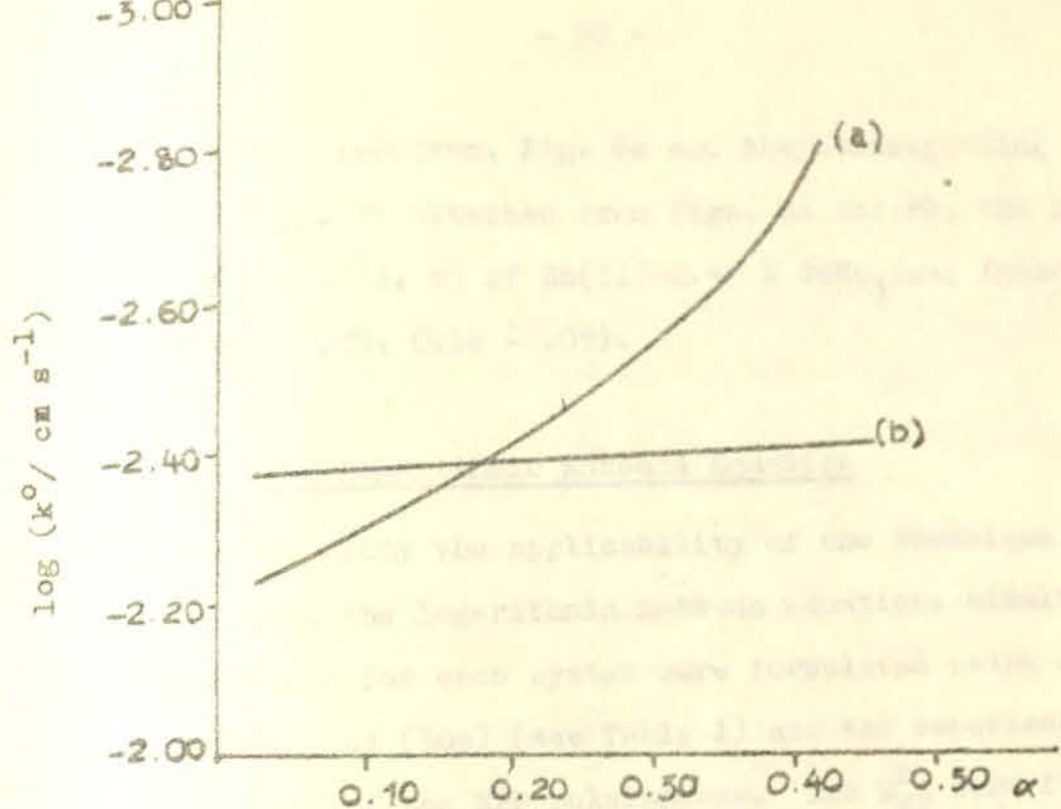


Fig. 9a $\log k^0$ vs α diagram at (a) $E_{3/4} - E_{y4} = -0.046$ V;
 b) $E^0 - E_{y2} = 0.006$ V of Zn(II)-0.49M NaNO₃ system

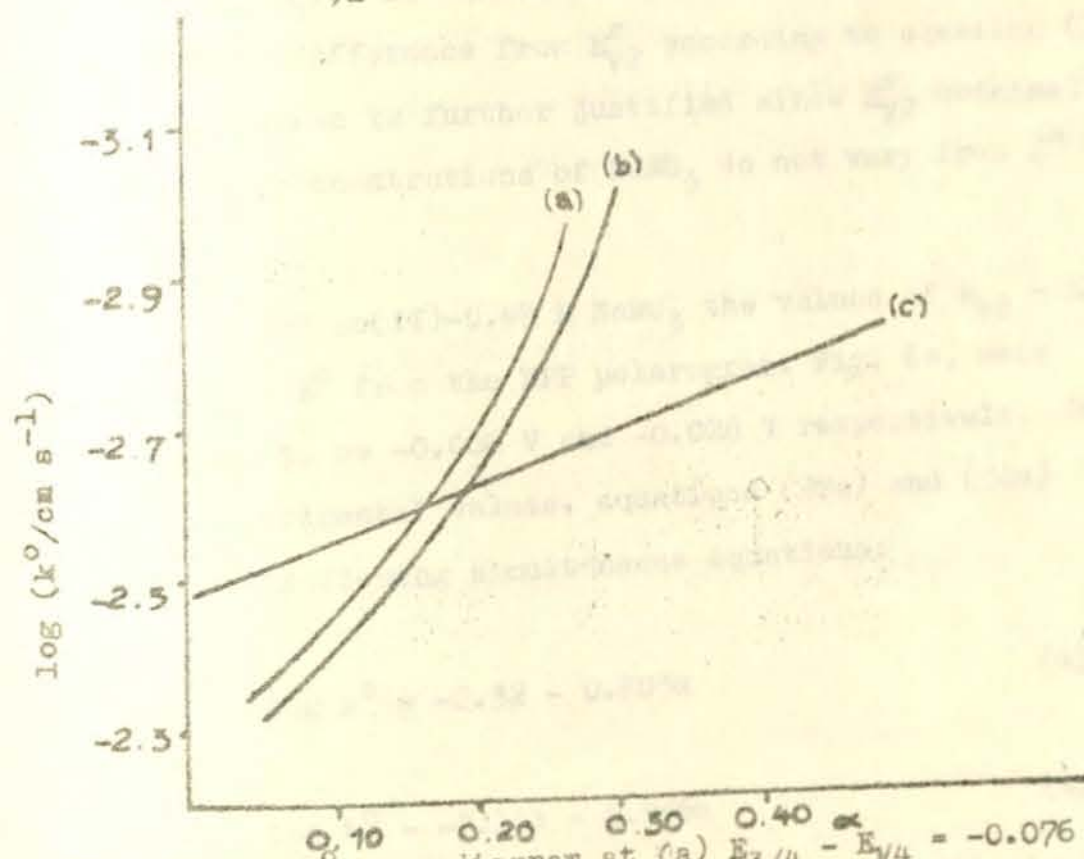


Fig. 9b $\log k^0$ vs α diagram at (a) $E_{3/4} - E_{y4} = -0.076$ V;
 (b) $E_{3/4} - E_{y4} = -0.068$ V; (c) $E^0 - E_{y2} = 0.018$ V of Zn(II)
 1.05M and -2.45M NaNO₃ systems

of the NPP polarogram, Fig. 6c and the corresponding plots in Fig. 9b obtained from Figs. 8a and 8b, the pair: $[\log (k^{\circ}/\text{cm s}^{-1}), \alpha]$ of Zn(II)-2.45 M NaNO_3 was found to be $(-2.60 \pm .05, 0.16 \pm .05)$.

4.1.1.3 The Logarithmic Matsuda Equation

To study the applicability of the technique deduced from the logarithmic Matsuda equation, simultaneous equations for each system were formulated using equations (29a) and (30a) (see Table 1) and the experimental $E_{1/2}$ and $E_{3/4}$ of the NPP polarograms. The $E_{1/2}^R$ term found in the equation is identified as E° in all the systems. Since $(D_o/D_R)^{1/2}$ is almost unity the value of E° has a negligible difference from $E_{1/2}^R$ according to equation (12d). The assumption is further justified since $E_{1/2}^R$ obtained at different concentrations of NaNO_3 do not vary from E° Zn^{2+}/Zn .

For Zn(II)-0.49 M NaNO_3 the values of $E_{1/2} - E^{\circ}$ and $E_{3/4} - E^{\circ}$ from the NPP polarogram, Fig. 6a, were evaluated to be -0.006 V and -0.028 V respectively. Using these experimental values, equations (29a) and (30a) yield the following simultaneous equations:

$$\log k^{\circ} = -2.32 - 0.203\alpha \quad (41a)$$

$$\log k^{\circ} = -2.113 - 0.946\alpha \quad (41b)$$

The values of $\log (k^{\circ}/\text{cm s}^{-1})$ and α calculated

via equations (41a) and (41b) are -2.37 and 0.28 respectively.

To determine the kinetic parameters of the Zn(II)-1.05 M NaNO₃ system, the experimental values, $E_{1/2} - E^0 = -0.018$ V and $E_{3/4} - E^0 = -0.058$ V, with equations (29a) and (30a) yield:

$$\log k^0 = -2.50 - 0.682\alpha \quad (42a)$$

$$\log k^0 = -2.207 - 1.960\alpha \quad (42b)$$

$\log (k^0/\text{cm s}^{-1})$ and α were then computed to be -2.66 and 0.23 respectively.

In the same way as the previous cases, for Zn(II)-2.45 M NaNO₃ the following simultaneous equations from $E_{1/2} - E^0 = 0.018$ V and $E_{3/4} - E^0 = -0.058$ V were formulated:

$$\log k^0 = -2.501 - 0.682\alpha \quad (43a)$$

$$\log k^0 = -2.209 - 2.027\alpha \quad (43b)$$

The pair: $[(\log k^0/\text{cm s}^{-1}), \alpha]$ was then calculated to be (-2.65, 0.22).

4.1.2 Discussion

The experimental values of the kinetic parameters of the three techniques and the literature

values in the varying concentration of NaNO_3 are listed in Table 6. Comparison of the results shows a reasonable agreement between the values of the three techniques. The agreement of the literature values of k^0 at $\theta_s = 20$ ms and 40 ms, with the experimental k^0 (at $\theta_s = 190$ ms) further consolidates the fact that the effect of θ_s on the rate constant is not so significant.

In addition to the simplicity of the technique developed from the logarithmic form of Matsuda's equation, the agreement of its result and the previously established procedures of P. Merican et al. [1] and J.H. Christie et al. [13] demonstrates the reliability of the obtained values as well as the validity of the method. The results also confirm the applicability of the P. Merican et al. technique to the quasi-reversible electrode reduction of Zn(II) .

With regard to the effect of the concentration of the supporting electrolyte on the rate of reduction of Zn(II) the results of the J.H. Christie technique unravels a decrease of k^0 value with an increase of NaNO_3 concentration implying a decrease in the rate of discharge of Zn(II) at DME. The value of k^0 of the logarithmic Matsuda's equation and the technique of P. Merican disclose a different tendency in transition from 1.05 M to 2.45 M NaNO_3 . This variation in the trend of rate constant may be because of the polarograms of Zn(II) -2.45 M NaNO_3 which are inconvenient for analysis. This con-

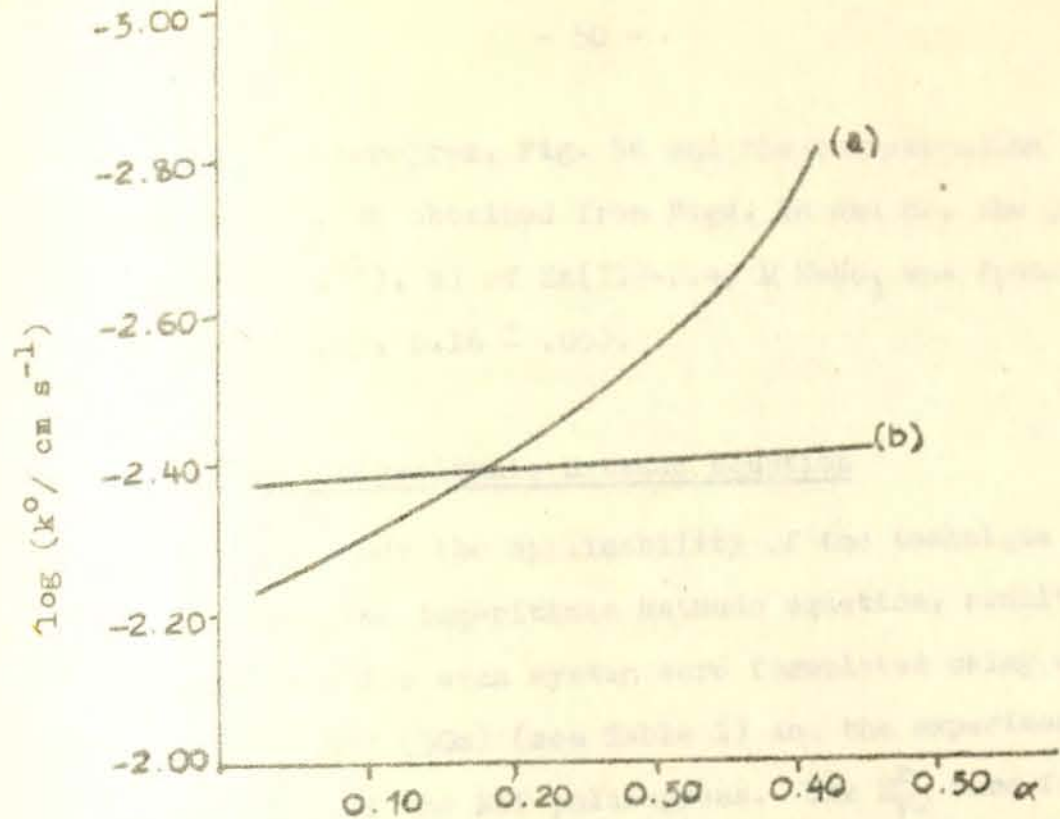


Fig. 9a $\log k^0$ vs α diagram at (a) $E_{3/4} - E_{y4} = -0.046$ V;
 b) $E^0 - E_{y2} = 0.006$ V of Zn(II)-0.49M NaNO₃ system

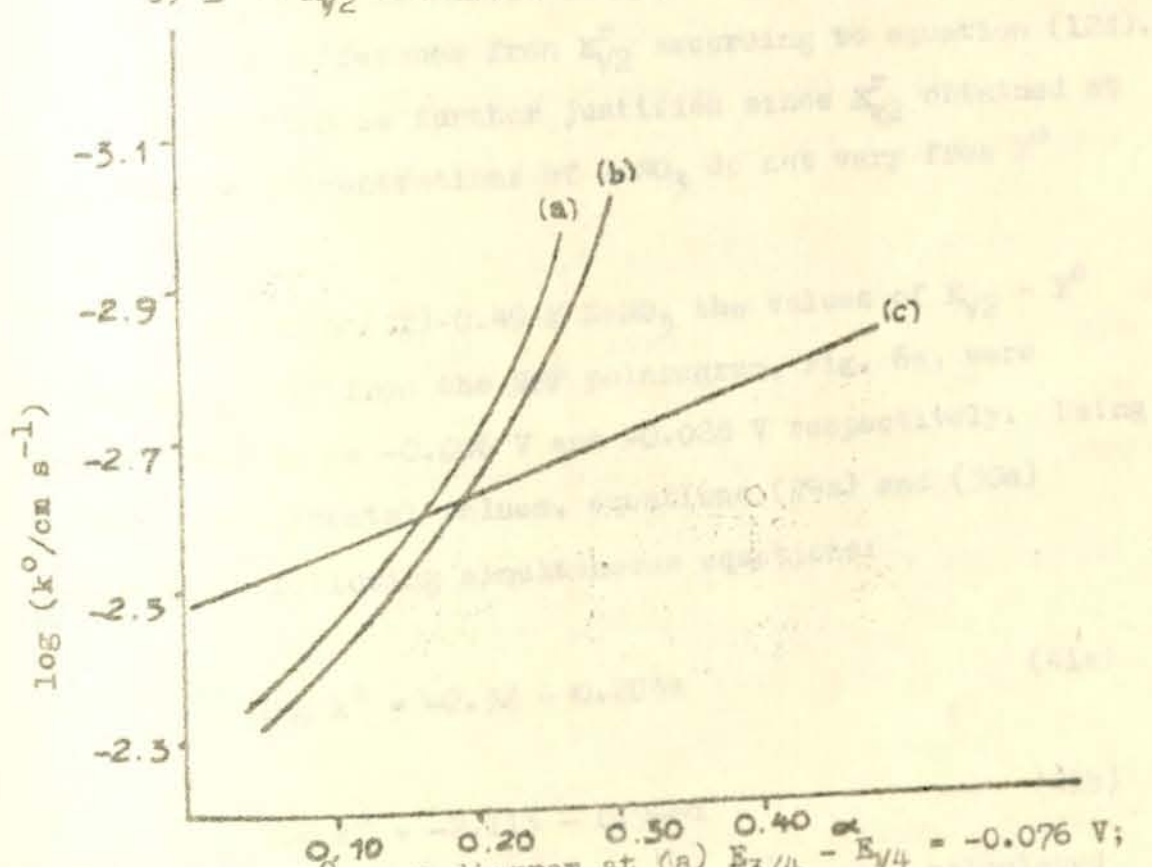


Fig. 9b $\log k^0$ vs α diagram at (a) $E_{3/4} - E_{y4} = -0.076$ V;
 (b) $E_{3/4} - E_{y4} = -0.068$ V; (c) $E^0 - E_{y2} = 0.018$ V of Zn(II)
 1.05M and -2.45M NaNO₃ systems

of the NPP polarogram, Fig. 6c and the corresponding plots in Fig. 9b obtained from Figs. 8a and 8b, the pair: $[\log (k^{\circ}/\text{cm s}^{-1}), \alpha]$ of $\text{Zn(II)}-2.45 \text{ M NaNO}_3$ was found to be $(-2.60 \pm .05, 0.16 \pm .05)$.

4.1.1.3 The Logarithmic Matsuda Equation

To study the applicability of the technique deduced from the logarithmic Matsuda equation, simultaneous equations for each system were formulated using equations (29a) and (30a) (see Table 1) and the experimental $E_{1/2}$ and $E_{3/4}$ of the NPP polarograms. The $E_{1/2}^r$ term found in the equation is identified as E° in all the systems. Since $(D_o/D_R)^{1/2}$ is almost unity the value of E° has a negligible difference from $E_{1/2}^r$ according to equation (12d). The assumption is further justified since $E_{1/2}^r$ obtained at different concentrations of NaNO_3 do not vary from E° Zn^{2+}/Zn .

For $\text{Zn(II)}-0.49 \text{ M NaNO}_3$ the values of $E_{1/2} - E^{\circ}$ and $E_{3/4} - E^{\circ}$ from the NPP polarogram, Fig. 6a, were evaluated to be -0.006 V and -0.028 V respectively. Using these experimental values, equations (29a) and (30a) yield the following simultaneous equations:

$$\log k^{\circ} = -2.32 - 0.203\alpha \quad (41a)$$

$$\log k^{\circ} = -2.113 - 0.946\alpha \quad (41b)$$

The values of $\log (k^{\circ}/\text{cm s}^{-1})$ and α calculated

via equations (41a) and (41b) are -2.37 and 0.28 respectively.

To determine the kinetic parameters of the Zn(II)-1.05 M NaNO₃ system, the experimental values, $E_{1/2} - E^0 = -0.018$ V and $E_{3/4} - E^0 = -0.058$ V, with equations (29a) and (30a) yield:

$$\log k^0 = -2.50 - 0.682\alpha \quad (42a)$$

$$\log k^0 = -2.207 - 1.960\alpha \quad (42b)$$

Log ($k^0/\text{cm s}^{-1}$) and α were then computed to be -2.66 and 0.23 respectively.

In the same way as the previous cases, for Zn(II)-2.45 M NaNO₃ the following simultaneous equations from $E_{1/2} - E^0 = 0.018$ V and $E_{3/4} - E^0 = -0.058$ V were formulated:

$$\log k^0 = -2.501 - 0.682\alpha \quad (43a)$$

$$\log k^0 = -2.209 - 2.027\alpha \quad (43b)$$

The pair: [$(\log k^0/\text{cm s}^{-1}), \alpha$] was then calculated to be (-2.65, 0.22).

4.1.2 Discussion

The experimental values of the kinetic parameters of the three techniques and the literature

values in the varying concentration of NaNO_3 are listed in Table 6. Comparison of the results shows a reasonable agreement between the values of the three techniques. The agreement of the literature values of k^0 at $\theta_s = 20$ ms and 40 ms, with the experimental k^0 (at $\theta_s = 190$ ms) further consolidates the fact that the effect of θ_s on the rate constant is not so significant.

In addition to the simplicity of the technique developed from the logarithmic form of Matsuda's equation, the agreement of its result and the previously established procedures of P. Merican et al. [1] and J.H. Christie et al. [13] demonstrates the reliability of the obtained values as well as the validity of the method. The results also confirm the applicability of the P. Merican et al. technique to the quasi-reversible electrode reduction of Zn(II) .

With regard to the effect of the concentration of the supporting electrolyte on the rate of reduction of Zn(II) the results of the J.H. Christie technique unravels a decrease of k^0 value with an increase of NaNO_3 concentration implying a decrease in the rate of discharge of Zn(II) at DME. The value of k^0 of the logarithmic Matsuda's equation and the technique of P. Merican disclose a different tendency in transition from 1.05 M to 2.45 M NaNO_3 . This variation in the trend of rate constant may be because of the polarograms of Zn(II) -2.45 M NaNO_3 which are inconvenient for analysis. This con-

Table 6 Apparent Values of the Kinetic Parameters for Zn(II) Reduction for Various Concentration of HNO_3

Concentration of HNO_3 in Molarity	Literature Values [5] of $\log(k^0/\text{cm}^5\text{-}1)$ at $\theta_s=20\text{ms}$ $\theta_s=40\text{ms}$	Exp'l values using J. Christie method at $\theta_s=190\text{ms}$	α	Exp'l values using logarithmic method at $\theta_s=190\text{ms}$	α	Exp'l values using F. Kerlcam method at $\theta_s=190\text{ms}$	α
0.49	-2.40	-2.36	0.21	-2.38	0.28	-2.40 \pm .05	0.20 \pm .05
1.05	-2.47	-2.68	0.21	-2.66	0.23	-2.61 \pm .05	0.19 \pm .05
2.45	-2.62	-2.72	0.22	-2.65	0.22	-2.60 \pm .05	0.15 \pm .05

tradiction of the results may be solved if the studies were performed at higher concentration of NaNO_3 , for the studies in more concentrated solution give a proper insight into the reduction rate response [20,32].

The trend of k^0 observed in the results obtained using the J.H. Christie technique had also been observed by Koryta [14] in his study by rapid de polarography and by J.H. Christie et al. [13] using NPP at the two sampling times of 20 ms and 40 ms. Such dependences of k^0 of Zn(II) reduction in various types of supporting electrolyte have also been shown [19] using different electrochemical methods. For Zn(II)-NaNO_3 system it has been shown [14] that the decrease of the rate of electrode reduction of Zn(II) is due to the decrease of the potential difference in the double layer which in its most part is caused by electrostatic effect of the ionic part of the double layer.

4.2 Cr(III)-NaClO_4 System

In the study of the electrode kinetics of Cr(III) the proposal suggested by P. Mericam et al. [1] for the totally irreversible electrode reaction is applied and tested. The irreversibility of the electrode reaction is checked using the method of Oldham and Parry with a further use of this technique to evaluate the kinetic parameters. The technique of the logarithmic Matsuda equation is also

Table 7. Equations Used for the Analysis of the
Ni(II)-KNO₃ and Cr(III)-NaClO₄ Systems

Method of analysis	Equations used	Equation numbers	Comment
Oldham and Parry	$E_{1/2} = E^0 + \frac{RT}{\alpha nF} \ln \left[2.31 k^0 \sqrt{\frac{\theta_s}{D_0}} \right]$	21	Used for determination of $\log k^0$
	$\frac{2.3031T}{2\alpha nF} \log \left[\frac{x^2(1.75+x^2)}{(1-x)} \right] = E_{1/2} - E_2$	38	Used for determination of α ($\log Y$ vs E_2)
P. Merican	$E_{3/4} - E_{1/4} = \frac{RT}{2\alpha nF} \ln 0.029$	35	Used for the determination of α
Logarithmic Matsuda Equation	$\log k^c = \log a + \frac{\alpha nF}{2.303RT} (E_{1/2} - E^0)$	37a	
	$\log k^c = \log a + 0.358 + \frac{\alpha nF}{2.303RT} (E_{3/4} - E^0)$	37b	

employed to extract the kinetic parameters. The equations of the different techniques are listed in Table 7. The study was performed in 0.2M, 0.5M and 1M NaClO₄.

The values of diffusion coefficients of Cr³⁺ and Cr²⁺ used in all the three methods were obtained from literature [21] and were $D_{Cr^{3+}} = 5.6 \times 10^{-6} \text{ cm}^2 \text{ s}^{-1}$ and $D_{Cr^{2+}} = 7.9 \times 10^{-6} \text{ cm}^2 \text{ s}^{-1}$. E^0 (Cr³⁺/Cr²⁺) at the different concentration of NaClO₄ were determined by R. Andreu et al. [20] and has values of -0.665 V, -0.650 V, and -0.645 V versus SCE for 0.2M, 0.5M, and 1M NaClO₄ respectively.

4.2.1 Determination of Kinetic Parameters

4.2.1.1 Method of Oldham and Parry

In the study of Cr(III)-NaClO₄ system using the technique of Oldham and Parry, the irreversibility of the Cr(III) reduction in each concentration of NaClO₄ was first confirmed using the relation established in equation (38) (see Table 7). From the respective NPP polarogram, the experimental i/i_d ($i/i_d = x$) at different potentials were determined. Log y, where

$$\log y = \log \left[\frac{x^2(1.75 + x^2)}{(1 - x)} \right] \quad (44)$$

was then plotted against (-E). The linearity of

the plot demonstrates the electrode reduction to be totally irreversible (see equation (38)).

The value of α of each system was determined from the slope, where the slope = $(2\alpha n/0.0592) \text{ V}^{-1}$ according to equation (38). The value of $E_{1/2}$ obtained from the intercept of the plot of $\log y$ vs $(-E)$ should coincide with the experimental $E_{1/2}$ of the NPP polarogram according to equation (38). The values of k^0 of each system were then calculated using an alternative expression of equation (21):

$$k^0 = \frac{1}{2.31} \sqrt{\frac{D_0}{e_s}} \left\{ \text{antilog} \left[\frac{\alpha n F}{RT} (E_{1/2} - E^0) \right] \right\} \quad (45)$$

and the values of the experimental $E_{1/2}$ together with the literature values of $D_{\text{Cr}^{3+}}$ and $E_{\text{Cr}^{3+}/\text{Cr}^{2+}}^0$

For $\text{Cr(III)-0.2M NaClO}_4$, the plot of $\log y$ versus $(-E)$, Fig. 11 was found to be linear showing the electrode reduction to be irreversible. The value of α was computed from the slope, and found to be 0.78. The experimental $E_{1/2}$ of the NPP polarogram, -0.781 V , (Fig. 10a) agrees well with the intercept of the respective plot in Fig. 11, -0.782 V , in accordance with the theoretical prediction of equation (38). Using the relation of equation (45) and the experimental $E_{1/2}$ value, $\log(k^0/\text{cm s}^{-1})$ was calculated to be -4.75 .

Extending the technique to $\text{Cr(III)-0.5M NaClO}_4$

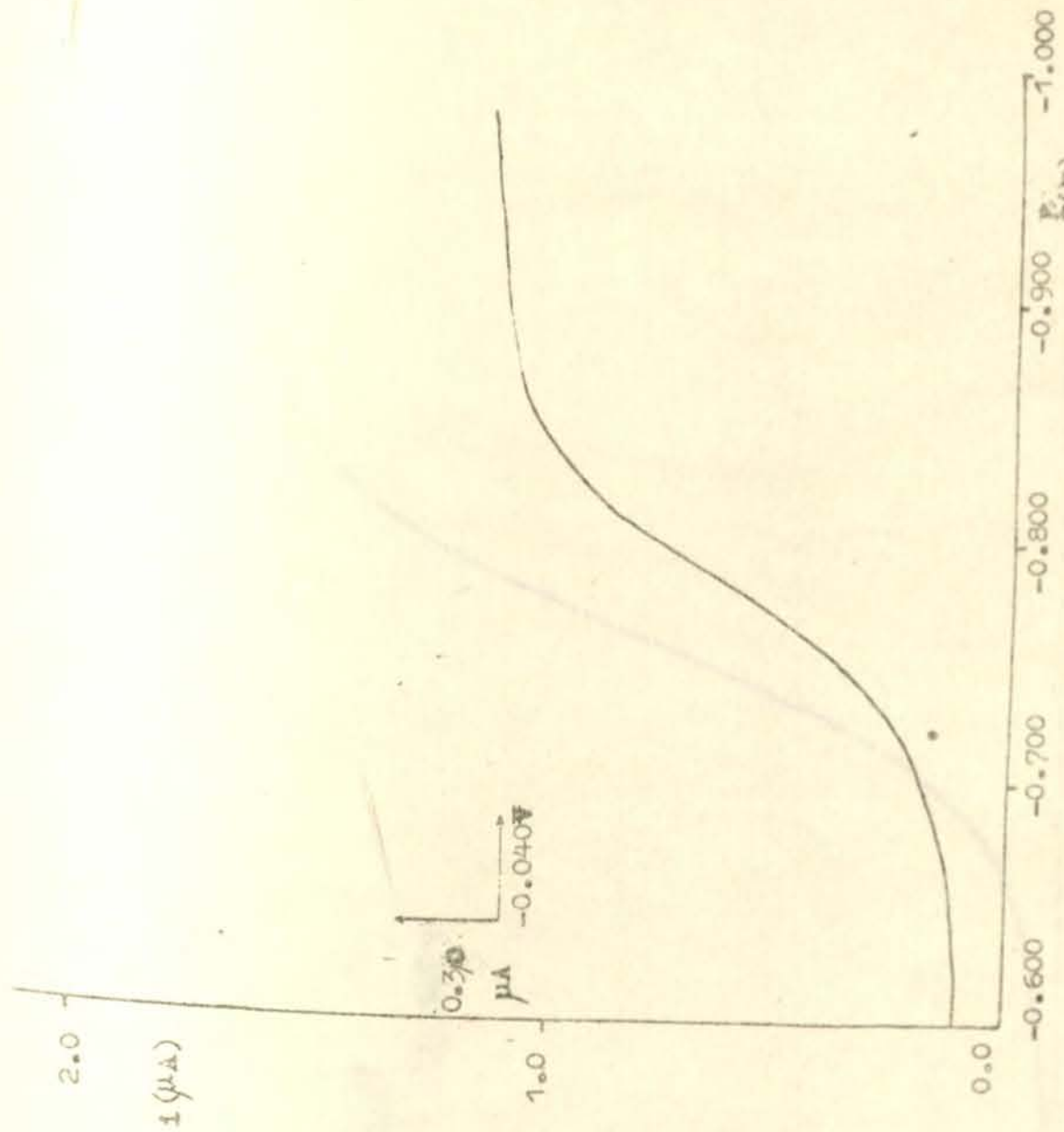


Fig. 10a NPP polarogram of 0.2mM Cr(III) in 0.2M NaClO₄

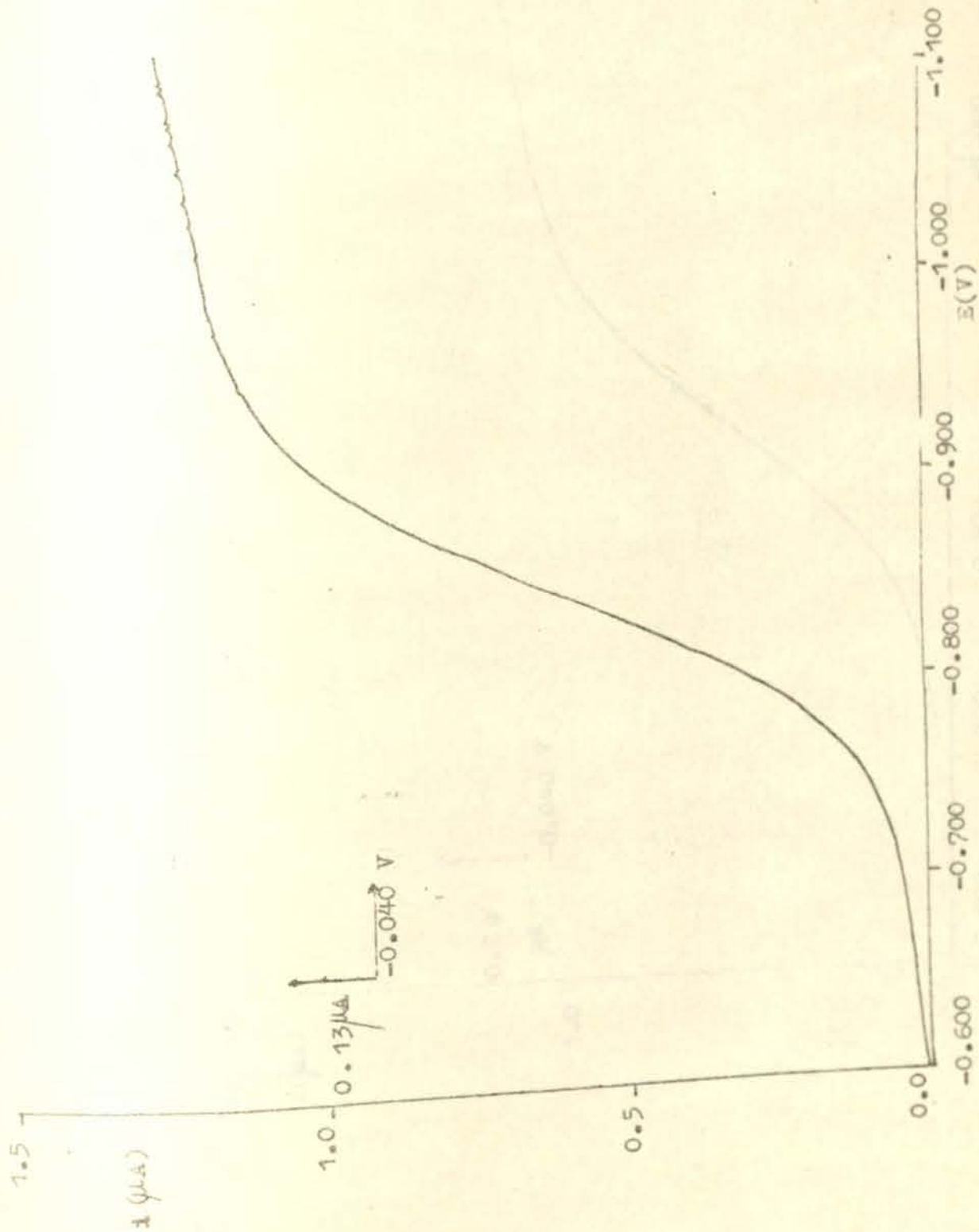


FIG. 10b NPP polarogram of 0.2mM Cr(III) in 0.5 M NaClO₄

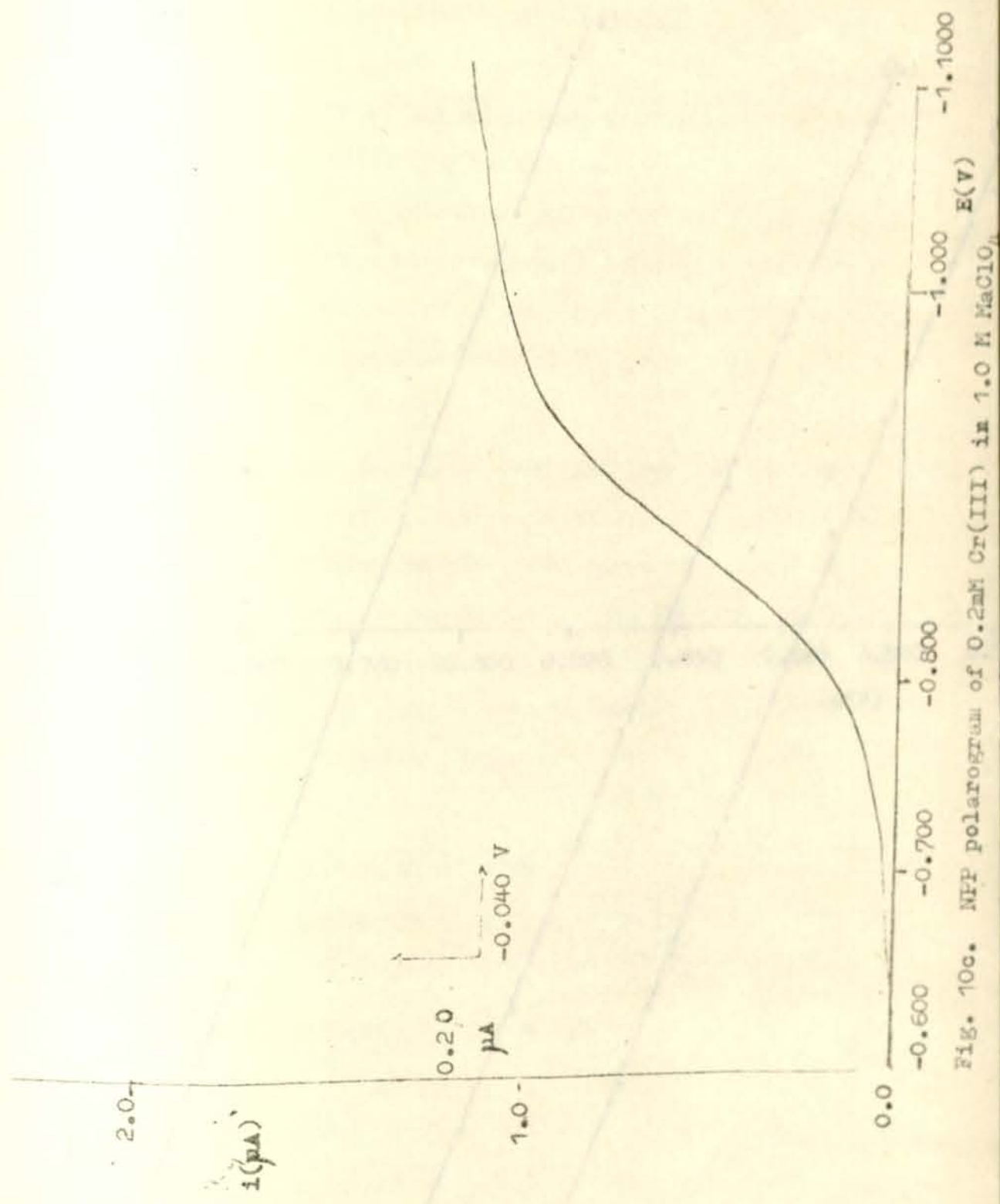


Fig. 10c. MPP polarogram of 0.2mM Cr(III) in 1.0 M NaClO₄

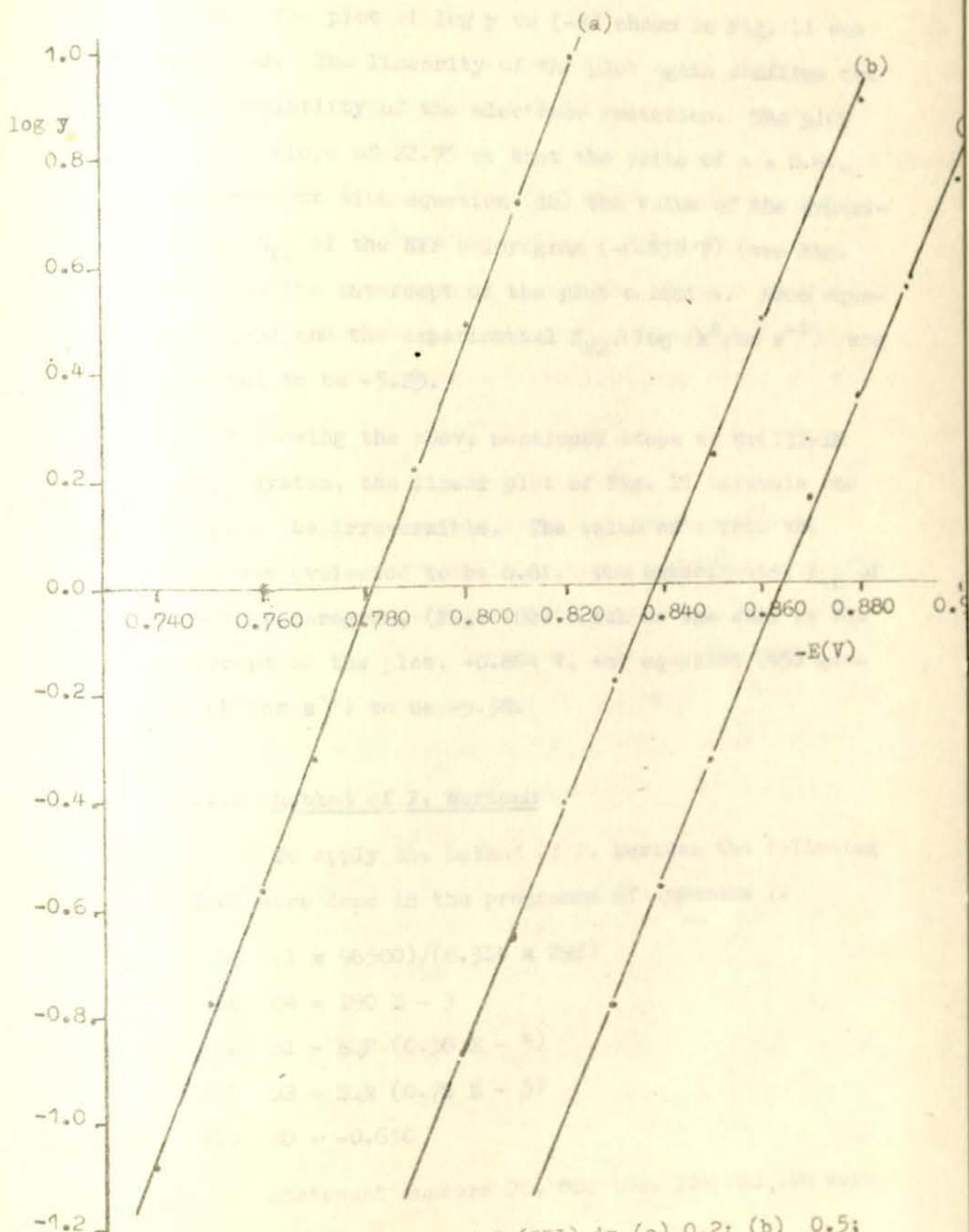


Fig.11 $\log y$ Vs $-E$ plot of Cr(III) in (a) 0.2; (b) 0.5; and (c) 1.0 M of NaClO_4

system, the plot of $\log y$ vs $(-E)$ shown in Fig. 11 was obtained. The linearity of the plot again confirms the irreversibility of the electrode reduction. The plot gives a slope of 22.75 so that the value of $\alpha = 0.67$. In agreement with equation (38) the value of the experimental $E_{1/2}$ of the NPP polarogram (-0.838 V) (see Fig. 10b) and the intercept of the plot coincide. From equation (45) and the experimental $E_{1/2}$, $\log (k^0/\text{cm s}^{-1})$ was computed to be -5.25.

Following the above mentioned steps to Cr(III)-1M NaClO_4 system, the linear plot of Fig. 11 unravels the system to be irreversible. The value of α from the slope was evaluated to be 0.62. The experimental $E_{1/2}$ of the NPP polarogram, (Fig. 10c) which is the same as the intercept of the plot, -0.864 V, and equation (45) give $\log (k^0/\text{cm s}^{-1})$ to be -5.38.

4.2.1.2 Method of P. Merican

To apply the method of P. Merican the following changes were done in the programme of Appendix I.

```
70 (1 * 96500)/(8.314 * 298)
80 C4 = 190 E - 3
100 D1 = SQR (0.56 E - 5)
105 D2 = SQR (0.79 E - 5)
110 E0 = -0.650
```

statement numbers 70, 80, 100, 105 and 110 were

changed in order to take into account the values of $n = 1$ for the $\text{Cr}^{3+}/\text{Cr}^{2+}$ system, the experimental sampling time $\theta_s = 190$ ms, the diffusion coefficients $D_{\text{Cr}^{3+}}$, $D_{\text{Cr}^{2+}}$ and $E_{\text{Cr}^{3+}/\text{Cr}^{2+}}^0 = -0.650$ V vs SCE. The theoretical calculations were performed for $0.4 \leq \alpha \leq 1$ (with successive addition of 0.05) and $10^{-4} \geq (k^0/\text{cm s}^{-1}) \geq 10^{-8}$ (with successive addition of the exponent by -0.05). The same computer as in the previous case was used with a computer time of 1:45 hours to complete the calculations. From the calculated values, the theoretical plots shown in Fig. 12 were obtained.

To judge the applicability of the P. Merican's method to the irreversible system of Cr(III), α of each system was calculated from the experimental wave width using equation (35). The method was then crosschecked by considering the agreement of the theoretically calculated irreversible values of $E_{3/4} - E_{1/4}$ at the experimental value of α with the experimental wave width, Appendix II a. The irreversible wave width value for each α corresponds to the $E_{3/4} - E_{1/4}$ value in the region where the wave width is independent of the value of $\log k^0$ [1]. If the technique was found to be valid from the agreement of the theoretical and experimental results, the value of k^0 was evaluated from the theoretical plot $E^0 - E_{1/2}$ vs $\log k^0$ at the experimental α of Fig. 12.

From the experimental wave width of the NPP polarogram (Fig. 10a) -0.060 V, the value of α of Cr(III)-0.2M

$(E^0 - E_{1/2})/mV$

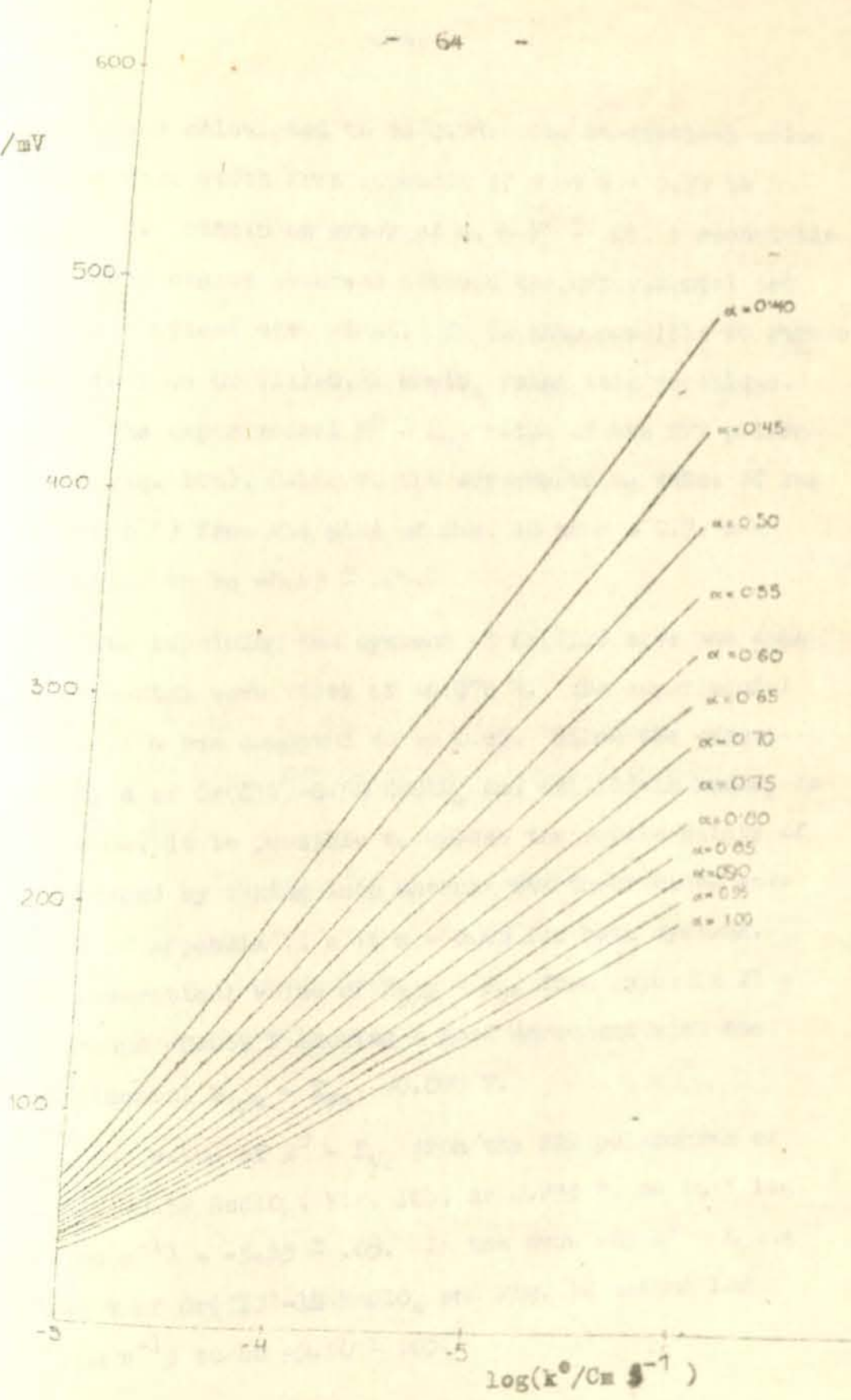


Fig. 12 $(E^0 - E_{1/2})$ Vs $\log k^0$ diagram at various α values for the analysis of the Cr(III)- $NaClO_4$ systems

NaClO_4 was calculated to be 0.76. The theoretical value of the wave width from Appendix II a at $\alpha = 0.75$ is -0.059 V. Within an error of α , $0.75 \pm .05$, a reasonable agreement can be observed between the experimental and the theoretical wave width. It is thus possible to pursue our study on $\text{Cr(III)}-0.2\text{M NaClO}_4$ using this technique. Using the experimental $E^0 - E_{1/2}$ value of the NPP polarogram (Fig. 10a), 0.162 V, the corresponding value of $\log(k^0/\text{cm s}^{-1})$ from the plot of Fig. 12 at $\alpha = 0.75$ was evaluated to be $-4.63 \pm .05$.

The remaining two systems of Cr(III) have the same experimental wave width of -0.070 V. The experimental value of α was computed to be 0.65 . Since the experimental α of $\text{Cr(III)}-0.5\text{M NaClO}_4$ and $\text{Cr(III)}-1\text{M NaClO}_4$ is the same, it is possible to assess the applicability of the method by taking into account the theoretical wave width of Appendix II a at $\alpha = 0.65$ for both systems. The theoretical value of $E_{3/4} - E_{1/4}$ from Appendix II a is around -0.069 V showing a good agreement with the experimental $E_{3/4} - E_{1/4}$, -0.070 V.

The value of $E^0 - E_{1/2}$ from the NPP polarogram of $\text{Cr(III)}-0.5\text{M NaClO}_4$, Fig. 10b, is 0.233 V, so that $\log(k^0/\text{cm s}^{-1}) = -5.15 \pm .05$. In the same way $E^0 - E_{1/2} = 0.264$ V of $\text{Cr(III)}-1\text{M NaClO}_4$ and Fig. 12 define $\log(k^0/\text{cm s}^{-1})$ to be $-5.50 \pm .05$.

4.2.1.3 The Logarithmic Matsuda Equation

To study the irreversible electrode reaction of

Cr(III) the simplified logarithmic Matsuda equations, Eqs. (37a) and (37b) (see Table 7) of totally irreversible systems were used.

For Cr(III)-0.2M NaClO₄, the experimental ($E_{1/2} - E^{\circ}$) -0.264 V and $E_{3/4} - E^{\circ}$ -0.190 V and equations (37a) and (37b) respectively furnish the following simultaneous equations:

$$\log k^{\circ} = -2.62 - 2.74 \alpha \quad (46a)$$

$$\log k^{\circ} = -2.26 - 3.21 \alpha \quad (46b)$$

From the solution of the simultaneous equations $\log (k^{\circ}/\text{cm s}^{-1})$ and α were found to be -4.70 and 0.77 respectively.

In the case of Cr(III)-0.5M NaClO₄ the values $E_{1/2} - E^{\circ}$ and $E_{3/4} - E^{\circ}$ were found to be -0.233 V and -0.267 V. Using these values and equation (37a) and (37b) the simultaneous equations below were formulated:

$$\log k^{\circ} = -2.62 - 3.94 \alpha \quad (47a)$$

$$\log k^{\circ} = -2.26 - 4.51 \alpha \quad (47b)$$

The values of $\log (k^{\circ}/\text{cm s}^{-1})$ and α then computed to be -5.10 and 0.63 respectively.

Following the same steps, the simultaneous equations:

$$\log k^0 = -2.52 - 4.46 \alpha \quad (48a)$$

$$\log k^0 = -2.26 - 5.07 \alpha \quad (48b)$$

were obtained for Cr(III)-1M NaClO₄. The pairs: [$\log(k^0/\text{cm s}^{-1}), \alpha$] were then calculated to be (-5.25, 0.59).

4.2.2 Discussion

The values of $\log k^0$ and α of the three techniques are presented in Table 8. The results in Table 8 show the agreement of the evaluated kinetic parameters at the various concentration of NaClO₄. The reliability of the values determined by the method of P. Mericam is thus confirmed. The same justification is also extended to the technique deduced from the logarithmic form of Matsuda's equation.

Similar to Zn(II) reduction in NaNO₃, within the range of NaClO₄ concentration used, an increase in the supporting electrolyte concentration is accompanied with a decrease in the apparent value of the rate constant for reduction of Cr(III) as shown in Table 8. This result discloses the fact that the rate of reduction of Cr(III) diminishes with an increase of the NaClO₄ concentration. This is in agreement with the tendency of the rate response of Cr(III) observed in the works of R. Anderu et al. [20] at a concentration of NaClO₄ lower than 3M

Table 8. Apparent Values of the Kinetic Parameters of Cr(III) Reduction
for Various Concentrations of NaClO_4^- .

NaClO_4^- M	Oldham and Ferry Method		P. Mericom Method		Logarithmic Matsuda Equation	
	$\log(k^0/\text{cm s}^{-1})$	α	$\log(k^0/\text{cm s}^{-1})$	α	$\log(k^0/\text{cm s}^{-1})$	α
0.20	-4.75	0.78	-4.63 ± 0.05	0.75 ± 0.05	-4.70	0.77
0.50	-5.25	0.67	-5.15 ± 0.05	0.65 ± 0.05	-5.10	0.63
1.00	-5.38	0.62	-5.50 ± 0.05	0.65 ± 0.05	-5.25	0.59

Note: Literature [14,33] values of the pairs: $[\log(k^0/\text{cm s}^{-1}), \alpha]$ at 0.5 and 1.0M of NaClO_4^- using dc polarographic technique are $(-5.09, 0.60)$ and $(-5.10, 0.55)$ respectively.

and others [21,33] using dc polarographic method. Such trend of the rate constant was also observed by other workers [34,35].

However, the moderate concentration of NaClO_4 in which the study was performed cannot reveal a clear picture of the effect of NaClO_4 concentration on the electrode kinetics of Cr(III) . Contrary to the rate of reduction of Cr(III) at concentrations lower than 3M, R. Andreu et al. [20] found that the rate constant was increased noticeably for concentration of NaClO_4 greater than 3M. Thus an appropriate insight into the influence of the supporting electrolyte concentration on the rate response of Cr(III) can only be achieved if the studies were done in a wider concentration range [20].

4.3 Ni(II)- KNO_3 System

The applicability of the three techniques already employed in the Cr(III)-NaClO_4 systems were tested on the electrode reduction of Ni(II) in various concentrations of KNO_3 as supporting electrolyte.

The values of the kinetic parameters were referred to $E_{\text{Ni}^{2+}/\text{Ni}}^0 = -0.250 \text{ V vs NHE}$ [36]. The diffusion coefficient of Ni(II) used was the value at infinite dilution at 25°C , $D_{\text{Ni}^{2+}} = 0.69 \times 10^{-5} \text{ cm}^2 \text{ s}^{-1}$ [37]. Since the amalgam diffusion coe-

fficient of simple metals are nearly equal to the diffusion coefficient of the corresponding aquo-complex in dilute aqueous solution [38] it was assumed that $D_{\text{Ni}^- \text{Hg}} = D_{\text{Ni}^{2+}} = 0.69 \times 10^{-5} \text{ cm}^2 \text{ s}^{-1}$. The same equations listed in Table 7 were used for the analysis of the system.

The inconvenient nature of the NPP polarograms obtained at higher concentrations of KNO_3 limit our study of Ni(II) reduction to 0.10, 0.15, 0.20 and 0.26 M of KNO_3 . This problem may be due to the two reduction steps that Ni(II) shows at high salt concentrations as stated by Sanborn and Orlenann [39]. The experimental NPP polarograms for the above mentioned concentration of KNO_3 are shown in Figs. 13a, 13b, 13c, and 13d.

4.3.1 Determination of Kinetic Parameters

The irreversibility of the Ni(II) reduction in the different concentrations of KNO_3 was checked using the method of Oldham and Parry in much the such way as that done for the Cr(III)- NaClO_4 systems. The linearity of the plots of $\log y$ of equation (44) versus $-E$ of Fig. 14 deduced from the experimental data of the respective NPP polarograms) show that the Ni(II)- KNO_3 systems are irreversible. The value of $E_{V/2}$ obtaine from the intercept of each plot coincide with the experimental $E_{V/2}$ of the NPP polarograms (Figs. 13a, 13b, 13c, and 13d) justi-

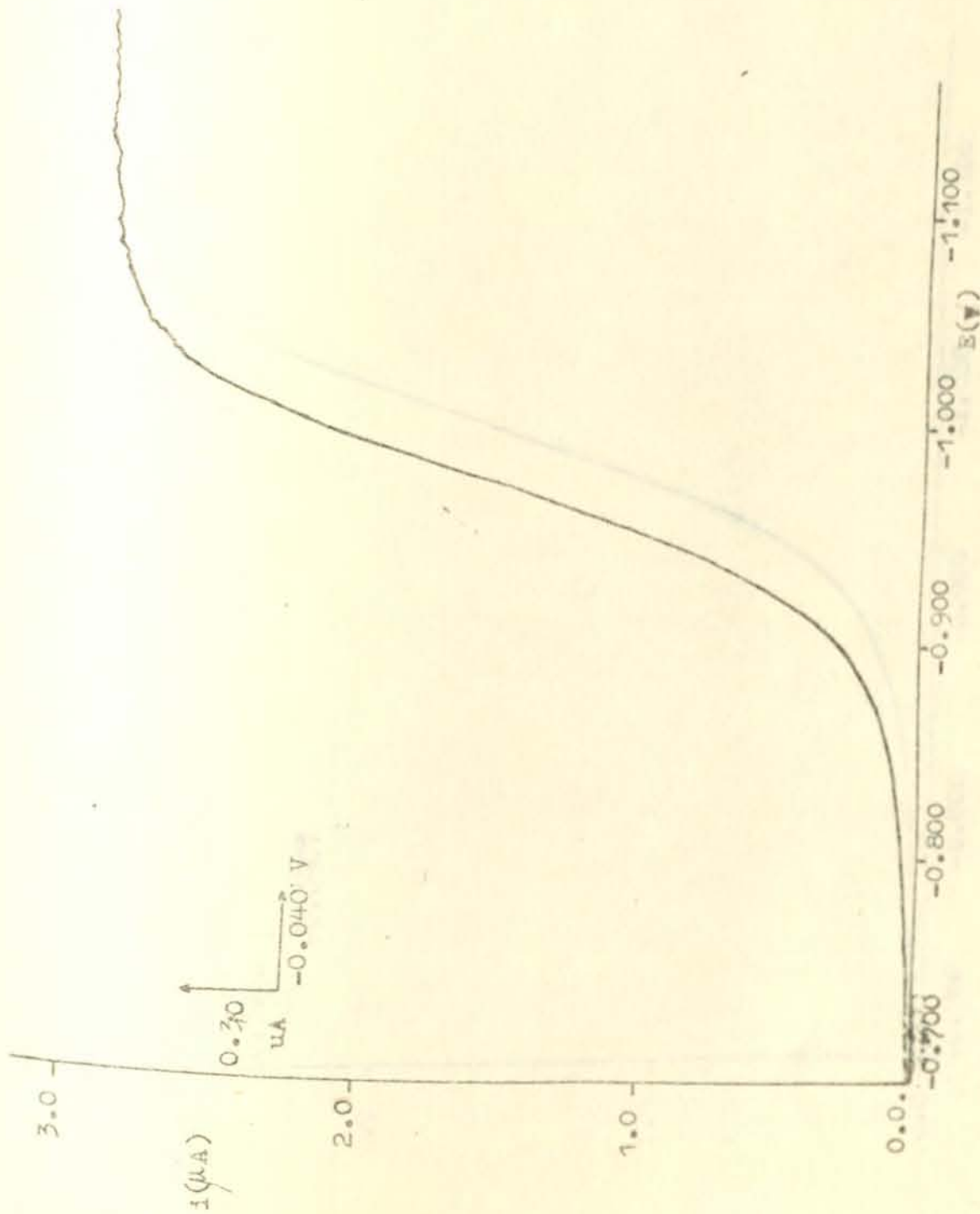


FIG. 13a NPP polarogram of 0.2mm Ni(II) in 0.1M KNO₃.

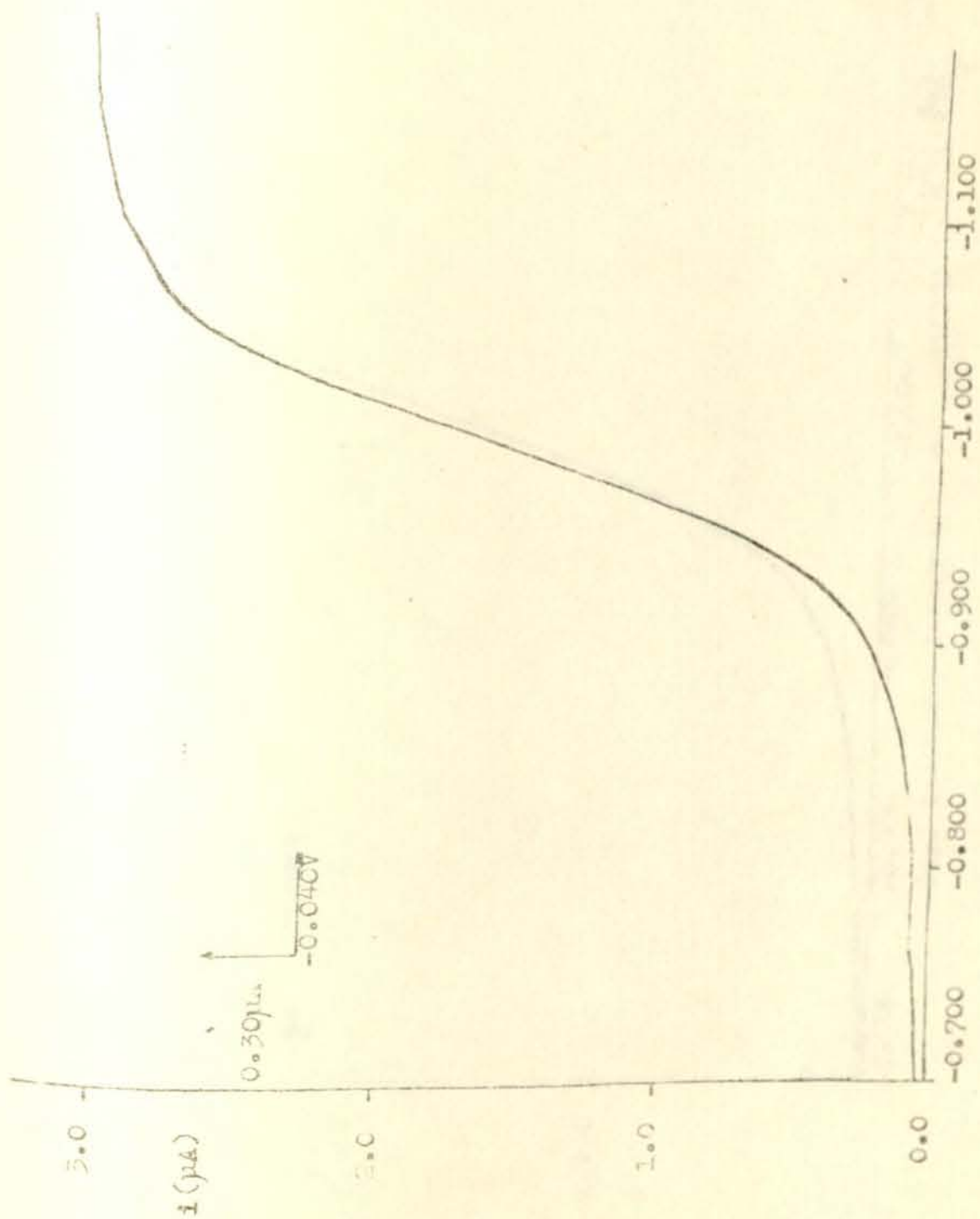


Fig. 13b NPP polarogram of 0.2 mM Ni(II) in 0.15M KNO_3

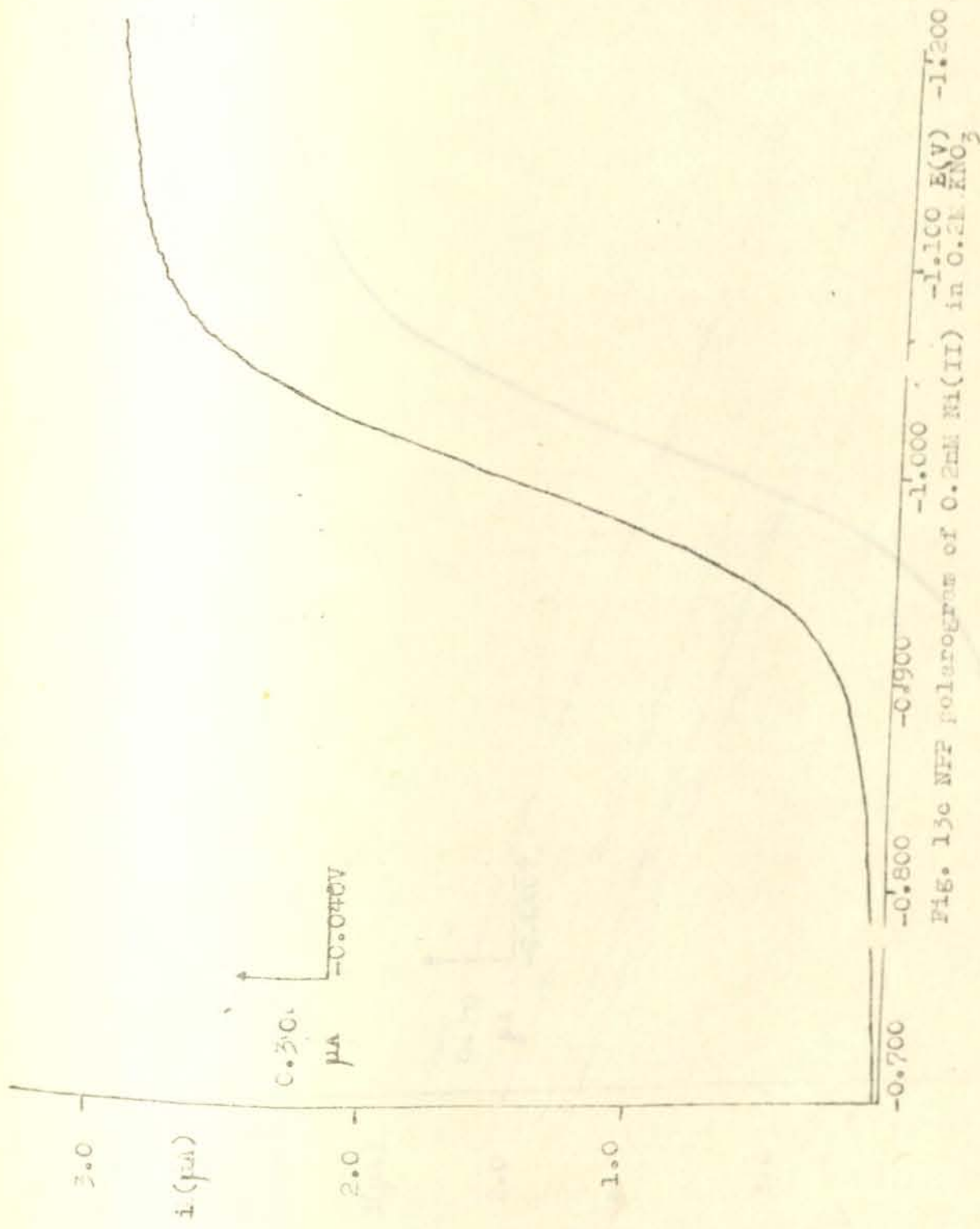


Fig. 13c NPP polarogram of 0.2M Ni(II) in 0.2M KNO_3

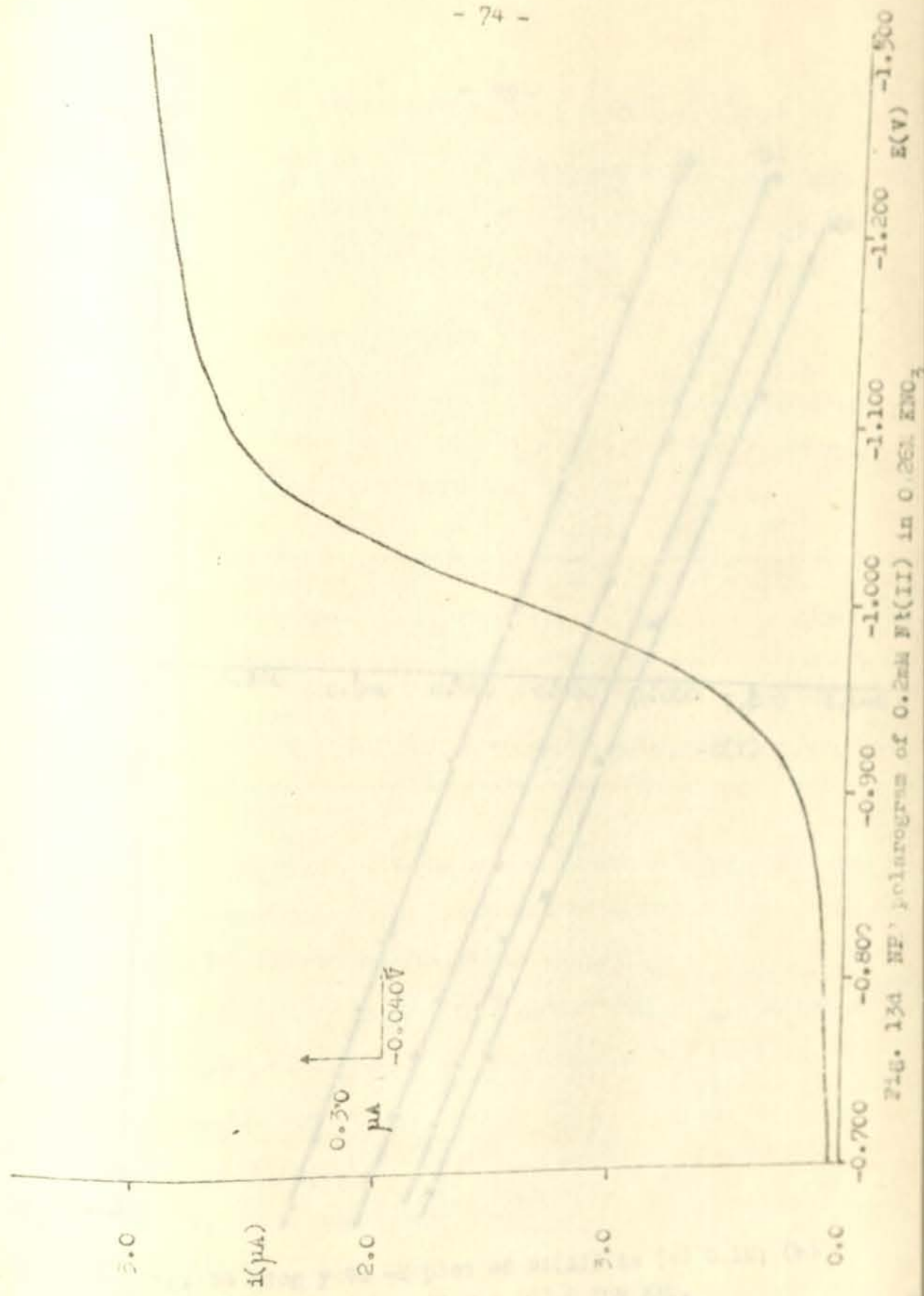


Fig. 134 NP polarogram of 0.2mM Pt(II) in 0.263 KNO₃

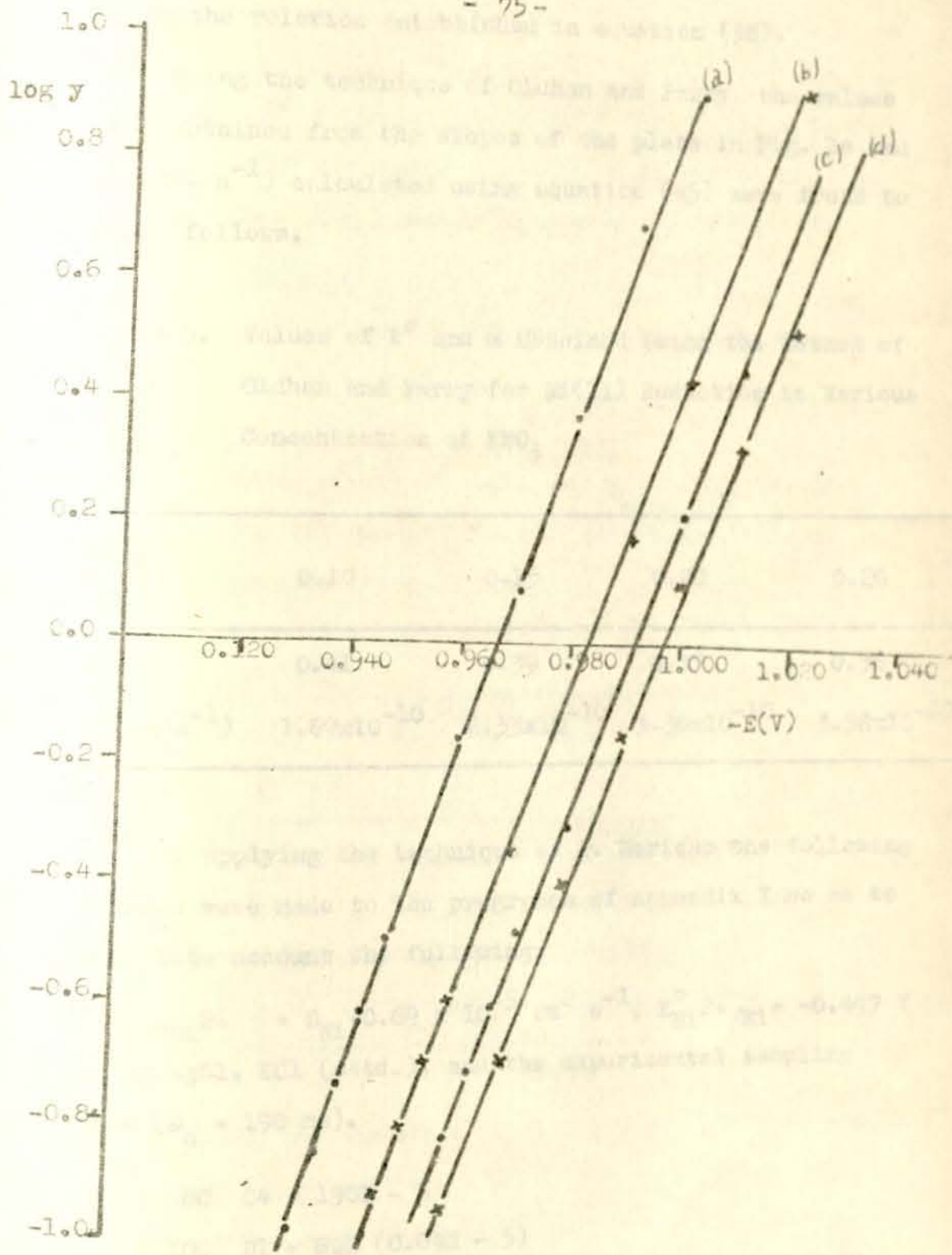


Fig. 14 $\log y$ Vs $-E$ plot of Ni(II) in (a) 0.1M; (b) 0.15; (c) 0.20 and (d) 0.26M KNO_3

ifying the relation established in equation (38).

Using the technique of Oldham and Parry, the values of α obtained from the slopes of the plots in Fig. 14 and k^0 (cm. s^{-1}) calculated using equation (45) were found to be as follows.

Table 9. Values of k^0 and α Obtained Using the Method of Oldham and Parry for Ni(II) Reduction in Various Concentration of KNO_3

KNO_3 M	0.10	0.15	0.20	0.26
α	0.41	0.39	0.37	0.38
$k^0(\text{cm s}^{-1})$	1.69×10^{-10}	2.33×10^{-10}	5.36×10^{-10}	3.58×10^{-10}

In applying the technique of P. Merican the following changes were made to the programme of Appendix I so as to take into account the following:

$D_{\text{Ni}^{2+}} = D_{\text{Ni}} = 0.69 \times 10^{-5} \text{ cm}^2 \text{ s}^{-1}$, $E_{\text{Ni}^{2+}/\text{Ni}}^0 = -0.447 \text{ V}$
vs $\mu\text{g}/\text{AgCl}$, KCl (std.), and the experimental sampling time ($\theta_s = 190 \text{ ms}$).

80 C4 = 190E - 3
100 D1 = SQR (0.69E - 5)
105 D2 = SQR (0.69E - 5)
110 E0 = -0.447

Using the same microcomputer employed in the previous cases theoretical calculations were performed for $0.2 \leq \alpha \leq 0.65$ and $10^{-6} \geq (k^0/\text{cm s}^{-1}) \geq 10^{-12}$ with successive addition of 0.05 to the former case and -0.05 to the exponent of the latter. The computer time used was 1:45 hours.

The experimental values of $E^0 - E_{1/2}$ and $E_{3/4} - E_{1/4}$ extracted from the corresponding NPP polarograms of each system are listed in Table 10.

Table 10. Experimental $E^0 - E_{1/2}$ and $E_{3/4} - E_{1/4}$ Values for the Reduction of Ni(II) in the Various Concentration of KNO_3

KNO_3 M	$E^0 - E_{1/2}$ V	$E_{3/4} - E_{1/4}$ V
0.10	0.519	-0.056
0.15	0.535	-0.058
0.20	0.545	-0.064
0.26	0.549	-0.066

Following the procedure of P. Merican for irreversible electrode reaction the values of α were calculated from the experimental wave widths of Table 8 using equation (35) and their values were found to be 0.41, 0.39, 0.36, and 0.35 for Ni(II) in 0.1, 0.15, 0.20, and 0.26M of KNO_3 respectively. The validity of the method was then tested

by taking into account the theoretical irreversible values of $E_{3/4} - E_{1/4}$ from the computer output at α values of 0.35 and 0.45 shown in Appendix II b. The values of $E_{3/4} - E_{1/4}$ in the irreversible region where the wave width is independent of k^0 are around -0.063 V at $\alpha = 0.35$ and -0.055 V at $\alpha = 0.40$ showing a reasonable agreement within the error of α , $\alpha \pm .05$, with the experimental values of Table 10. It is thus possible to extend our study to the evaluation of k^0 using the theoretical plots of $E^0 - E_{1/2}$ versus $\log k^0$ of Fig. 15 which contains a set of straight lines as in the case of Cr(III). From the experimental $E^0 - E_{1/2}$ values of Table 10 and the plots at α of 0.35 and 0.40 of Fig. 15 the values of $\log (k^0/\text{cm s}^{-1})$ were found to be $-9.61 \pm .05$, $-9.82 \pm .05$, $-9.03 \pm .05$, and $-9.08 \pm .05$ for the Ni(II) reduction in the successively increasing concentrations of KNO_3 .

The logarithmic Matsuda equations, equations (36a) and (37a) for totally irreversible reactions were applied together with the experimental results presented in Table 11.

Table 11. Experimental Values of $E_{1/2} - E^0$ and $E_{3/4} - E^0$ for the reduction of Ni(II) in the Various Concentrations of KNO_3 .

KNO_3 M	$E_{1/2} - E^0$ V	$E_{3/4} - E^0$ V
0.10	-0.519	-0.545
0.15	-0.535	-0.565
0.20	-0.545	-0.577
0.26	-0.549	-0.583

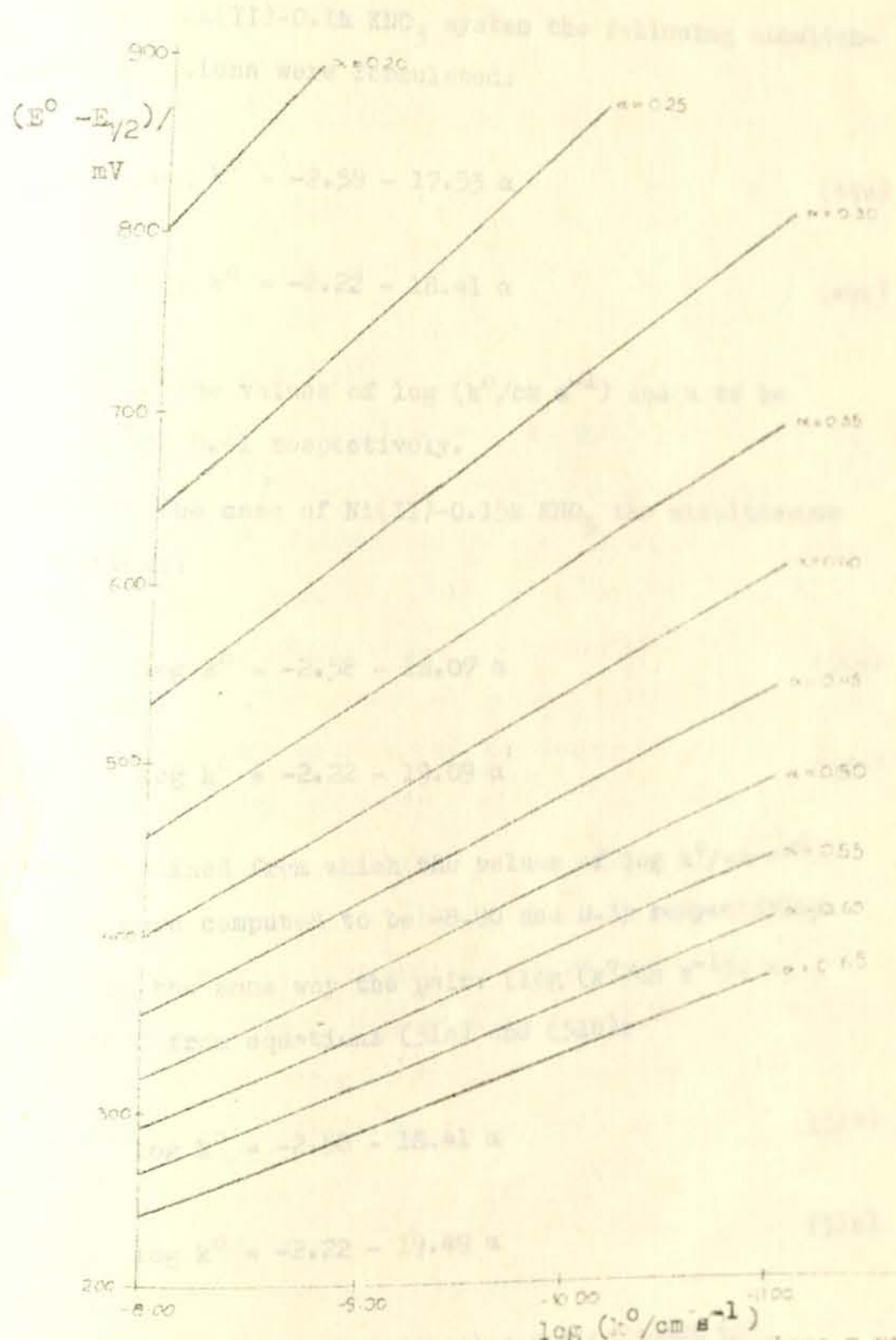


Fig. 15. $(E^\circ - E_{1/2})$ Vs $\log k^\circ$ diagram at various α values for the analysis of the Ni(II)- KNO_3 system.

For Ni(II)-0.1M KNO₃ system the following simultaneous equations were formulated:

$$\log k^0 = -2.58 - 17.53 \alpha \quad (49a)$$

$$\log k^0 = -2.22 - 18.41 \alpha \quad (49b)$$

yielding the values of $\log (k^0/\text{cm s}^{-1})$ and α to be -9.75 and 0.41 respectively.

In the case of Ni(II)-0.15M KNO₃ the simultaneous equations:

$$\log k^0 = -2.58 - 18.07 \alpha \quad (50a)$$

$$\log k^0 = -2.22 - 19.09 \alpha \quad (50b)$$

were obtained from which the values of $\log k^0/\text{cm s}^{-1}$ and α were computed to be -8.90 and 0.35 respectively.

In the same way the pair: [$\log (k^0/\text{cm s}^{-1})$, α] obtained from equations (51a) and (51b):

$$\log k^0 = -2.58 - 18.41 \alpha \quad (51a)$$

$$\log k^0 = -2.22 - 19.49 \alpha \quad (51b)$$

were found to be (-8.72, 0.33) for Ni(II)-0.2M KNO₃ and from equations (52a) and (52b):

$$\log k^0 = -2.58 - 18.55 \alpha \quad (52a)$$

$$\log k^0 = -2.22 - 19.70 \alpha \quad (52b)$$

the pair was evaluated to be (-8.33, 0.31) for the remaining Ni(II)-0.26M KNO₃ system.

4.3.2 Discussion

In supporting electrolytes such as alkali-perchlorates or nitrates that do not form complexes with nickel the reduction of hexaquonickel ion is supposed [40] to follow an irreversible path due to the fact that the half wave potential is 0.5 V more negative than the reversible standard potential for the nickel couple. This is in agreement with our result deduced using the proposal of Oldham and Ferry [15].

To see the agreement of the values extracted by means of the three techniques, k^0 and α values of the three methods are listed in Table 12. For the Ni(II)-0.1M KNO₃ system a reasonable agreement can be observed. The slight variation of the result of P. Mericam can be explained in terms of the theoretical errors of α , $\alpha \pm .05$, and $\log k^0$, $\log k^0 \pm .05$ associated with the procedure. However, at higher concentrations of KNO₃ the values of each technique show a significant variation with a pronounced deviation in the results obtained using the logarithmic Matsuda equation.

Ni(II) at high salt concentration of supporting electrolyte was taken to follow a two-step reduction mechanism by Sanborn and Orlemann [39] and subsequently disproved by Girest [41] who considered, the mechanism to be charge transfer preceded by a relatively slow dehydration step. In view of these facts, the electrode reaction of Ni(II) is likely to be different from simple electrode reactions at the higher concentrations of KNO_3 , so that the anomalies observed in the concentrations of KNO_3 greater than 0.1M by no means disqualify the validity of the logarithmic Matsuda equation or the technique of P. Mericam for electrode reactions.

The existence of the above mentioned mechanism influence easily the wave of the NPP polarogram in the top region where the only experimental parameter $E_{3/4}$ in addition to $E_{1/2}$ used in the logarithmic Matsuda equations is found. This shows that the effect of the appearance of such mechanism have a pronounced impact on the values of this technique compared with the other techniques which use the experimental values of the whole region of the NPP wave. In addition, the exaggerated change in the value of k^0 of this technique compared with others may indicate the fact that the shift of the simple electrode reaction mechanism of Ni(II) to other type lies in the transition of the concentration of KNO_3 from 0.1M to 0.15M.

With regard to the change of the value of k^0 as function of concentration, there is an increase with in-

Table 12. Apparent Values of k^0 and α for the Reduction of Ni(II) in Various Concentrations of KNO_3 .

KNO_3 M	Method of Glabau and Perry		Method of F. Lippman		Logarithmic Rate Law Equation	
	$\log(k^0/cm s^{-1})$	α	$\log(k^0/cm s^{-1})$	α	$\log(k^0/cm s^{-1})$	α
0.10M	-9.77	0.41	$-9.61 \pm .05$	$0.40 \pm .05$	-9.75	0.41
0.15M	-9.63	0.39	$-9.82 \pm .05$	$0.40 \pm .05$	-8.9	0.35
0.20M	-9.57	0.37	$-9.03 \pm .05$	$0.35 \pm .05$	-8.72	0.33
0.26M	-9.45	0.37	$-9.08 \pm .05$	$0.35 \pm .05$	-8.33	0.31

Note: Literature [18] values of $\log(k^0/cm s^{-1})$ at $E = 0V$ (NHE) and α for the Ni(II)-0.1M KNO_3 system using dc polarographic technique are -13.70 and 0.40 respectively.

creasing concentrations of KNO_3 in all values obtained using the three techniques with the exception of that evaluated from Oldham and Parry technique at the value of 0.26M KNO_3 . The variation in the case of Oldham and Parry can be due to the inconvenient nature of the NPP polarogram at this concentration of KNO_3 . The supporting electrolyte dependence of k^0 which is different from that observed for the Zn(II) and Cr(III) systems may be due to the appearance of a different reduction mechanism with increasing salt concentrations as proposed by the above mentioned workers. Such tendency of the rate constant had also been observed [19] in Cl^- , Br^- , or I^- media and this can be explained in terms of adsorption [42,43] of Cl^- , Br^- , or I^- which makes the ϕ_2 of equation (10b) more negative, thereby increasing the apparent values of k^0 with increasing concentration of the supporting electrolyte.

5. CONCLUSION

The validity of the graphical procedure that has recently been established by P. Merican et al. [1] for the determination of kinetic parameters of simple electrode reaction by normal pulse polarography has been tested on the quasi-reversible system of Zn(II). The method had been applied to the reduction of Zn(II) in 2M KNO_3 by the same workers, but in this present work the study has been extended to the reduction of Zn(II) in 0.49, 1.05, and 2.45M NaNO_3 . The method has been found to yield results in good agreement with those obtained using other techniques. A proposal had also been made by P. Merican et al. to use this graphical procedure for the determination of kinetic parameters of totally irreversible electrode reaction and the present work has confirmed its applicability to the polarographic reduction of Cr(III) in NaClO_4 and Ni(II) in KNO_3 . Cr(III) has been studied in 0.2, 0.5, and 1.0M NaClO_4 and the kinetic parameters obtained by the graphical method were found to agree with values evaluated using other techniques. The studies for the Ni(II) reduction were made in 0.1, 0.15, 0.20, and 0.26M KNO_3 . The values determined for the Ni(II)-0.1M KNO_3 system were in reasonable agreement with those obtained by other techniques whereas anomalies were observed at the higher concentrations of KNO_3 .

A relatively more convenient means of extracting kinetic parameters of simple electrode reaction by NPF

has been developed. The technique has been deduced from the logarithmic form of Matsuda's equation for the rate constant. The equation has been split into two independent and separate equations incorporating $E_{1/2}$ and $E_{3/4}$ terms as the only experimental parameters to be used for the analysis of the NPP polarogram. Simultaneous equations were then formulated using the experimental $E_{1/2}$ and $E_{3/4}$ values and the theoretical relations, from which the values of the kinetic parameters were determined. The technique has been tested on the above mentioned quasi-reversible system of Zn(II) yielding values in good agreement with those obtained using other methods. The method has further been simplified for totally irreversible systems. The technique has been applied for the foregoing reductions of Cr(III) and Ni(II). For reduction of Cr(II) in all concentration of NaClO_4 , reasonable agreement has been observed with values evaluated employing previously established methods. anomalies have still been found for the Ni(II) reduction in all concentrations of KNO_3 except 0.1M KNO_3 .

6. APPENDIX

- I. Computer Programme for the Theoretical Calculation of $(E^{\circ} - E_{1/2})$ and $(E_{3/4} - E_{1/4})$ for Simple Electrode Reaction as Functions of $\log k^{\circ}$ and α

Temperature (°C)	$E_{1/2}$ (V)	$E_{3/4}$ (V)
25	1.00	1.00
30	1.00	1.00
35	1.00	1.00
40	1.00	1.00
45	1.00	1.00
50	1.00	1.00
55	1.00	1.00
60	1.00	1.00
65	1.00	1.00
70	1.00	1.00
75	1.00	1.00
80	1.00	1.00
85	1.00	1.00
90	1.00	1.00
95	1.00	1.00
100	1.00	1.00
105	1.00	1.00
110	1.00	1.00
115	1.00	1.00
120	1.00	1.00
125	1.00	1.00
130	1.00	1.00
135	1.00	1.00
140	1.00	1.00
145	1.00	1.00
150	1.00	1.00
155	1.00	1.00
160	1.00	1.00
165	1.00	1.00
170	1.00	1.00
175	1.00	1.00
180	1.00	1.00
185	1.00	1.00
190	1.00	1.00
195	1.00	1.00
200	1.00	1.00

II. Theoretical Values of $(E^0 - E_{1/2})$ and $(E_{3/4} - E_{1/2})$ for the Analysis of Irreversible Electrode Reactions

IIa. Cr(III)-NaClO₄ System

Temperature (°C)	$E_{1/2}$ (V)	$E_{3/4}$ (V)
25	1.00	1.00
30	1.00	1.00
35	1.00	1.00
40	1.00	1.00
45	1.00	1.00
50	1.00	1.00
55	1.00	1.00
60	1.00	1.00
65	1.00	1.00
70	1.00	1.00
75	1.00	1.00
80	1.00	1.00
85	1.00	1.00
90	1.00	1.00
95	1.00	1.00
100	1.00	1.00
105	1.00	1.00
110	1.00	1.00
115	1.00	1.00
120	1.00	1.00
125	1.00	1.00
130	1.00	1.00
135	1.00	1.00
140	1.00	1.00
145	1.00	1.00
150	1.00	1.00
155	1.00	1.00
160	1.00	1.00
165	1.00	1.00
170	1.00	1.00
175	1.00	1.00
180	1.00	1.00
185	1.00	1.00
190	1.00	1.00
195	1.00	1.00
200	1.00	1.00

KU	$E_0 - E_{1/2}$	$E_3/4 - E_{1/4}$
.001	.048	-.054
8.912414E-04	.0511	-.0563
7.94378E-04	.0542	-.0563
7.07946E-04	.0582	-.0571
6.309478E-04	.0621	-.0594
5.623418E-04	.066	-.0594
5.011874E-04	.0699	-.0594
4.46604E-04	.0738	-.0618
3.981474E-04	.0777	-.061
3.548137E-04	.0816	-.0618
3.162782E-04	.0855	-.0641
2.818387E-04	.0902	-.0625
2.511891E-04	.0941	-6.490001E-02
2.230725E-04	9.880001E-02	-6.490001E-02
1.996765E-04	.1027	-.0641
1.770783E-04	.1074	-.0672
1.584896E-04	.1121	-6.490001E-02
1.41234E-04	.116	-.0657
1.258929E-04	.1207	-.0672
1.122021E-04	.1253	-.0657
1.000002E-04	.1292	-.0672
8.912527E-05	.1339	-.0672
7.943297E-05	.1386	-.0665
7.079469E-05	.1433	-6.800001E-02
6.309574E-05	.1472	-.0672
5.623413E-05	.1519	-.0665
5.011871E-05	.1566	-.0688
4.466234E-05	.1613	-.0672
3.981067E-05	.1652	-.0672
3.548126E-05	.1699	-.0688
3.162272E-05	.1746	-.0672
2.818376E-05	.1792	-.0672
2.51188E-05	.1839	-6.800001E-02
2.230713E-05	.1878	-.0665
1.996755E-05	.1925	-6.800001E-02
1.770772E-05	.1972	-6.800001E-02
1.584886E-05	.2019	-.0665
1.41253E-05	.2066	-.0688
1.258918E-05	.2113	-.0672
1.122012E-05	.2162	-.0672
9.995936E-06	.2199	-.0688
8.912445E-06	.2246	-.0672
7.943218E-06	.2292	-.0672
7.079404E-06	.2339	-6.800001E-02
6.309521E-06	.2378	-.0672
5.623361E-06	.2425	-6.800001E-02
5.011828E-06	.2472	-.0688
4.466793E-06	.2519	-.0665
3.981035E-06	.2566	-6.800001E-02
3.541098E-06	.2613	-6.800001E-02
3.162243E-06	.2652	-.0672
2.81835E-06	.2699	-.0688
2.511858E-06	.2746	-6.800001E-02
2.230694E-06	.2792	-.0672
1.9967236E-06	.2839	-.0688
1.770757E-06	.2878	-6.800001E-02
1.584872E-06	.2925	-6.800001E-02
1.412517E-06	.2972	-.0688
1.258906E-06	.3019	-.0665
1.122002E-06	.3066	-6.800001E-02
9.995844E-07	.3113	-6.800001E-02
8.912375E-07	.3152	-.0672
7.943146E-07	.3199	-.0688
7.079339E-07	.3246	-6.800001E-02
6.30947E-07	.3292	-.0665
5.623317E-07	.3339	-.0688
5.011782E-07	.3386	-6.800001E-02
4.466752E-07	.3425	-.0672
3.980999E-07	.3472	-.0688
3.548065E-07	.3519	-.0672
3.162218E-07	.3566	-.0672
2.818324E-07	.3613	-6.800001E-02
2.511835E-07	.3652	-.0672
2.230676E-07	.3699	-6.800001E-02
1.9967221E-07	.3746	-6.800001E-02
1.770741E-07	.3792	-.0665
1.584807E-07	.3839	-6.800001E-02
1.412506E-07	.3886	-.0672
1.258996E-07	.3925	-.0672

IIb. Ni(II)-KNO₃ System

6.309862E-07	.3057	-.0641
5.623399E-07	.3096	-.0641
5.011861E-07	.3135	-.0633
4.466823E-07	.3182	-.0625
3.961056E-07	.3221	-.0618
3.548122E-07	.3268	-.0618
3.162264E-07	.3307	-.0641
2.818369E-07	.3346	-.0633
2.511875E-07	.3393	-.0633
2.238709E-07	.3432	-.0618
1.99525E-07	.3479	-.0618
1.778269E-07	.3518	-.0641
1.584882E-07	.3557	-.0633
1.412527E-07	.3604	-.0633
1.258916E-07	.3643	-.0625
1.122008E-07	.369	-.0618
9.999911E-08	.3729	-.0641
8.912422E-08	.3768	-.0633
7.943208E-08	.3815	-.0633
7.079366E-08	.3854	-.0625
6.309513E-08	.3901	-.0625
5.623354E-08	.394	-.0625
5.011808E-08	.3979	-.0633
4.466781E-08	.4026	-.0633
3.96102E-08	.4065	-.0625
3.548089E-08	.4112	-.0625
3.162235E-08	.4151	-.0625
2.818346E-08	.4197	-.0633
2.511851E-08	.4237	-.0633
2.238691E-08	.4276	-.0625
1.995234E-08	.4322	-.0625
1.77825E-08	.4362	-.0625
1.584868E-08	.4408	-.0641
1.412514E-08	.4447	-.0641
1.258905E-08	.4487	-.0625
1.121999E-08	.4533	-.0625
9.999832E-09	.4572	-.0618
8.912352E-09	.4619	-.0641
7.943146E-09	.4658	-.0641
7.07933E-09	.4697	-.0633
6.309446E-09	.4744	-.0625
5.623303E-09	.4783	-.0618
5.011769E-09	.483	-.0618
4.466746E-09	.4869	-.0641
3.960988E-09	.4908	-.0633
3.548061E-09	.4955	-.0633
3.16221E-09	.4994	-.0618
2.818317E-09	.5041001	-.0618
2.511832E-09	.5080001	-.0641
2.238668E-09	.5119	-.0633
1.995216E-09	.5156	-.0633
1.778236E-09	.5205	-.0625
1.584855E-09	.5252	-.0618
1.412503E-09	.5291	-.0641
1.258895E-09	.533	-.0633
1.12199E-09	.5377	-.0633
9.999727E-10	.5416	-.0626
8.91227E-10	.5453	-.0626
7.943063E-10	.5502	-.0641
7.079265E-10	.5541	-.0633
6.309397E-10	.5588	-.0633
5.623258E-10	.5627	-.0625
5.01173E-10	.5674	-.0626
4.466711E-10	.5713	-.0626
3.960957E-10	.576	-.0633
3.548024E-10	.5799	-.0633
3.162181E-10	.5838	-.0625
2.818294E-10	.5885	-.0626
2.511805E-10	.5924	-.0625
2.23865E-10	.5971	-.0641
1.9952E-10	.601	-.0633
1.77822E-10	.6049	-.0625
1.584841E-10	.6096	-.0625
1.412491E-10	.6135	-.0618
1.258882E-10	.6182	-.0641
1.12198E-10	.6221	-.0641
9.999661E-11	.626	-.0625
8.912188E-11	.6307	-.0625
7.943E-11	.6346	-.0618
7.079209E-11	.6393	-.0641
6.309338E-11	.6432	-.0641
5.623191E-11	.6471	-.0633
5.011672E-11	.6518	-.0625
4.466664E-11	.6557	-.0618
3.96092E-11	.6604	-.0618
3.548E-11	.6643	-.0641
3.162E-11	.6682	-.0633

6.309562E-07	.2674	-.0555
5.623399E-07	.2705	-.0547
5.011861E-07	.2744	-.0555
4.466823E-07	.2783	-.0547
3.981056E-07	.2822	-.0547
3.548122E-07	.2854	-.0555
3.162264E-07	.2893	-.0555
2.818369E-07	.2932	-.0547
2.511875E-07	.2971	-.0555
2.238709E-07	.3002	-.0547
1.99525E-07	.3041	-.0555
1.778269E-07	.308	-.0547
1.584882E-07	.3112	-.0555
1.412527E-07	.3151	-.0547
1.258916E-07	.319	-.0547
1.122008E-07	.3229	-.0555
9.999911E-08	.326	-.0555
8.912422E-08	.3299	-.0555
7.943208E-08	.3338	-.0547
7.079386E-08	.3377	-.0547
6.309513E-08	.3408	-.0547
5.623354E-08	.3447	-.0555
5.011808E-08	.3487	-.0547
4.466781E-08	.3518	-.0555
3.98102E-08	.3557	-.0547
3.548089E-08	.3596	-.0555
3.162235E-08	.3635	-.0555
2.818346E-08	.3666	-.0555
2.511851E-08	.3705	-.0547
2.238691E-08	.3744	-.0547
1.995234E-08	.3783	-.0563
1.77825E-08	.3815	-.0555
1.584868E-08	.3854	-.0555
1.412514E-08	.3893	-.0547
1.258905E-08	.3932	-.0555
1.121999E-08	.3963	-.0547
-9.999832E-09	.4002	-.0555
8.912352E-09	.4041	-.0547
7.943146E-09	.4072	-.0555
7.07933E-09	.4112	-.0547
6.309446E-09	.4151	-.0547
5.623303E-09	.419	-.0563
5.011769E-09	.4221	-.0555
4.466746E-09	.426	-.0555
3.980986E-09	.4299	-.0547
3.548051E-09	.4338	-.0555
3.16221E-09	.4369	-.0547
2.818317E-09	.4408	-.0555
2.511832E-09	.4447	-.0547
2.238668E-09	.4479	-.0555
1.995216E-09	.4518	-.0547
1.778236E-09	.4557	-.0547
1.584855E-09	.4596	-.0555
1.412503E-09	.4627	-.0555
1.258895E-09	.4666	-.0555
1.12199E-09	.4705	-.0547
9.999727E-10	.4744	-.0555
8.91227E-10	.4776	-.0547
7.943063E-10	.4815	-.0555
7.079265E-10	.4854	-.0547
6.309397E-10	.4885	-.0555
5.623258E-10	.4924	-.0547
5.01173E-10	.4963	-.0547
4.466711E-10	.5002	-.0555
3.980957E-10	.5033	-.0555
3.548024E-10	.5072	-.0555
3.162181E-10	.5112	-.0547
2.818294E-10	.5151	-.0563
2.511805E-10	.5182	-.0547
2.23865E-10	.5221	-.0555
1.9952E-10	.526	-.0547
1.77822E-10	.5299	-.0555
1.584841E-10	.533	-.0547
1.412491E-10	.5369	-.0555
1.258882E-10	.5408	-.0555
1.12198E-10	.544	-.0555
9.999661E-11	.5479	-.0547
8.912189E-11	.5518	-.0547
7.943E-11	.5557	-.0563
*7.079209E-11	.5588	-.0555
6.309338E-11	.5627	-.0555
5.623191E-11	.5666	-.0547
5.011677E-11	.5705	-.0555
4.466664E-11	.5737	-.0547
3.98092E-11	.5776	-.0555
3.548E-11	.5815	-.0547

Appendix III

In this appendix the derivation of Eq. (19a) using Eqs. (11), (17), and (18) will be shown.

Eq. (11) can be rewritten as

$$\phi (\lambda_2 \sqrt{v} \theta_s) = x (1 + \exp(\xi_2)) \quad (\text{A-1})$$

with x defined as in Eq. (15b).

Inserting Eq. (A-1) into Eq. (17), yields

$$\lambda_2 \sqrt{v} \theta_s = \frac{\sqrt{3}}{4} \left\{ x \left[\frac{1.75 + x^2 [1 + \exp(\xi_2)]^2}{1 - x [1 + \exp(\xi_2)]} \right]^{1/2} \right\} (1 + \exp(\xi_2)) \quad (\text{A-2})$$

λ_2 of Eq. (18) can be rewritten as:

$$\lambda_2 = \left\{ \frac{k^0}{vD} \exp(-\alpha \xi_2) [1 + \exp(\xi_2)] \right\} \quad (\text{A-3})$$

with λ_2 and D defined as in Eqs. (12c) and (13b).

Substituting this expression of λ_2 in Eq. (A-2) yields, upon some rearrangement

$$\exp(-\alpha \xi_2) = \frac{vD \sqrt{3}}{k^0 4 \sqrt{v} \theta_s} \left\{ x \left[\frac{1.75 + x^2 (1 + \exp(\xi_2))^2}{1 - x [1 + \exp(\xi_2)]} \right]^{1/2} \right\} \quad (\text{A-4})$$

Introducing the definition of ξ_2 given in Eq. (12c)

$$E_2 = E^x - \frac{RT}{\alpha nF} \ln \left\{ x \left[\frac{1.75 + x^2 (1 + \exp(\xi_2))^2}{1 - x [1 + \exp(\xi_2)]} \right] \right\} \quad (\text{A-5})$$

with E^x defined in Eq. (19b).

9. REFERENCES

1. F. Merican, M. Astruc, and X. Andrieu, J. Electroanal. Chem., 169, (1984) 207.
2. H. Matsuda, Bull. Chem. Soc. Japan, 53, (1980) 3439.
3. G.C. Barker and A.W. Gardner, Z. Anal. Chem., 173, (1960) 70.
4. E.P. Parry and R.A. Osteryoung, Anal. Chem. 37, (1965) 1634.
5. J.B. Flato, Anal. Chem., 38 (1966) 54.
6. A.J. Bard and L.R. Faulkner, "Electrochemical Methods," Wiley, 1980, p. 186.
7. A.M. Bond, "Modern Polarographic Methods in Analytical Chemistry," Marcel Dekker, New York, 1980, Chap. 6.
8. J. Galvez and A. Bern, J. Electroanal. Chem., 69 (1976) 145.
9. A.A.M. Brinkman and J.M. Los, J. Electroanal. Chem., 14, (1967) 269.
10. K.B. Oldham, Anal. Chem., 40 (1968) 1025.
11. I. Ruzic, J. Electroanal. Chem., 75, (1977) 25.
12. G.C. Barker and A.W. Gardner, C/R 2297 A.E.R.E., Harwell, 1958.
13. J.H. Christie, E.P. Parry and R.A. Osteryoung, Electrochim. Acta., 11, (1966) 1525.
14. J. Koryta, Electrochim. Acta., 6, (1962) 67.

15. K.B. Oldham and E.P. Parry, Anal. Chem., 40, (1968) 65.
16. L. Camacho, J.L. Avila, A.M. Heras and F. Garico - Blanco, J. Electroanal. Chem., 182, (1985) 173.
17. J.W. Dillard, J.J. O'Dea and R.A. Osteryoung, Anal. Chem., 51 (1979) 115.
18. K. Morinaga, Bull. Chem. Soc. Japan, 29 (1956) 793.
19. R. Tamamushi, "Kinetic Parameters of Electrode reactions of Metallic Compounds," Butterworths, London (1975).
20. R. Andreu, M. Rueda, D. Goxalez - Arjona and F. Sanchez, J. Electroanal. Chem., 175, (1984) 251.
21. F.C. Anson, W. Rathjen and R.D. Frisbee, J. Electrochem. Soc., 117, (1970) 477.
22. R. Parsons and E. Passeron, J. Electroanal. Chem., 12, (1966) 524.
23. B.E. Conway, "Theory and Principles of Electrode Process," Ronald, New York, 1965, Chap. 6.
24. J.O.M. Bockris and A.K.N. Reddy, "Modern Electrochemistry," Vol. 2, Plenum, New York, Chap. 8.
25. R. Parsons, "Handbook of Electrochemical Constants," Butterworths, London (1959), p 79.
26. A.I. Vogel, "A Text Book of Quantitative Inorganic Analysis" 3rd Ed., Longmans, 1961, p. 1021.
27. Ref. 26 p. 433.

28. H. Matsuda, Y. Ayabe and K. Adachi, Ber. Bunsen. Phys. Chem., 67, (1963) 593.
29. R. Tamamushi and N. Tanaka, Z. Phys. Chem., (Frankfurt) 39, (1983).
30. S. Vairicka and J. Koryta, Colln. Czech. Chem. Commun., 32, (1967) 2346.
31. J. Crank, "The Mathematics of Diffusion," Clarendon Press, Oxford, 1975, p. 375.
32. R. Anderu, M. Slyters - Rehabach, A.G. Remijnse and J.H. Sluyters, J. Electroanal. Chem., 134, (1982) 101.
33. C.W. de Kreuk, M. Slutyers - rehbach, J.H. Sluyters, J. Electroanal. Chem., 28, (1970) 391.
34. M. Zielinska - Ignacink and Z. Galus, J. Electroanal. Chem., 50 (1974) 41.
35. M.J. Weaver and F.C. Anson, J. Electroanal. Chem., 65., (1975) 711.
36. D.A. Skoog and D.M. West, "Fundamentals of Analytical Chemistry" 2nd Ed., Holt, Rihart and Winston Inc., 1969, p. 813.
37. I.M. Kolthoff and J.J. Lingane, "Polarography" 2nd Ed., 1955, Interscience Pub. New York, p. 52.
38. L. Meites., "Polarographic Techniques" Willey, New York, 2nd Ed., 1965, p. 229.
39. R.H. Sanborn and E.F. Orlemann, J. Am. Chem. Soc., 78, (1956) 4852.

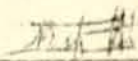
40. Ref. 37 p. 486.
41. P. Delahay, "Double Layer and Electrode Kinetics,"
Wiley - Interscience, New York, 1954, p. 216
42. Ref. 6 Chap. 12.
43. Ref. 41 Chap. 9.
44. Ref. 23 Chaps. 4 and 5

D E C L A R A T I O N

I, the undersigned, declare that this thesis is my work and that all sources of material used for the thesis have been duly acknowledged.

Name Eizuneh Workie

Signature



Place and date of submission:

Chemistry Department

Addis Ababa University

June 1986